Applications of UV-Vis-NIR

Optical Characterization of Materials Using Spectroscopy

Application Compendium

Agilent

Trusted Answers

Table of contents

Introduction

Ultraviolet, visible, near-infrared (UV-Vis-NIR) spectrophotometry provides valuable information on the properties of materials by measuring wavelengths of light from the UV (175 nm), through visible, to the NIR (3300 nm). It is a non-destructive technique that includes various measurement modalities enabling the analysis of a range of sample-types. These attributes make UV-Vis-NIR spectrophotometry a powerful and convenient tool for the characterization of samples via the spectral signatures of molecular vibrational modes and atomic electronic transitions.

This application compendium covers a broad range of spectrophotometric solutions relevant to material science including research, product development, manufacturing, and quality control/quality assurance (QA/QC) of final goods.

We have endeavored to present some of the most common applications of the technique, spanning industries from optics, optoelectronics, and semiconductors to ceramics (glass), fine/bulk chemicals (catalysts), and personal protective equipment. If you would like to discover how these examples can be extended to meet your specific measurement or material characterization needs—or for other application inquiries—contact your local Agilent representative.

Optics

The effective, efficient control and use of light is foundational to every aspect of our everyday lives. Optical devices are used across a range of applications from lighting and visual displays (phones, monitors) to telecommunications (fiber optic cables) and energy (solar)—with new applications in continuous development. Depending on the function of the device, mirrors, lenses, light sources, and detectors are used to redirect, create, or sense light at specific wavelengths. To characterize the transmission, reflection, and scattering properties of these optical components, UV-Vis-NIR spectrophotometers are used. The technique can measure various sized components, use different measurement modes, and provide the photometric performance needed to support this important industry.

Application Note

Materials

Agilent

Trusted Answers

Characterizing Sub-Nanometer Narrow Bandpass Filters Using an Agilent Cary UV-Vis-NIR

Author

Travis Burt
Agilent Technologies, Inc.

Abstract

Bandpass filters can provide an inexpensive alternative to grating monochromators for isolating narrow wavelength regions. Many commercial bandpass filters have full-width half-maximum (FWHM) bandwidths of 10 nm. This application note describes Cary UV-Vis-NIR spectrophotometer techniques for characterizing sub-nanometer FWHM bandpass filters and presents the results of a filter with a FWHM bandwidth of 3.1 Å and two filters with FWHM bandwidths of 1.2 Å.

Discussion

Instrument parameters and sample mounting require careful attention to ensure successful characterization of sub-nanometer FWHM bandpass filters. These can be challenging samples to the spectroscopist but when approached correctly the method clearly confirms the abilities of Cary UV-Vis-NIR spectrophotometers. It is recommended practice that the spectrophotometer be warmed up for a 1 hour period and then re-initialized (reset) by turning it off and then on again immediately. A wavelength validation test should also be performed using the validation software application and checked before any measurements are attempted.

The function of bandpass filters are based on interferometric principles and so they are sensitive to the angle of the incident light. The peak wavelength shifts (decreases) to shorter wavelengths with increasing angle. Conversely, peak wavelength increases slightly with temperature. To account for temperature variations narrow bandpass filters are measured at specified temperatures, generally 23 °C.
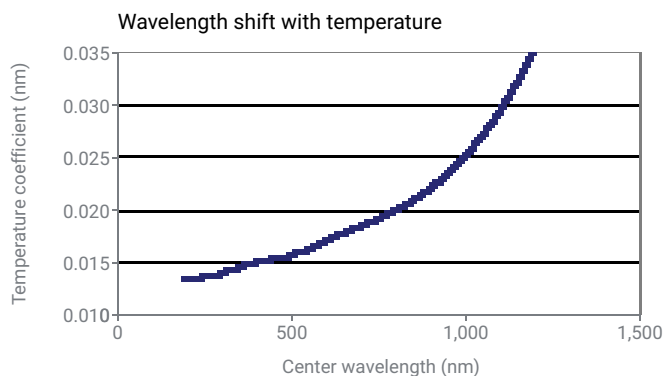
Figure 1. Filter temperature dependance.
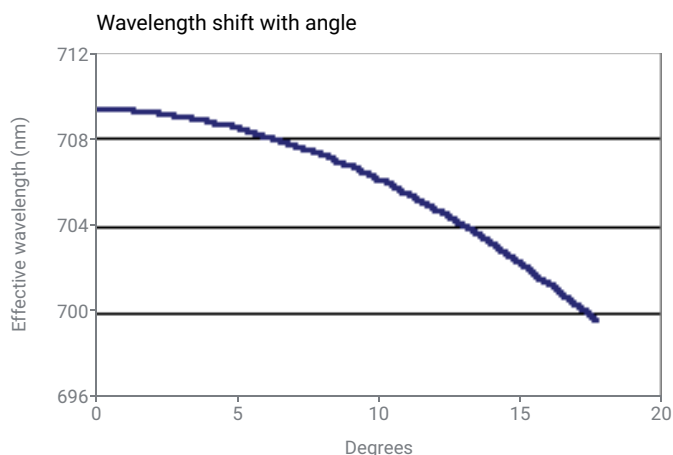
Figure 2. Filter angular dependance.

It is clear from Figures 1 and 2 that attention should be paid to the large temperature variations that are present in some laboratories but a 1° angle of incidence is not likely to be exceeded unless the sample holder is installed incorrectly or some foreign material becomes lodged between the filter and the solid sample slide.

Equation 1 may be used to determine wavelength shifts of a filter in collimated light with incident angle of up to 15 degrees.

Equation 1. $I_\theta = I_o[1 - (N_e/N\star)^2 \sin^2\theta]^{1/2}$

Where;

I_θ = wavelength at angle of incidence

I_o = wavelength at normal incidence

N_e = refractive index of external medium

$N\star$ = effective refractive index of filter (refer to manufactures specifications)

θ = angle of incidence.

For convergent or divergent light the wavelength shift is slightly less where the dependent variable is the cone angle. A good approximation for determining wavelength shift with cone angle is to define θ as the cone angle and divide the result of Equation 1 by two.

The Figures 1 and 2 show the general trends of peak wavelength shifts with temperature and angle. Broadly speaking a temperature change of 5 °C or 1° in the angle of incidence will move the peak wavelength by up to 0.05 nm.

Instrument considerations

The spectrophotometer should be configured to reduced slit height, double beam mode. The independent control tab should be activated to enable spectral bandwidth (SBW) values below 0.040 nm to be entered. The SBW and data interval should be set to ensure an adequate number of data points are collected across the bandwidth of the filter. The strong dependence of FWHM and peak wavelengths on the SBW can be seen in Figure 3. The decrease in the peak wavelength and the maximum percent transmission can be seen as SBW is increased.
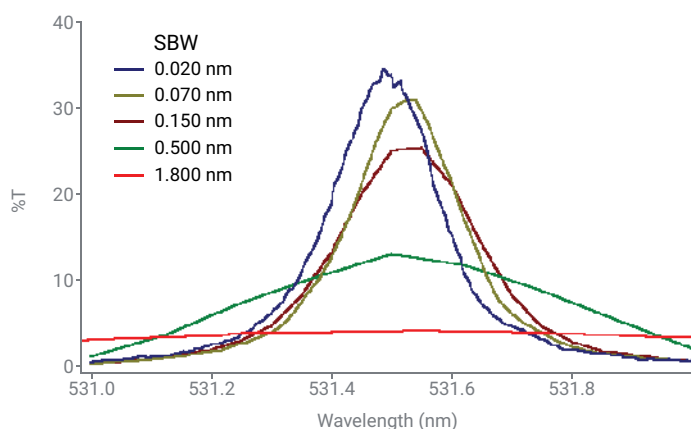
Figure 3. Filter SBW dependance.

In the Cary UV-Vis-NIR the reduced slit height cone angle can be reduced from a maximum of 5.0 to 0.6 degrees using 1 mm apertures at positions of 50 mm prior to, and 50 mm after, the sample. A cone angle of 0.6 degrees will minimize the shift in the peak wavelength of a narrow bandpass filter to less than 0.05 nm. Care must be taken to ensure that the 1 mm apertures are located at the center of the beam profile and that they are parallel to the beam axis. This is achieved by maximizing flux throughput before the sample is inserted into the instrument.

First, the front sample beam aperture is inserted and the instrument is set to idle at the filters center wavelength at a practical SBW (eg. 1.5 nm). The aperture is moved up and down until the maximum signal is achieved in the %T display, then locked into place using the locking nut. A 5 mm aperture is then inserted into the front and rear stands of the rear beam and the signal is minimized. The 5 mm apertures are used in the rear beam because they are easier to align than the 1 mm apertures but the full dynamic range of the spectrophotometer needs to be preserved by placing an attenuator in the rear beam. A 1.1 Abs rear beam attenuator (RBA) was sufficient to bring the baseline scan below 100% during its collect. Finally, after the two 5 mm apertures and RBA are positioned in the rear beam, the second 1 mm aperture is inserted into the back of the sample beam. Once again, the aperture height is optimized to achieve maximum signal throughput and then locked into place.

The front and rear aperture alignment may need to be revisited to ensure optimum throughput has been achieved. Both 100%T and 0%T background scans need to be performed before the sample is measured. Averaging time should be chosen such that an acceptable signal to noise ratio is achieved. For sub-nanometer FWHM bandpass filters this value is likely to be at least above 5 seconds. This amounts to approximately 20 minutes per scan for a visible spectral region of 3 nm. Alternatively, the signal-to-noise (S/N) control feature of the software can be used to minimize scan times. By selecting a desired S/N value scan rates will automatically increase in less noisy regions of the spectrum. Spectra of three different narrow bandpass filters can be seen in Figures 4 and 5.

Figure 4. Spectrum of narrow bandpass filter.
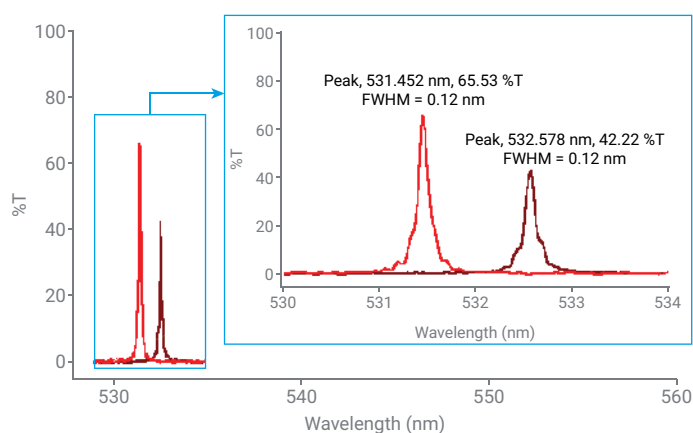
Figure 5. Spectrum of narrow bandpass filters.

Conclusion

Successful measurement of sub-nanometer bandpass filters can be performed on a Cary 5000/6000i or Cary 7000 UMS, UV-Vis-NIR spectrophotometer. Two 1 mm apertures are used 50 mm either side of the sample in the front beam and two 5 mm apertures with 1.1 Abs rear beam attenuation are used in the rear beam. Correct alignment of the apertures is critical to achieving optimum throughput of the spectrophotometer prior to measurement. The FWHM, peak wavelength and peak transmission for three narrow bandpass filters were measured and found to be, respectively:

0.31 nm, 709.277 nm, 26.17 %T,
0.12 nm, 531.452 nm, 65.53 %T,
0.12 nm, 532.578 nm, 42.22 %T.

www.agilent.com/chem/cary5000

Agilent
Trusted Answers

Agilent

Trusted Answers

Evaluation of the Cary Absolute Specular Reflectance Accessory for the Measurement of Optical Constants of Thin Films

Author

Stuart White
Physics Department,
Sydney University, Sydney,
New South Wales

Abstract

The optical constants of thin absorbing films can be determined using photometry, in which the transmittance (T) and the reflectance from the front (R) and rear (R[1]) of the substrate-film system are measured as a function of the wavelength of incident unpolarized light. This information and the film thickness (t) can be used to obtain the dispersion, $n(\lambda)$ and the extinction coefficient, $k(\lambda)$. From these a variety of useful quantities, such as the dielectric function and absorption coefficient, can be calculated.

The method of determining the optical constants from photometric data which adequately overcomes the difficulties of missing or multiple solutions is discussed in detail by McPhedran *et al.*[1]

Using an Agilent Cary UV-Vis-NIR spectrophotometer, R, R[1], and T are routinely measured for wavelengths between 200 and 3,000 nm (the instrument has a range of 185 to 3,152 nm).

To measure film and substrate transmittance is straightforward: the baseline is recorded, the instrument is zeroed, then the slide is placed in the sample beam and the resultant spectrum is recorded. The effect of finite substrate thickness is removed by calculation[1], assuming that the optical properties of the substrate material are known. For transmittance measurements, it is not the usual practice to place an uncoated slide in the reference beam.

The calculation of optical constants assumes that the film is of homogeneous composition and uniform thickness and the films we measure approximate this ideal well. This means that the reflectance is predominantly specular and so we do not normally require an integrating reflectance accessory which would limit the wavelength range and reduce the signal-to-noise ratio.

An Agilent Cary VW absolute specular reflectance accessory (SRA) was used in this evaluation.

Figure 1 is an optical schematic of the SRA. Note that:

– The sample beam undergoes three reflections from aluminum-coated mirrors in the reference, or V, position.

– The reference beam symmetrically undergoes three reflections.
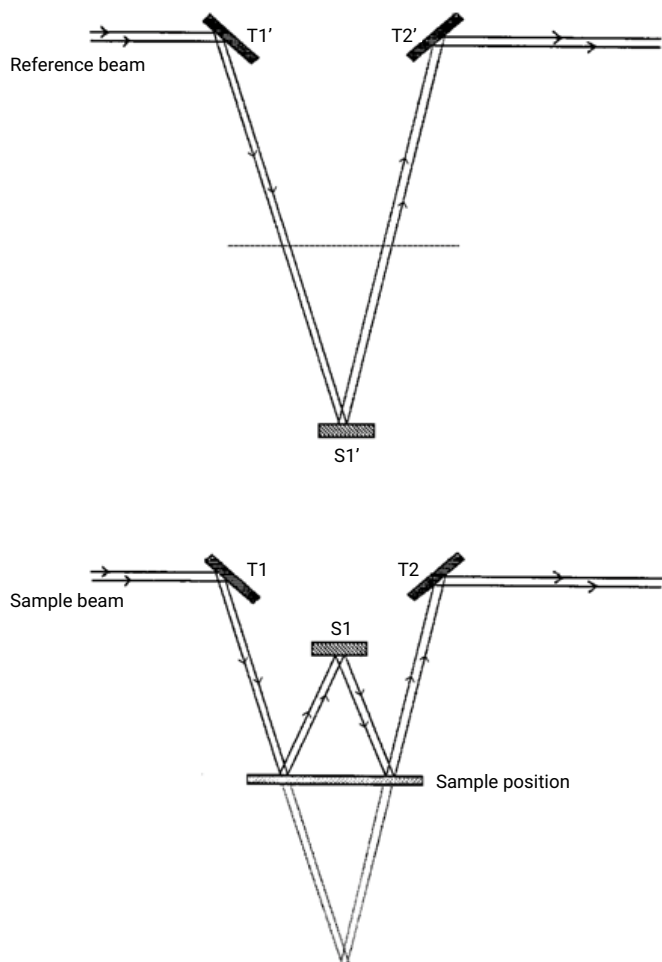
Figure 1. The optical design of the Agilent Cary absolute specular reflectance accessory (SRA).

Aluminum is used as a coating for the SRA mirrors because it has a uniformly high reflectance in the UV-Vis-NIR. Despite this, the light losses can be quite large after several reflections, particularly around 820 nm where the aluminum absorbs significantly. The reflectivity of the three mirror design is indicated in Figure 2.
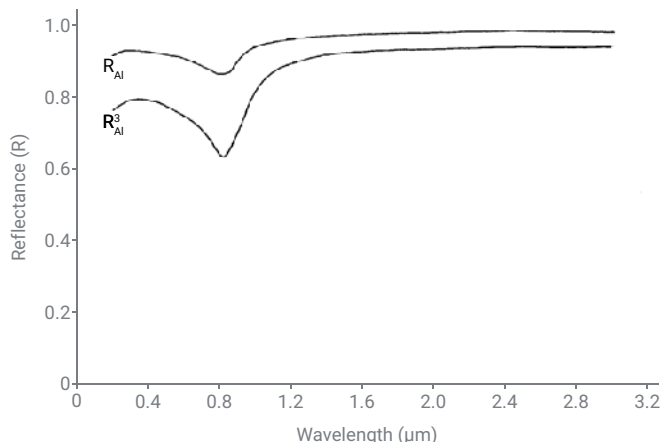
Figure 2. The cumulative reflectivity effects of aluminum surfaces.

Optical performance

It is convenient to use polished wafers of single crystal silicon as a standard when assessing a reflectance instrument such as this one. Although evaporated metal films such as aluminum or silver have a higher reflectance, the value for such films can significantly depend on deposition and post deposition conditions. Thus, in practice, it is preferable to use a single crystal material. Uncertainties deriving from the presence of an oxide layer and surface roughness have a major effect on the normal incidence reflectance only in the UV, so comparison with the literature is reasonable.

Figure 3 shows the reflectance of a mechanically polished <100> oriented silicon wafer as measured by the SRA, in the wavelength region around 800 nm. Also shown are the reflectance values determined by Aspnes and Studna[3], from measurements using spectroscopic ellipsometry.

The region around 800 nm is problematic for two reasons:

1. The changeover from the photomultiplier to the PbS detector occurs at 800 nm. This means that both detectors are operating at the edge of their region of best performance. Therefore, with low light signals, the signal-to-noise ratio and photometric linearity of the PbS detector in particular will be impaired.

2. This is also the region where the light loss due to absorption in the SRA mirrors is greatest, as discussed before and shown in Figure 2.
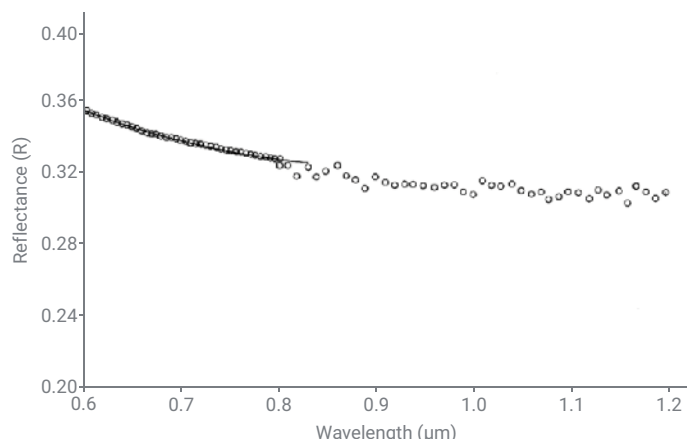
Figure 3. Reflectance of single crystal <100> silicon. Circles represent data obtained using the SRA.

Alignment tests

It is important to determine the effect of misalignment of the sample in a specular reflectance accessory. This was performed in two ways.

In the first instance, a B270 glass slide, 2 mm thick, with a freshly deposited aluminum film was rotated about a vertical axis by using shims inserted under either end. This geometry is shown in Figure 4.

Figure 5 shows the decrease in reflectance relative to zero rotation for both accessories. As is illustrated, measurements using the accessory are sensitive to rotation.
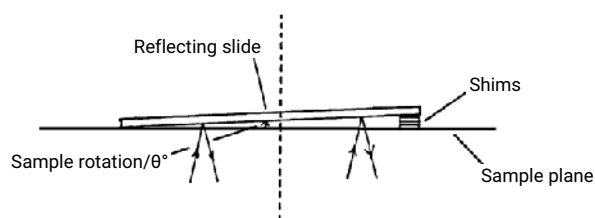
Figure 4. The geometry used to determine the sensitivity of the reflectance to rotation of the sample.
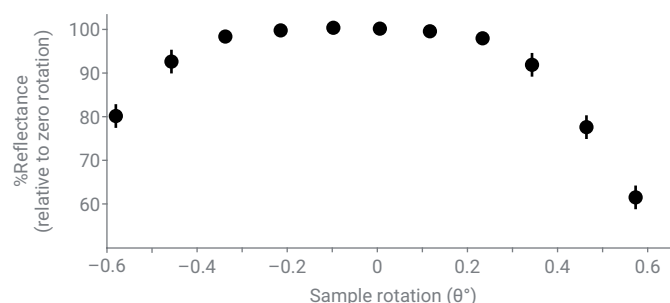
Figure 5. Reflectance of the slide as a function of the angle of rotation, relative to zero rotation.

It should be noted that:

– The reflectance is unaffected by rotations of up to 0.2° in either direction.

– The SRA can be readily aligned by the user, thus any asymmetry can be eliminated.

The second alignment test involved a displacement of the reflecting surface from the sample plane by varying amounts, as shown in Figure 6.
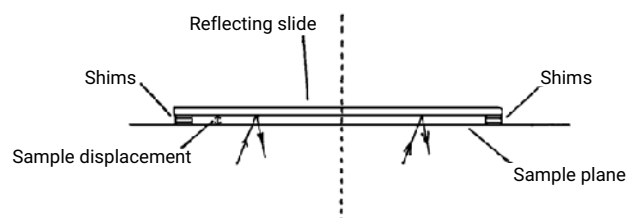
Figure 6. The geometry used to determine the sensitivity of the reflectance to displacement of the sample away from the sample plane.

This is particularly important in our work, because we have a need to measure the reflectance of thin films from the rear of the film, which results in a 0.5 mm displacement of the most reflecting interface from the sample plane.

The measured reflectance of the aluminum-coated slide varied by less than 1.5% for displacements of the slide of up to 1 mm.

Conclusion

Preliminary tests on the Agilent Cary SRA indicate that it has excellent signal-to-noise performance, particularly in the wavelength region where aluminum absorbs: above and near 800 nm.

The symmetry of the front and rear beam path means that it is possible to store baseline correction values over the entire UV-Vis-NIR range of wavelengths.

The sample mounting configuration offers two key advantages to the user:

– The ability to measure smaller samples.

– The front loading of the sample ensures greater visibility and less risk of sample mismounting or damage.

The sensitivity to misalignment of the sample is not likely to cause a problem and the mirror alignment can easily be carried out by the user.

References

1. McPhedran Ross, C. *et al.* Unambiguous Determination of Optical Constants of Absorbing Films by Reflectance and Transmission Measurements. *Applied Optics* **1984**, *23*, 1197.

2. Gourlet, D. L. Spectrophotometric Measurements Of Filters, Laser Reflections and Optical Materials. *Instruments At Work* **1982**, UV-23, 3.

3. Aspnes, D. E.; Studna, A. A. Dielectric Functions and Optical Parameters of Si, Ge, GaP, GaAs, GaSb, InP1, InAs and InSb from 1.5 to 6.0 eV. *Phys. Rev. B* **1983**, *27*, 985.

www.agilent.com/chem/vw-sra

Agilent
Trusted Answers

Agilent

Trusted Answers

Gaining Deeper Insights into Thin Film Response

Overcoming spectral oscillations using the Agilent Cary universal measurement accessory
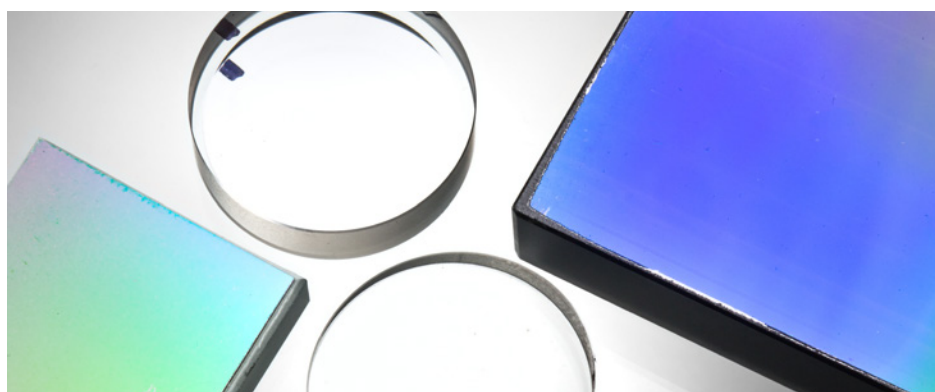
Authors

Robert Francis and Travis Burt
Agilent Technologies, Inc.
Mulgrave, Victoria
Australia

Introduction

A more detailed account of this work was first published in Optics Express 16129, 2 July 2012, Vol. 20, No. 14.[1]

Designers and manufacturers of high-quality multilayer optical coatings require reliable methods to measure optical constants of thin film materials with a high degree of accuracy. This is normally achieved using UV-visible-IR spectrophotometry to acquire normal and quasi-normal transmittance (T) and reflectance (R) spectra of a sample. Understanding the accuracy of the data produced and the source of any errors (random or systematic) will lead to more reliable sample characterization.[2,3]

Random errors (random noise) vary from one point to another in the measurement data set, and have been shown to have minimal impact on the characterization results.[2] However, systematic errors that result in an offset of spectral characteristics as a whole, or cause large-scale wavelength variations of T and R curves, are especially critical for the accurate determination of thin film parameters.[2]

Valuable information relating to data accuracy is provided by calculating the total losses (TL) of the thin film sample[4,5] using $TL(\lambda) = 100\% - R(\lambda) - T(\lambda)$. Typically, in the spectral range where the substrate and the thin film are nonabsorbing and nonscattering, zero total losses would be expected, whereas with absorbing films, $TL(\lambda)$ decreases with increasing λ.

When analyzing spectra for TL, researchers often observe oscillations, which may cause doubt about the quality of the data. Sources of such oscillations include:

- The difference in angles of incidence (AOI) at which T and R are measured
- Absorption in a thin film acting in combination with interference effects
- A slight thickness nonuniformity of the film

A full report on the origins of oscillations in TL is discussed in reference 1.[1] This application note demonstrates how an Agilent Cary 5000 UV-Vis-NIR spectrophotometer equipped with a universal measurement accessory (UMA) is able to provide previously unreported insights into thin film characterization due to its ability to measure T and R without moving the sample.

Experimental

Samples

A Ta_2O_5 film of 292 nm thickness was deposited onto a Suprasil substrate of 25 mm diameter and 6.35 mm thickness using a magnetron-sputtering Leybold Optics HELIOS plant.[1] A second, preprepared Ta_2O_5 sample with a slightly different film thickness was also used. Transmittance data for s-polarized light were measured at 7° and 10°, and s-polarized reflectance data were measured at 10°.

Instrumentation

- Agilent Cary 5000 UV-Vis-NIR spectrophotometer
- Agilent universal measurement accessory

The UMA is a highly automated, variable-angle, absolute specular reflectance and transmittance system. The linearly polarized beam that illuminates the sample can be measured in transmission, and by rotating the detector assembly about

an axis through the sample and perpendicular to the plane of incidence, in reflection, as indicated in Figure 1. Therefore, the same spot on the sample is used for both T and R measurements. This multiple measurement mode capability of the UMA results in more accurate, rapid, and complete optical characterization of thin films. These data could also have been collected on a Cary 7000 universal measurement spectrophotometer (UMS).

Results and discussion

Traditionally, reflectance and transmittance measurements have been performed using spectrophotometers fitted with different accessory attachments. In practice, different areas of the sample surface may be tested. If the deposition process produces a film with a nonuniform thickness, it is reasonable to expect that reflectance and transmittance measurements are affected.

With the development of the UMA, it is now possible to measure T and R at the same sample point, overcoming one source of oscillations on the results. In this study, an Agilent Cary 5000 double beam UV-Vis-NIR spectrophotometer equipped with a UMA was used to acquire transmittance data for s-polarized light at 7° and 10°, and s-polarized reflectance data at 10°. To verify the capabilities of the UMA, the same sample was reanalyzed a few months later using a second UMA unit and different sample mounts.
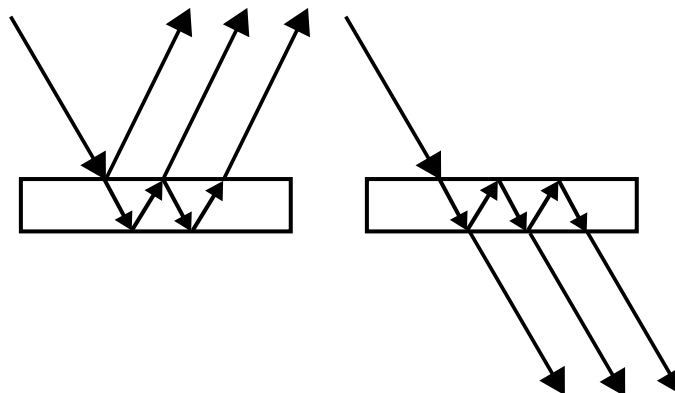

Figure 1. Schematic of the Agilent UMA, an absolute variable-angle reflectance and transmission accessory capable of front and back surface reflection (left) and direct and inter-reflected transmission (right) measurement.

The first experiment considered TL calculated on the basis of T and R measurements taken at different AOI using the first UMA unit according to: $TL^{(s)}(\lambda) = 100\% - T^{(s)}(7°, \lambda) - R^{(s)}(10°, \lambda)$. The experimental total losses are plotted in Figure 2A (red line). Oscillations of approximately 0.4% magnitude are clearly observed. The solid curve (black line) in Figure 2A presents a theoretical approximation of total losses as expected when T and R are measured at different angles of 7 and 10 degrees, respectively. There is good agreement between the experimental and theoretical results shown in Figure 2A. This agreement confirms that the oscillations are due to only the difference in AOI and that the effect of thickness nonuniformity does not contribute to total losses spectral behavior.

Figure 2B shows experimental total losses, calculated from T and R measurements taken at equal AOI: $TL^{(s)}(\lambda) = 100\% - T^{(s)}(7°, \lambda) - R^{(s)}(7°, \lambda)$.
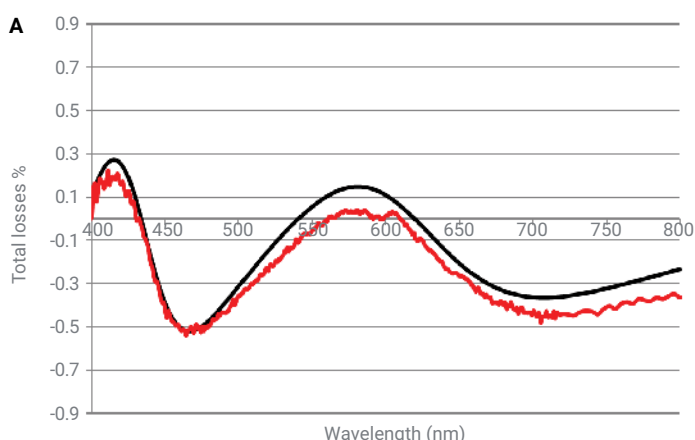
The absence of any oscillations is clearly observed. This is further confirmation that thickness nonuniformity does not affect total losses when T and R measurements are acquired at the same point of the sample.

The second experiment acquired T and R data from the original sample on a new sample mount using a different UMA unit coupled to the Cary 5000 spectrophotometer. The solid black curve in Figure 3A represents the data acquired using a UMA unit.

The same sample was re-analyzed using a different UMA unit four months later and the results are represented by the red line. Visually, both data sets are indistinguishable, demonstrating the excellent reproducibility between multiple UMA units. This gives confidence in results obtained from different UMA/UMS systems, for example, within a manufacturing environment where more than one instrument can be used.
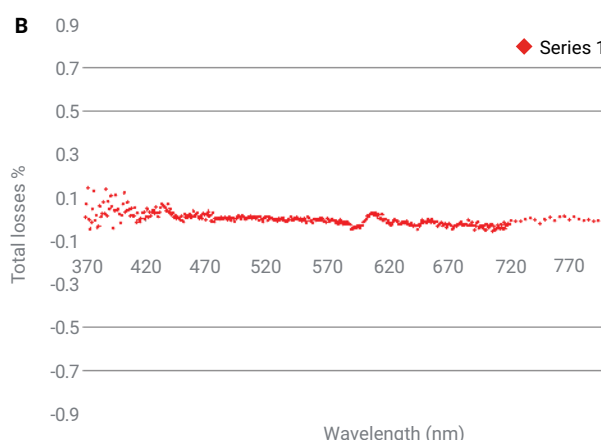
Figure 2. (A) Comparison of $TL^{(s)}(\lambda) = 100\% - T^{(s)}(7°, \lambda) - R^{(s)}(10°, \lambda)$ calculated from experimental data and $TL^{(s)}AOI(\lambda)$ calculated by theoretical equation.[1] (B) Total losses $TL^{(s)}(\lambda) = 100\% - T^{(s)}(7°, \lambda) - R^{(s)}(7°, \lambda)$ calculated from experimental data.
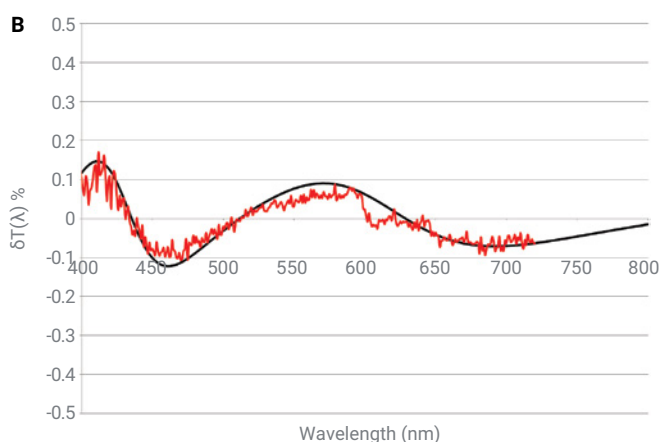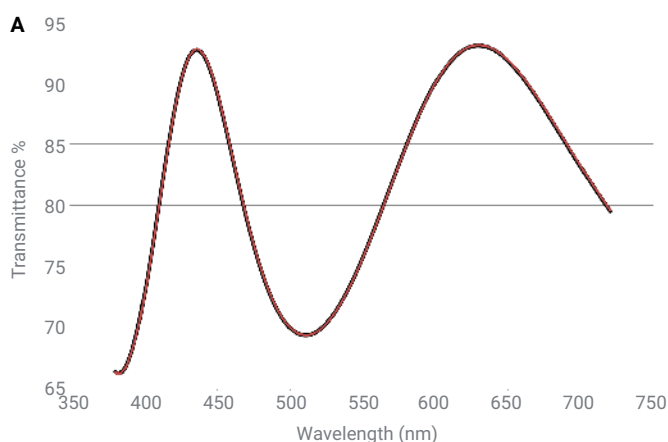
Figure 3. (A) Comparison of two transmittance spectra acquired using two different UMA accessories coupled to an Agilent Cary 5000 spectrophotometer. The data relate to the same Ta_2O_5 sample. (B) Comparison of $T^{(s)}(\lambda) = T^{(s,1)}(7°, \lambda) - T^{(s,2)}(7°, \lambda)$ calculated from experimental data (red line) and by theoretical equations (black line).[1]

The difference between the two transmittance spectra is indicated by the red line in Figure 3B. Oscillations of approximately 0.15% in magnitude can clearly be observed. The solid curve (black line) in Figure 3B indicates a theoretical approximation of total losses calculated with Δd = −0.3 nm. This thickness nonuniformity value corresponds to approximately 0.1% of the geometrical film thickness (d = 292 nm). This is in full agreement with the thickness nonuniformity level in the HELIOS deposition plant.

Conclusions

One cause of oscillations in total losses spectra arise from slight thickness nonuniformity of the thin film sample. However, this source of error can be small when compared to variations in AOI between T and R measurements. AOI errors can be eliminated using an advanced spectrophotometric accessory (developed by Agilent Technologies) fitted to an Agilent Cary 5000 UV-Vis-NIR spectrophotometer. The UMA is a variable-angle specular reflectance and transmittance system that acquires T and R data without moving the sample or the incident beam onto the sample.

The results presented in this report demonstrate that the residual oscillations observed after eliminating AOI variations are minimal and are in full agreement with the theoretical values. The findings confirm that the effect of thickness nonuniformity does not contribute to total losses spectral behavior when an instrument capable of T and R measurement at the same point of the investigated sample is used. The latest in multiangle spectral photometry provides researchers with more accurate spectroscopic information for the characterization of thin films than has been available previously.

References

1. Amotchkina, T. V. *et al.* Oscillations in Spectral Behavior of Total Losses (1−R−T) in Thin Dielectric Films. *Optics Express*, 2 July **2012**, 20(14), 16129−44.

2. Tikhonravov, A. V. *et al.* Effect of Systematic Errors in Spectral Photometric Data on the Accuracy of Determination of Optical Parameters of Dielectric Thin Films. *Appl. Opt.* **2002**, *41*, *2555−2560*.

3. Woollam, J. Ellipsometry, Variable Angle Spectroscopic, *Wiley Encyclopedia of Electrical and Electronics Engineering*, J. Webster, ed. (Wiley, New York, 2000). Supplement 1.

4. Tikhonravov, A. V. *et al.* Optical Parameters of Oxide Films Typically Used in Optical Coating Production. *Appl. Opt.* **2011**, *50*, C75−C85.

5. Tikhonravov, A. *et al.* Reliable Determination of Wavelength Dependence of Thin Film Refractive Index. *Proc. SPIE* **2003**, *5188*, *331−342*.

www.agilent.com/chem/cary5000

Agilent

Trusted Answers

Agilent

Trusted Answers

High Volume Optical Component Testing

Using an Agilent Cary 7000 Universal Measurement Spectrophotometer (UMS) with Solids Autosampler

Author

Travis Burt

Farinaz Haq

Agilent Technologies, Inc.

Introduction

Manufacturers of high quality multilayer optical coatings require reliable methods to accurately measure optical performance of thin film materials. Traditionally this is accomplished using two separate measurements: normal incidence transmission (T), typically conducted within the sample chamber of a spectrophotometer, and near normal reflectance (R) measurements, which require the use of a separate reflectance accessory. Ensuring that both measurements are made from exactly the same patch on the sample is difficult using this approach due to sample repositioning during changes in instrument configuration between R and T measurements. However, the Cary 7000 UMS overcomes this limitation by measuring multi-angle transmission and absolute reflection measurements from exactly the same point of a sample's surface, without sample repositioning. This method eliminates systematic errors often introduced due to small variations in angle of incidence (AOI) when a variety of %R and %T measurement techniques are employed.

QA/QC of optical thin film coatings

Effective quality assurance and quality control (QA/QC) of optical thin film coatings has relied on accurate spectroscopic measurements taken during and at completion of a coating procedure. Current QA/QC testing is typically limited to representative witness pieces introduced into the coating process for testing purposes. Witness piece testing is preferred to comprehensive testing of large numbers of finished-goods because of the prohibitively high cost-per-analysis in high volume multiple sample testing.

In this study, we demonstrate increased productivity and reduced cost-per-analysis with automated, unattended multi-angle R/T analysis for multiple samples of uncoated fused silica using an Agilent Cary 7000 UMS fitted with an Agilent Solids Autosampler.

Experimental

Instrumentation

* Agilent Cary 7000 Universal Measurement Spectrophotometer
* Agilent Solids Autosampler

The Cary 7000 UMS is the latest generation of high performance UV-Vis-NIR spectrophotometers designed for Multi-Angle Photometric Spectroscopy (MPS) applications over the wavelength range 250–2500 nm. MPS measures the absolute reflectance and/or transmittance of a sample across a range of angles from near normal to oblique incidence (1). The UMS performs variable angle transmission and absolute reflectance measurements from the same patch of a sample's surface. The linearly polarized beam that is incident on the sample can be used to measure transmission, and by rotating the detector assembly about an axis through the sample and perpendicular to the plane of incidence, in reflection. The UMS also functions as a goniospectrophotometer providing further capability for diffuse reflectance measurements of non-specular surfaces and diffuse transmittance measurements of translucent materials. The addition of an automated polarizer further enables accurate measurement at S, P or user specified polarization angles.

The accessory component of the Cary 7000 UMS, the Cary UMA (Universal Measurement Accessory), is available as an upgrade option for existing Cary 4000/5000/6000i UV-Vis-NIR spectrophotometer users.

The Solids Autosampler is an independently controlled sample holder designed specifically for the Cary 7000 UMS and UMA. It can be mounted inside the Cary 7000 UMS measurement chamber as shown in Figure 1a. In addition to the angle of incidence (AOI) control (Θ_i) provided by the UMS, the Solids Autosampler provides two additional degrees of freedom; radial (z) and rotational direction (Φ) about the incident beams axis (I_o). A variety of sample holders allow mounting of multiple individual samples (up to 32 x 1 inch

diameter), Figure 1b, or single large diameter samples (8 inch diameter).

Studies have shown that the inclusion of MPS data at angles beyond near normal incidence provides better reverse engineering of complex thin films (2). Additionally multi-angle photometric spectroscopic data has also provided insight into oscillations in the total losses in thin dielectric films (3). Measurements made using MPS measurements performed on a Cary 7000 UMS have been used to validate and optimize reverse engineering strategies applied during coating production runs (4).

Figure 1a. Plan view of the Cary 7000 UMS measurement chamber with the Solids Autosampler installed.

Figure 1b. A multi-sample holder with capacity to mount up to 32 x 1 inch diameter samples.
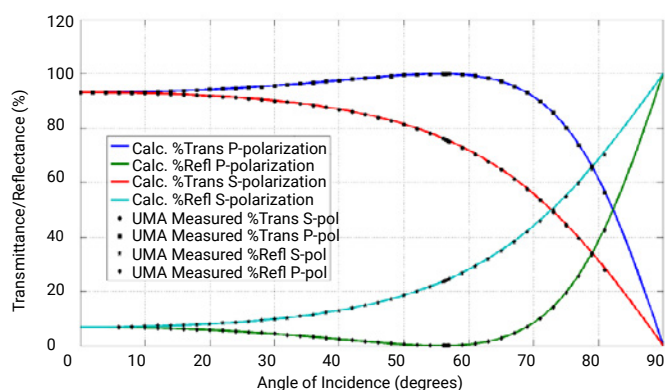
Figure 2. Absolute reflectance and transmittance of a 1mm thick silica sample plate as a function of angle of incidence. The solid lines are calculated from the Fresnel equations and the symbols are values measured using the Cary 7000 UMS. Measurement wavelength: 500 nm; physical size of the fused silica sample limited AOI range to 0−82°.

Results and discussion

Single-sample analysis

The Cary UMS was used to provide sequential multi-angle measurements for both absolute specular reflectance and direct transmittance on the same patch of sample of 1 mm thick fused silica without repositioning of the sample (Figure 2). This simple measurement of the transmission and reflection from a 1 mm thick plate of fused silica was conducted at angles of incidence ranging from 0 to 82° in transmission and 6 to 82° in reflection in both S and P polarization. The physical size of the silica sample limited the measurable range of angle of incidence to <82° without the incident beam falling off the sample surface. The measurements shown include contributions from both the front and internal rear surface reflections and transmissions. The individual points represent the measured values and the underlying solid lines indicate the total reflectance and total transmittance predicted by the Fresnel equations:

Reflection (R) and Transmission (T) Coefficients for s and p polarized light

$$R_s = \left| \frac{n_1\cos\theta_i - n_2\cos\theta_t}{n_1\cos\theta_i + n_2\cos\theta_t} \right|^2 \qquad R_p = \left| \frac{n_1\cos\theta_t - n_2\cos\theta_i}{n_1\cos\theta_t + n_2\cos\theta_i} \right|^2$$

$$T_s = 1 - R_s \qquad T_p = 1 - R_p$$

n_1 = refractive index of incident medium
n_2 = refractive index of sample
θ_i = angle of incidence
θ_t = angle of transmission
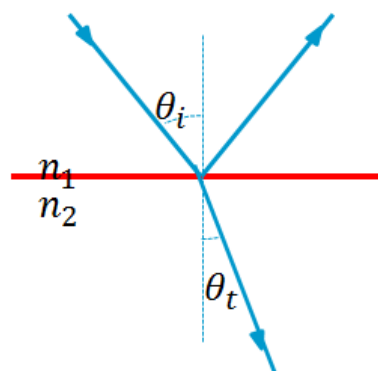
Where n_1 was taken to be 1.00 (air) and n_2 the refractive index of fused silica as determined by the Sellmeier Equation:

$$n_2(\lambda) = 1 + \sum_i \frac{B_i\lambda^2}{\lambda^2 - C_i}$$

λ = wavelength
B_i and C_i = Sellmeier coefficients

Sellmeier coefficients are typically supplied with the optical data sheets of transparent materials.
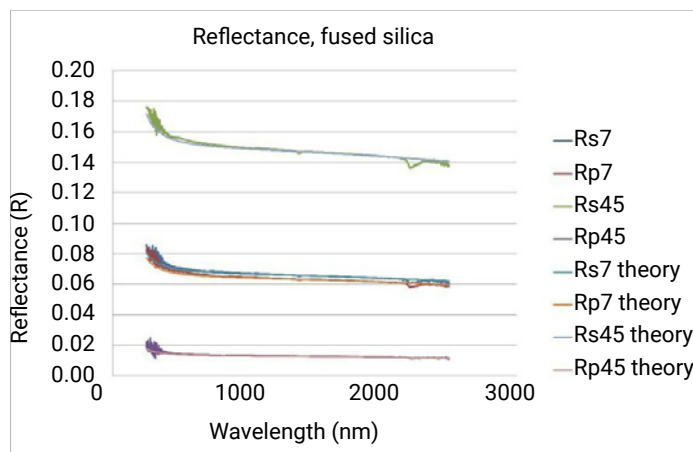
Figure 3a. Reflectance of fused silica at sample position #1 in the multi-sample holder. Theoretical lines are calculated from the Fresnel equations. Measured results were made using the Cary 7000 UMS with Solids Autosampler.
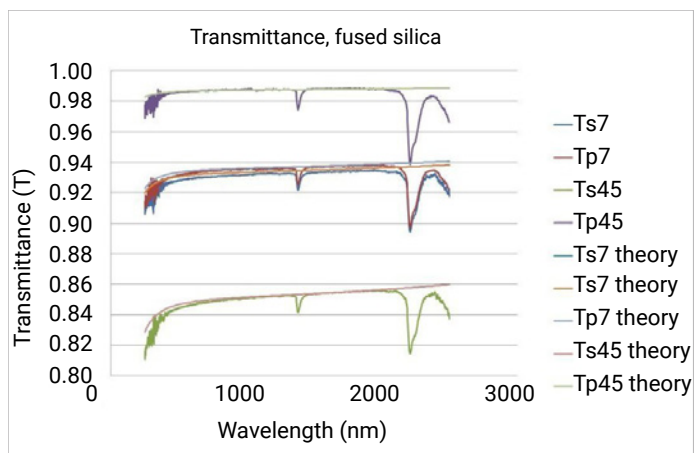
Figure 3b. Transmittance of fused silica at sample position #1 in the multi-sample holder. Theoretical lines are calculated from the Fresnel equations. Measured results were made using the Cary 7000 UMS with Solids Autosampler.
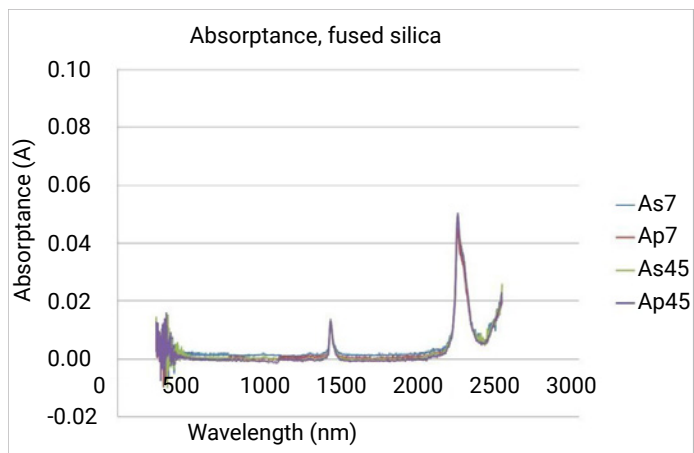
Figure 3c. Absorptance (A) of fused silica at sample position #1 in the multi-sample holder. Absorptance data is calculated from T, and R data using A = 1 − R − T. Aside from the water absorption band at ~1400 nm, absorptance data 500−2000 nm is expected to be approx 0.00.

Multi-sample analysis

The Solids Autosampler was used to extend MPS measurements from a single piece of fused silica to 11 individual pieces of uncoated fused silica (38 mm x 42.5 mm x 1 mm), over the wavelength range of 250 – 2500 nm. Each sample was measured in R and T, at AOI ±7° and AOI ±45°, under S and P polarization. The positive(+) and negative(-) collection angles were automatically averaged post data collect and the final spectra denoted as; Ts7, Rs7, Tp7, Rp7, Ts45, Rs45, Tp45, Rp45. The time taken to collect the 16 spectra per sample was approx 40 minutes and the total collect time for the 11 samples was less than 8 hours. Data was collected in a single unattended overnight run without further user intervention. Absorptance, defined as

A=1-R-T, was calculated for each angle and polarization.

Full spectral range results of sample #1 are presented in Figures 3a, b and c, showing close agreement with theory over a wide range of signal levels, angles, polarization states and wavelength. Residual errors, calculated as the difference from Fresnel theory for the central wavelength 1500 nm, are given in Table 1.

Factors that may affect the accuracy of these measurements include the residual uncertainty in the symmetry of the system, sample mounting and long term drift of the instrument.

- Spectral data from the positive(+) and negative(-) angles were averaged to help correct for any optical asymmetries in the measurement.

- Samples were located by the perimeter of their front face against a precision machined surface. They were then clamped between two plates to help ensure they were reproducibly located and perpendicular to the incoming beam I_o.

- The fully automated collection of the data was conducted unattended, without any need to open the measurement chamber. An initial baseline was collected prior to analyzing the 11 samples. Drift correction was not applied.

The quality of the data obtained, and the close agreement between the measured and theoretical results, indicate that the reproducibility and stability of the system is sufficient for fully automated and unattended data collection and that the symmetry of the Cary 7000 UMS was very close to optimal.

21

Table 1. Residual error calculated for the 8 collect conditions for each of the 11 samples in the multi-sample holder.

Residuals	Sample number											Average	StDev.
	1	2	3	4	5	6	7	8	9	10	11		
Ts7	0.01	-0.01	-0.02	-0.01	-0.01	-0.01	-0.02	-0.03	-0.03	-0.05	-0.07	0.02	0.019
Rs7	-0.06	-0.05	-0.06	-0.06	-0.05	-0.06	-0.06	-0.05	-0.05	-0.07	-0.05	0.06	0.005
Tp7	0.00	-0.02	-0.02	-0.01	-0.02	-0.03	-0.04	-0.05	-0.06	-0.08	-0.10	0.04	0.030
Rp7	0.02	0.02	0.02	0.02	0.02	0.02	0.02	0.02	0.02	0.02	0.01	0.02	0.004
Ts45	-0.04	-0.06	-0.07	-0.07	-0.05	-0.07	-0.08	-0.08	-0.09	-0.10	-0.12	0.08	0.024
Rs45	-0.16	-0.16	-0.16	-0.16	-0.16	-0.16	-0.16	-0.16	-0.17	-0.17	-0.17	0.16	0.004
Tp45	-0.04	-0.05	-0.06	-0.05	-0.05	-0.06	-0.07	-0.08	-0.09	-0.11	-0.14	0.07	0.031
Rp45	0.03	0.03	0.03	0.03	0.03	0.03	0.03	0.03	0.03	0.03	0.02	0.03	0.002
Average	0.04	0.05	0.05	0.05	0.05	0.06	0.06	0.06	0.07	0.08	0.09		
StDev.	0.049	0.048	0.048	0.050	0.048	0.047	0.044	0.048	0.047	0.049	0.056		

Conclusion

The Agilent Cary 7000 UMS with Solids Autosampler has been shown to provide automated and unattended routine measurement of the optical properties of multi-samples of uncoated fused silica with good agreement between the measured and theoretical results. The total collect time for the 11 samples was less than 8 hours, acquired in a single unattended run, compared to days needed by non-MPS methodology. The increased productivity offered by the 7000 UMS would lead to a significant reduction in QA/QC cost-per-analysis of industrial optics.

Further, the Solids Autosampler provides a wide range of functionality which enables routine MPS measurements of both the absolute reflectance and transmittance from the same place on the surface of a wide range of specular and/or diffuse samples. The measurement of spectral data across a wide range of AOI provides better characterization of the performance of materials and coatings employed for precision optics. This data can also assist in the validation of optical coating designs by reducing the uncertainties encountered in reverse engineering of coating parameters.

References

1. Death, D.L.; Francis, R.J.; Bricker, C.; Burt, T.; Colley, C. *The UMA: A new tool for Multi-angle Photometric Spectroscopy*. Proceedings of the Optical Interference Coatings (OIC) OSA Topical Meeting, Canada, **2013**.

2. Tikho0nravov, A.V.; Amotchkina, T.V.; Trubetskov, M.K.; Francis, R.J.; Janicki, V.; Sancho-Parramon, J.; Zorc, H.; Pervak, V. Optical characterization and reverse engineering based on multiangle spectroscopy. *Appl. Opt.* **2012**, *51*, 245-254.

3. Amotchkina, T.V.; Trubetskov, M.K.; Tikhonravov, A.V.; Janicki, V. J.; Sancho-Parramon; Razskazovskaya, O; Pervak, V. Oscillations in the spectral behavior of total losses (1 − T − R) in the dielectric films. *Opt. Exp.* **2012,** 20, 16129-16144.

4. Amotchkina, T.V.; Trubetskov, M.K.; Tikhonravov, A.V. Schlichting, S., Ehlers, H., Ristau, D., Death, D., Francis, J.J. and Pervak, V. Quality control of oblique incidence optical coatings based on normal incidence measurement data. *Opt. Exp.* **2013**, 21, 21508-21522 (2013).

More information

A more detailed account of this work was first published in *Opt. Exp.* **2013**, 21, 18, 21508-21522.

www.agilent.com/chem

Agilent

Trusted Answers

Application Note

Glass, ceramics, optics

Agilent

Trusted Answers

Optical Characteristics and Thickness of 2-layered Structures

Refractive index and film thickness measured using a Cary 5000 with UMA accessory

Authors

Kozlova N.S., Kozlova A.P., Zabelina E.V., Goreeva Zh.A., Didenko I.S.[1]

[1]Laboratory "Single crystals and Stock on their Base" NUST "MISiS", Moscow, Russia

Introduction

Multilayer optical coatings are widely used in technologies that exploit the properties of light from the ultra-violet through to the infrared (*1*). Successful optical coating design and manufacturing demands high quality information about the refractive index, absorption coefficients and thickness of layered thin-film structures.

For the successful study of the properties of a thin-film structure use of non-destructive methods are preferred. The fundamental approaches to the characterization of layered thin-film structures differ fundamentally from optical characterization techniques for bulk materials. The optical properties of the films are typically characterized using ellipsometry—an optical technique based on the analysis of the polarization state of light reflected from the specimen. Now there is an alternative multipurpose nondestructive optical technique—multiangle spectrophotometry (*2, 3*).

Spectral and angular functions of reflectance and transmittance for incident polarized light is carried out using a spectrophotometer fitted with an accessory.

Although, optical parameters are very much dependent on

- substrate and film growth conditions
- film homogeneity
- substrate homogeneity and
- optical properties, *(4, 5)*

we expect here to maintain film homogeneity during the structures lifetime.

The aim of this work is to determine the parameters; thickness (d), refractive index (n) and extinction coefficient (k) of the films using the Agilent Cary 5000 spectrophotometer with a unique, and automated, Universal Measurement Accessory (UMA).

Experimental

The Cary 5000 spectrophotometer with UMA allows automated and unattended measurement of:

- absolute reflectance R (at 5−85° incidence) and transmittance T (at 0−85° deg incidence light) with a minimum step interval of 0.02° ;
- T and R measurements at different angles and polarization within one working sequence;
- a 190−2800 nm working wavelength range for unpolarized light;
- a 250−2500 nm wavelength range for *s*- and *p*-polarized light.

Thus, it is possible to obtain a full description of the sample, without moving it. The Cary 5000 with UMA is a universal measurement system that eliminates the need to use multiple consoles, replacement and/or reconfiguration. It provides high quality data, measuring all the characteristics from one area of the sample. A huge advantage of this accessory is the ability to measure the optical characteristics by varying the polarization of the incident light, at different angles of incident light, on the same region of the sample. The UMA scheme consists of a fixed light source, 360° rotatable sample holder and independent detector. The detector can move around the sample in a horizontal plane.

The refractive index and thickness of the films were characterized using double angle light incidence *(6)*. This method is only suitable for the spectral range in which the film is transparent or exhibits negligibly low absorption.

Results and Discussion

Two samples, each with a different substrate type (transparent or opaque in the visible wave range), were characterized :nanocomposite coatings Zr-Si-B-(N) films on

quartz substrates (transparent in the visible range) *(7)* and layered lithium niobate $LiNbO_3$ structure specimens on (001) single crystal silicon substrates (opaque in the visible range) *(8, 9)*.

Both structures were grown using high-frequency magnetron sputtering. The ability of the substrate to transmit light affects the choice of the measured parameter in this method: for transparent substrates we can use transmittance, for opaque substrates we can use reflectance.

To determine the thickness (d) for the first sample transmission spectra were obtained at two arbitrary different unpolarized light incidence angles, in this case, at normal incidence $\varphi_1 = 0°$ and $\varphi_2 = 20°$ (Fig. 1).
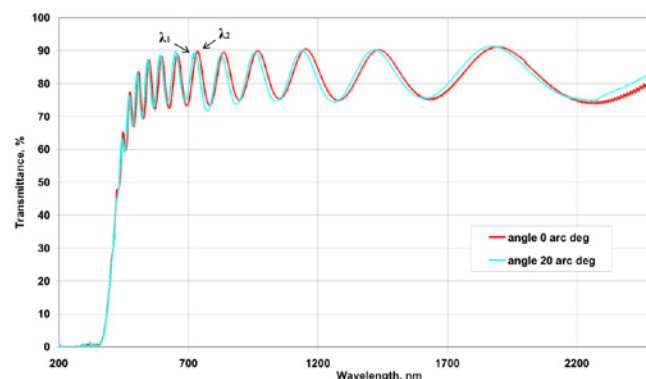
Figure 1. Transmission spectra of nanocomposite coatings Zr-Si-B-(N) films on quartz substrates at normal incidence (λ_2) and 20° (λ_1).

To evaluate the refractive index of the sputtered layer we used the spectral reflection dependences recorded at two different unpolarized light incidence angles, i.e. $\varphi_1 = 6°$ and $\varphi_2 = 20°$ (Fig. 2).
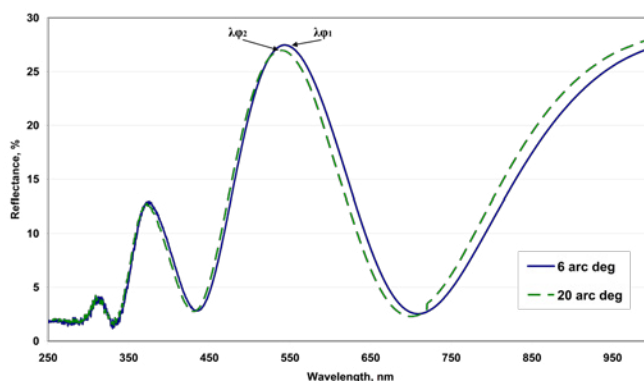

Figure 2. Reflection spectra of $LiNbO_3$ structure specimens on silicon substrates at two incidence angles 6° and 20°.

In the resultant spectra we select the wavelengths λφ1 and λφ2 corresponding to the same interference peak at the φ1 and φ2 incidence angles, respectively, and determine the refractive index of the film using the following formula *(6)*:

$$\left(\frac{n}{n_0}\right)^2 = \frac{\sin^2 \varphi_1 - \beta \sin^2 \varphi_2}{1 - \beta},$$

where n_0 is the refractive index of the medium (here, $n_0=1$ for air) and β is the coefficient determined as follows:

$$\beta = \left(\frac{\lambda_{\varphi 1}}{\lambda_{\varphi 2}}\right)^2,$$

The film refractive indices n calculated using the first equation are summarized below for both samples in Tables 1 and 2, respectively.

The optical thickness of the film *dn* was calculated based on the position of the adjacent interference maxima λ1 and λ2 at the same light incidence angle (the lower one of the two) using the formula *(6)*:

$$d \cdot n = \frac{\lambda_1 \cdot \lambda_2}{4(\lambda_2 - \lambda_1)},$$

The film thickness as determined by dividing the optical thickness of the film *dn* by the refractive index *n* was 250 nm ± 30 nm. Unfortunately, the refractive indices determined using this technique are quite sensitive to the peak wavelength measurement accuracy. Thus, this method is only suitable for the preliminary estimation of refractive indices aimed at selecting the initial approximations.

These films have heterogeneous structure, which was detected by optical microscopy. This heterogeneity is apparent in the value **n** measurement accuracy. The accuracy of determining **n** for the films is not worse than 0,01.

Table 1. Obtained results for Zr-Si-B-(N) films on quartz substrates.

$\lambda_{\varphi 1}$ (20°), nm	$\lambda_{\varphi 2}$ (0°), nm	*n*	*d*, nm
470	474	2.64	
502	507	2.44	
590	596	2.42	
650	657	2.35	
725	733	2.32	1380±5%
824	834	2.22	
883	895	2.20	
955	966	2.17	
1037	1050	2.17	

Table 2. Obtained results for layered LiNbO$_3$ structure on single crystal silicon substrates.

$\lambda_{\varphi 1}$ (6°), nm	$\lambda_{\varphi 2}$ (20°), nm	*n*	*d*, nm
543.62	539.25	2.58	
708.83	700.12	2.09	250±5%

Based on the obtained results, we constructed dispersion curves of the refractive indices for nanocomposite coatings Zr-Si-B-(N) films on quartz substrates, and for LiNbO$_3$ structure specimens on silicon substrates, refer to figure 3 and 4, respectively.
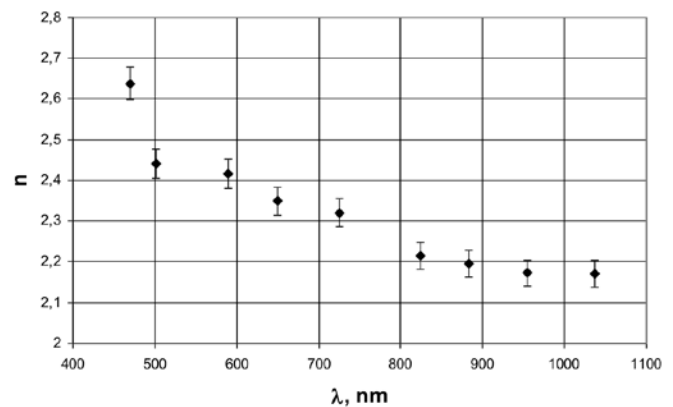

Figure 3. Dispersion curves of nanocomposite coatings Zr-Si-B-(N) films on quartz substrates.
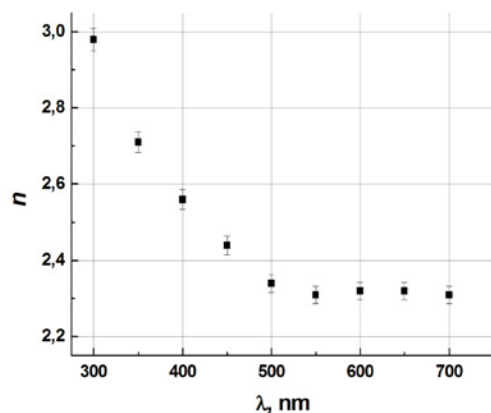
Figure 4. Dispersion curves of LiNbO$_3$ structure specimens on silicon substrates.

Conclusion

The refractive index of two samples was determined, using measurements performed on a Cary 5000 spectrophotometer, fitted with an Universal Measurement Accessory.

One sample consisted of a nanocomposite coating: Zr-Si-B-(N) films on a quartz substrate (transparent in the visible range). The second was a layered lithium niobate LiNbO$_3$ structure on a single crystal silicon substrate (opaque in the visible range).

The refractive index of both was calculated with an accuracy of ± 0.01. Film thickness was calculated from the determined reflective index for both samples.

References

1. D.P. Arndt, R.M.A. Azzam, J. M. Bennett, J. P. Borgogno, C. K. Carniglia, W. E. Case, J. A. Dobrowolski, U. J. Gibson, T. Tuttle Hart, F. C. Ho, V. A. Hodgkin, W. P. Klapp, H. A. Macleod, E. Pelletier, M. K. Purvis, D. M. Quinn, D. H. Strome, R. Swenson, P. A. Temple, and T. F. Thonn Multiple determination of the optical constants of thin-film coating materials, *Appl. Opt.* 23 (20) (**1984**), 3571 − 3596 https://doi.org/10.1364/AO.23.003571

2. A.V. Tikhonravov, M.K. Trubetskov, T.V. Amotchkina, G. DeBell, V. Pervak, A. Krasilnikova Sytchkova, M.L. Grilli, D. Ristau, Optical parameters of oxide films typically used in optical coating production, *Appl. Opt.* 50 (9) (**2011**) C1−C12, http://dx.doi.org/10.1364/AO.50.000C75

3. A.V. Tikhonravov, T.V. Amotchkina, M.K. Trubetskov, R.J. Francis, V. Janicki, J. Sancho-Parramon, H. Zorc, V. Pervak, Optical characterization and reverse engineering based on multiangle spectroscopy, *Appl. Opt.* 51 (2) (**2012**) 245−254, http://dx.doi.org/10.1364/AO.51.000245

4. W.-Ch Shih, Tz-L. Wang, X.-Y. Sun, M.-Sh Wu, Growth of c-axis-oriented LiNbO3 films on ZnO/SiO2/Si substrate by pulsed laser deposition for surface acoustic wave applications, *Jpn. J. Appl. Phys.* 47 (5) (**2008**) 4056−4059, http://dx.doi.org/10. 1143/JJAP.47.4056

5. A.Z. Simoes, A.H.M. Gonzalez, A. Ries, M.A. Zaghete, B.D. Stojanovic, J.A. Varela, Influence of thickness on crystallization and properties of LiNbO3 thin films, *Mater. Charact.* 50 (**2003**) 239−244, http://dx.doi.org/10.1016/S1044-5803(03)00089-5

6. B.M. Ayupov, I.A. Zarubin, V.A. Labusov, V.S. Sulyaeva, V.R. Shayapov, Searching for the starting approximation when solving inverse problems in ellipsometry and spectrophotometry, *J. Opt. Technol.* 78 (6) (**2011**) 350−354, http://dx.doi.org/10. 1364/JOT.78.000350

7. Ф.В. Кирюханцев-Корнеев, А.П. Козлова, Н.С. Козлова, Е.А. Левашов СТРУКТУРА, ФИЗИЧЕСКИЕ И ХИМИЧЕСКИЕ СВОЙСТВА НАНОКОМПОЗИТНЫХ ПОКРЫТИЙ Zr-Si-B-(N) Тезисы доклада Седьмой международной конференции «КРИСТАЛЛОФИЗИКА И ДЕФОРМАЦИОННОЕ ПОВЕДЕНИЕ ПЕРСПЕКТИВНЫХ МАТЕРИАЛОВ», Москва, 2017 г., с.104

8. N.S. Kozlova, V.R. Shayapov, E.V. Zabelina, A.P. Kozlova, R.N. Zhukov, D.A. Kiselev, M.D. Malinkovich, M.I. Voronova Spectrophotometric determination of optical parameters of lithium niobate films, *Modern Electronic Materials* 3 (**2017**), 122−126 http://dx.doi.org/10.1016/j.moem.2017.09.001

9. R.N. Zhukov, S.V. Ksenich, A.S. Bykov, D.A. Kiselev, M.D. Malinkovich, Yu.N. Parkhomenko, Synthesis and properties of the LiNbO$_3$ thin films intended for nanogradient structures, *PIERS Proc.* (**2013**) 98−101, http://dx.doi.org/10.1143/ JJAP.47.4056

www.agilent.com/chem

Agilent
Trusted Answers

Agilent

Trusted Answers

Optical Characterization of Thin Films

Using a Universal Measurement Accessory for
Agilent Cary UV-Vis-NIR spectrophotometers
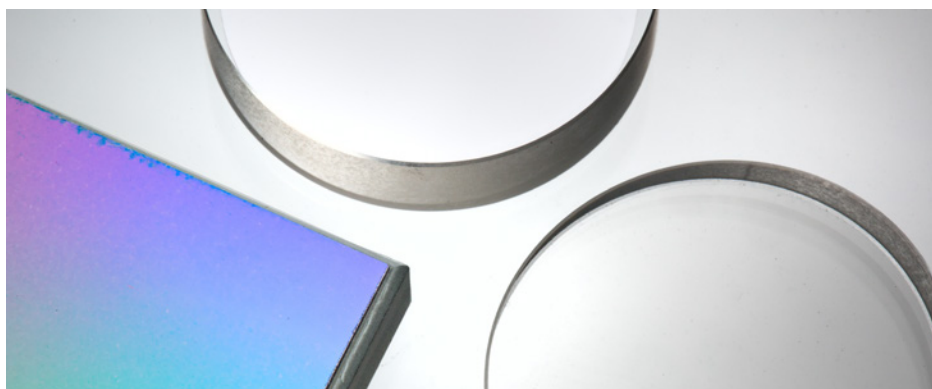
Authors

Robert Francis and Travis Burt
Agilent Technologies, Inc.
Mulgrave, Victoria
Australia

Introduction

A more detailed account of this work was first published in Applied Optics,
10 January 2012/Vol. 51, No. 2.[1]

The accurate determination of the optical parameters of thin films and multilayer coatings (using reverse-engineering of optical coatings) is paramount to the manufacturing of high-quality products. The data provide feedback to the design/production chain. Reverse-engineering results — where each layer is assessed in turn — can be used to adjust deposition parameters, recalibrate monitoring systems, and improve control of the thickness of individual layers.

Typically, optical characterization is based on the analysis of normal- or near-normal-incidence transmittance (T) or reflectance (R) data of a thin film sample on a transparent substrate using UV-visible-near-IR (UV-Vis-NIR) or Fourier transform IR (FTIR) spectrophotometry. However, optical characterization based on normal incidence T and R measurements and reliable reverse-engineering based on normal-incidence or near-normal-incidence T and R measurement data is challenging.

This application note demonstrates the applicability of multi-angle spectral photometric data to the optical characterization of single thin films and the reverse-engineering of multilayer optical coatings using an Agilent Cary 5000 UV-Vis-NIR spectrophotometer equipped with a universal measurement accessory (UMA). The study considers dense thin films and a multilayer produced by magnetron sputtering, as well as electron-beam (e-beam) evaporated thin films, which are typically more difficult to characterize. These data could also be collected on an Agilent Cary 7000 universal measurement spectrophotometer (UMS).

Experimental

Samples

This study measured two sets of experimental samples using two different deposition techniques: magnetron sputtering and e-beam evaporation. Details can be found in reference 1.

Instrumentation

– Agilent Cary 5000 UV-Vis-NIR spectrophotometer

– Agilent universal measurement accessory

The UMA is a highly automated variable-angle specular reflectance and transmittance system with full software control of the sample, detector, and polarizer positions. It provides accurate, rapid, and complete optical characterization of samples via transmission (%T) and absolute reflection (%R) measurements at various controllable angles of incident light (0 to 85 deg %T, and 5 to 85 deg %R). The linearly polarized beam that illuminates the sample can be measured in transmission. It can be measured in absolute reflectance by moving the detector assembly in a plane at a constant radius from the sample. This multiple measurement mode capability of the UMA results in improved productivity and more precise characterization of samples. A schematic of the UMA is presented in Figure 1.
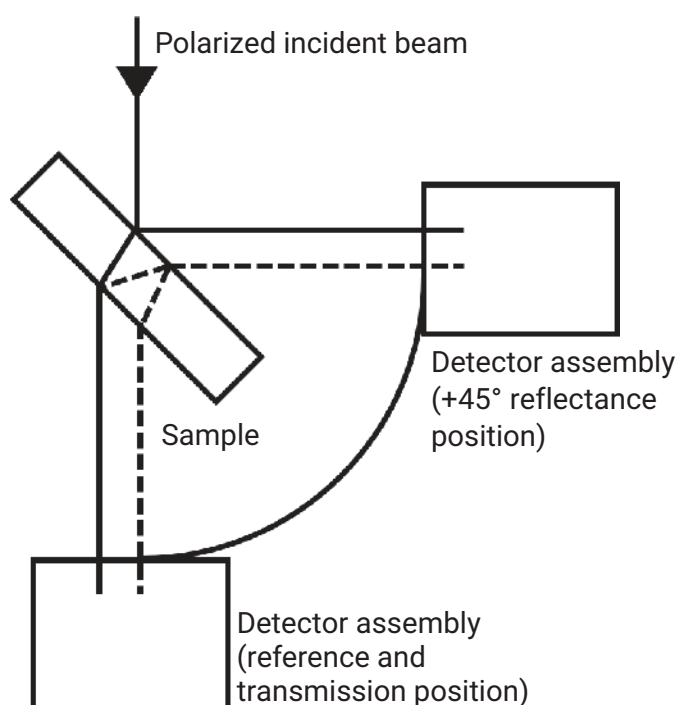
Figure 1. Schematic of the Agilent UMA, an absolute variable-angle reflectance and transmission accessory.

Results and discussion

Multi-angle spectral photometric measurements were performed for all samples in the spectral range from 300 to 2,500 nm at incidence angles of 7°, 10°, 20°, 30°, and 40° for s- and p-polarized light. In all optical characterization and reverse-engineering procedures throughout this study, only measurement data taken in the spectral range from 330 to 1,100 nm were used. Substrate internal absorption is significant above 1,100 nm wavelength, making estimation of accuracy uncertain.

Dense dielectric thin films

The UMA was used to acquire multi-angle spectral photometric data for the optical characterization of Ta_2O_5 and SiO_2 thin films produced by magnetron sputtering. Table 1 presents the numerical results of optical characterization: measured film thicknesses and refractive index values at λ = 600 nm. There is excellent consistency of the results obtained using T and R data measured at different incidence angles and with different polarization states. For both materials, deviations of thickness and refractive index values (n) from mean values in all columns of Table 1 are lower than 0.1%.

Table 1. Parameters of Ta_2O_5 and SiO_2 films found by using oblique-incidence T and R data acquired using the Agilent UMA.

Polarization State/Angle of Incidence	Ta_2O_5		SiO_2	
	Physical Thickness (nm)	n at 600 nm	Physical Thickness (nm)	n at 600 nm
s, 7°	292.3	2.162	401.4	1.486
s, 10°	292.5	2.160	401.7	1.485
s, 20°	292.4	2.161	401.5	1.484
s, 30°	292.4	2.161	401.9	1.484
s, 40°	292.4	2.161	401.6	1.483
p, 7°	292.7	2.159	401.9	1.484
p, 10°	292.5	2.160	401.4	1.485
p, 20°	292.5	2.160	401.5	1.484
p, 30°	292.5	2.160	401.9	1.486
p, 40°	292.4	2.161	401.7	1.483

Reliability of reverse-engineering based on multi-angle spectroscopy

To check the reliability of reverse-engineering based on multi-angle optical photometric data, a specially prepared 15-layer quarter-wave mirror with Ta_2O_5 and SiO_2 was analyzed as high and low index materials. The mirror was produced by magnetron sputtering by using time monitoring of layer thicknesses. During the deposition of this mirror, intentional errors of +5%, 7%, −5%, and +5% were imposed on the third, eighth, 14th, and 15th mirror layers, respectively. Various combinations of input measurement data were acquired using the UMA and the intentional thickness errors were reliably detected in all cases.[1] A typical example of the consistency of obtained results is presented in Figure 2.

Application of multi-angle spectroscopy to optical characterization of inhomogeneous e-beam evaporated thin films

Multi-angle spectral photometric measurement was also applied to the determination of optical parameters of e-beam-evaporated HfO_2 and SiO_2 films of various thicknesses. This was achieved by reverse-engineering of a specially prepared multilayer mirror. It was found that the optical properties of the e-beam evaporated HfO_2 films are dependent on film thickness. Results of all reverse-engineering attempts were consistent. The offsets of SiO_2 refractive indices determined in the course of reverse-engineering were in the range from 1.5% to 1.7% with respect to the nominal refractive index of SiO_2 found from characterization of the single SiO_2 layer. A good agreement in refractive indices of HfO_2 layers was also observed.
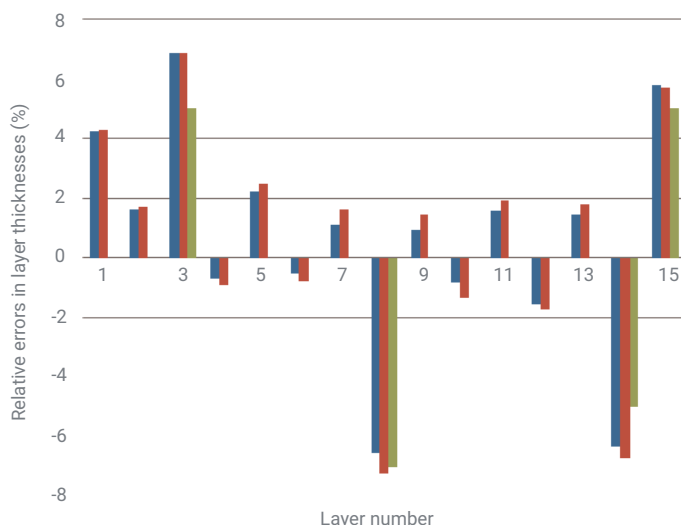
Figure 2. Comparison of errors in layer thicknesses of 15-layer quarter-wave mirror found on the basis of reflectance and transmittance data taken at 7°, 10°, 20°, 30°, and 40°, for the s-polarization case (blue bars) and the p-polarization case (red bars). Green bars show planned errors in the thicknesses of the third, eighth, 14th, and 15th layers.

The variations of HfO_2 refractive index values, determined from separate oblique incidence T and R measurements, did not exceed 0.5%. It can be seen in Figure 3 that the measured refractive index wavelength dependence of HfO_2 film is in agreement with reference wavelength dependencies from a previous study.[2] This agreement confirms the previous conclusion that the crystalline state of HfO_2 depends on film thickness.[3,4] As shown in these references, thin films are basically amorphous, while thicker films are partially crystalline, and the larger the crystalline fraction, the thicker the film. This can explain the difference in refractive indices of the HfO_2 films used in this study that were 197 nm thick in the case of a single layer, and approximately 50 nm thick in the case of a multilayer structure.

Figure 3. Nominal refractive index wavelength dependence of e-beam evaporated HfO$_2$ film (solid black curve), and reference refractive index wavelength dependencies of HfO$_2$ films produced by radio frequency sputtering (gray curve) and ion-beam sputtering (dashe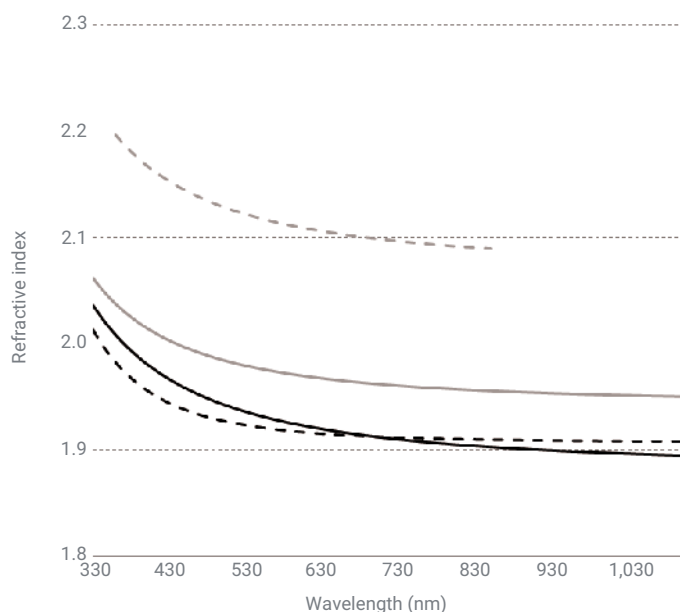d gray curve). The dashed black curve shows the refractive index of thin HfO$_2$ film found from measurement data related to a 12-layer quarter-wave mirror.

Conclusion

The applicability of multi-angle spectroscopy to the optical characterization of thin films and reverse-engineering of multilayer coatings was studied. The Agilent UMA, an advanced spectrophotometric accessory (fitted to an Agilent Cary 5000 UV-Vis-NIR spectrophotometer), supplied reflectance and transmittance data for multiple angle and s- and p-polarization states. The accuracy of measurement data was verified and it was confirmed that all measurement data were excellent over a wide spectral range from the UV to the NIR up to incidence angles of 40°.

Multi-angle spectral photometry provides researchers with more experimental information than conventional spectroscopy. This study demonstrates that the UMA spectrophotometer accessory provides experimental information that permits the solving of various optical coating characterization and reverse-engineering problems.

Comparative analysis of various combinations of input multi-angle spectroscopic data provides self-verification of the results obtained. Multi-angle spectral photometry is the perfect tool for the analysis of optical coatings under oblique light incidence or at diverged light illumination.

References

1. Tikhonravov, A. *et al.* Optical Characterization and Reverse-engineering Based on Multiangle Spectroscopy. *Appl. Opt.* **2012**, *51(2)*, 245−254.

2. Tikhonravov, A. *et al.* Optical Parameters of Oxide Films Typically Used in Optical Coating Production. *Appl. Opt.* **2011**, *50*, C75−C85.

3. Modreanu, M. *et al.* Solid Phase Crystallisation of HfO$_2$ Thin Films. *Mater. Sci. Eng. B* **2005**, *118*, 127−131.

4. Modreanu, M. *et al.* Investigation of Thermal Annealing Effects on Microstructural and Optical Properties of HfO$_2$ Thin Films. *Appl. Surface Sci.* **2006**, *253*, 328−334.

www.agilent.com/chem/cary5000

Agilent
Trusted Answers

Application Note

Glass, ceramics, optics

Agilent

Trusted Answers

Spectrophotometric Methods of Refractive Indices Measurement

Measuring the refractive index of single crystal optical materials using two methods

Authors

N.S. Kozlova[1], A.P. Kozlova[1], E.V. Zabelina[1], Zh.A. Goreeva[1], I.S. Didenko[1], T. Burt[2]

[1]Laboratory "Single crystals and Stock on their Base" NUST "MISiS", Russia

[2]Agilent Technologies, Australia.

Introduction

The production of advanced materials requires fast, accurate, and minimal labor-intensive determinations of material parameters. One of the main parameters required for the application of optical materials, in particular crystals, is refractive index (n).

There are three common methodologies for determining refractive index (*1-3*):

1) Goniometric method
A goniometer-spectrometer is used to measure transmission at angle, including the angles of minimum deviation of light and n is calculated from Snell's law.

This method demands a transparent sample in form of a large prism with precise angles between bottom plane and polished working planes.

2) Ellipsometric method
An ellipsometer is used to directly measure amplitude ratios and phase shifts of reflected light.

This method requires a specific optical model for each material. Standard optical models are included in commercial software packages but an optical model may not be included if you have an unknown or new materials.

3) Spectrophotometric methods

A spectrophotometer, with a sampling accessory, can be used to rotate the sample and the detector to angles that allow absolute specular reflectance data to be collected (or angular transmission data).

Spectrophotometric methods can be further broken down into 3 mostly commonly used methodologies:

3.1) The Fresnel formulas

Measurements of reflectance and transmittance of incident light, of p- and s- polarization, are made and **n** is calculated from the Fresnel equations. This method requires not only large polished sample surfaces but also software support to solve the Fresnel equations.

3.2) Brewster's law method

Measurement of reflectance for incident light of p- polarization at the Brewster angle (according Brewster's law). It is necessary to use samples with large surface area to achieve high accuracy measurements for the large angles.

3.3) Method of reflection at near-normal incidence

This method is based on measurement of the reflection spectrum from one surface at low angle of incidence close to the near normal angle (0 deg to approx. 10 deg). This method permits one to determine the dispersion component of the refractive index from a single polished plane of the sample in a single measurement.

Methods **3.2** and **3.3** do not require significant mathematical post data processing and can be introduced to any laboratory equipped with a Cary UV-Vis-NIR spectrophotometer and the Universal Measurement Accessory (UMA), Figure 1.

Figure 1. Cary-5000 with UMA accessory.

The Cary 5000 with the UMA eliminates the need to use multiple consoles, sample replacement and accessory reconfiguration.

Thus, it is possible to obtain a full description of the sample, without moving it.

The UMA scheme consists of a fixed light source, 360° rotatable sample holder and an independent detector that can move around sample holder in a horizontal plane in the range of angles from 10 to 350°.

The UMA provides high quality data, measuring all the characteristics from a single consistent area of the sample. An advantage of this accessory is the ability to measure the optical characteristics (absolute reflectance and transmittance) under varying incident light polarization and at different angles of incident light in the same area of the sample within one working sequence according to the scheme presented in Fig. 2.
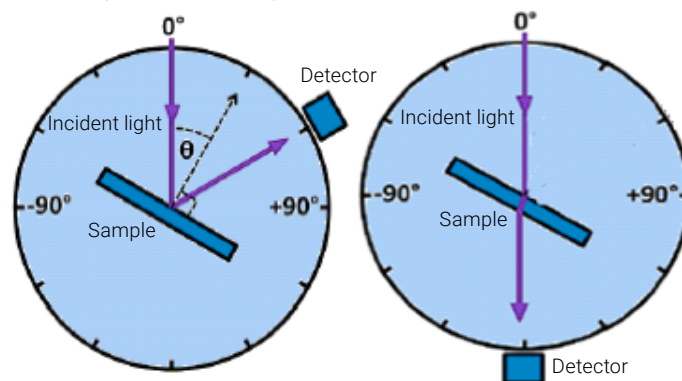
Figure 2. Scheme of measurement of reflectance (left) and transmittance (right).

The Cary 5000 with the UMA is a suitable and unique solution if you need to measure the refractive indices of samples and materials including difficult shaped samples, or when it is impossible to produce a sample in the form of a prism.

This study presents the results of the measurements of the refractive indices for new crystals $Gd_3Al_2Ga_3O_{12}$:Ce (GGAG) (4) using the Cary 5000 with the UMA by two spectrophotometric methods:

1. by Brewster's law (Method 3.2);

2. by the spectrum of reflection from one surface at low angle of incidence close to normal (Method 3.3).

Experimental

GGAG belongs to the cubic crystal system and, therefore, is characterized by a single refractive index *n*. We obtained the spectral and angular dependence of reflection coefficients of *p*- and *s*-polarized light in the range of angles (6 − 71°). For example, Figure 3 presents the angular dependence of reflection coefficients of *p*- and *s*-polarized light, *Rp* and *Rs*, respectively, for λ = 589 nm. The results have been published previously (*4*).
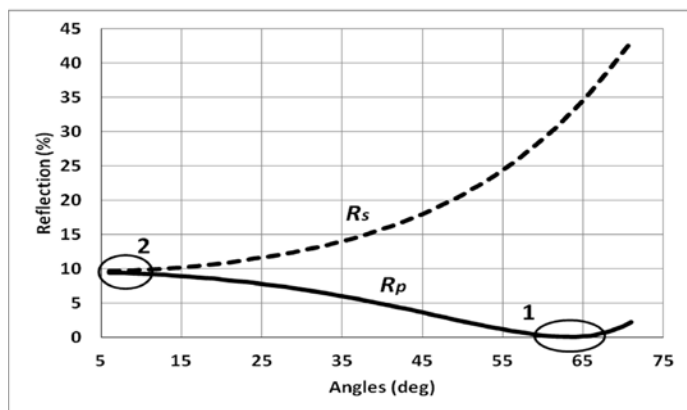

Figure 3. Angular dependence of the reflection of *p*- and *s*-polarized light at λ = 589 nm (*4*): 1 − the Brewster angle area, 2 − the area for the method of reflection from one surface at normal incidence of light.

Results and Discussion

Determination of refractive index according to Brewster's law (Method 3.2).

According to Brewster's law (*2*), if the incident light is polarized in the plane of incidence (*p*− polarization), at some angle of incidence reflectivity is close to zero $R \sim 0$. This angle is called the Brewster's angle θ and is associated with the refractive index *n* of the material through equation 1 (*2*):

$$\Theta_B = \arctan{(n/n_0)}$$

where n_0 is refractive index air (n_0=1).

To determine the values of the refractive index, we measured the spectral dependencies of the reflection coefficient at different angles of incidence of *p*- polarized light. Figure 3 presents the scheme of determination of the Brewster angle, for example, of the angular dependence of the reflection coefficient *p*-polarized light at the wavelength of 589 nm, where the angle of incidence was varied from 60° to 65°

in 1° increments (area 1). As a result, it was found that the Brewster angle is around 60°. For accurate determination of the minimum angle (the Brewster angle) we used the method of iterations by changing the pitch angle of the incident light from 1° to 0.04° steps. Then using equation (1) we determined *n*.

The same procedure can be applied to other wavelengths. In our case we measured the angular dependence of the *p*-polarized light reflection coefficient at: 400 nm, 425 nm, 589 nm, 650 nm, 700 nm, and 800 nm. For approximation of the refractive index experimental values we calculated the coefficients of the Cauchy equation (2) to obtain the dispersion dependences of refractive index (Figure 4).

$$n = A + \frac{B}{\lambda^2} + \frac{C}{\lambda^4} + \ldots$$
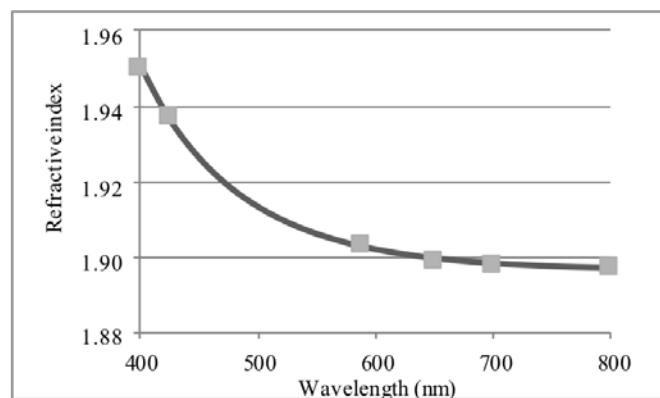
Figure 4. $Gd_3Al_2Ga_3O_{12}$:Ce refractive indices (*4*). Dotes − measured values, line − the Cauchy dispersion.

Hence, to determine the refractive index, the sequence of actions is as follows:

1) to measure the spectral dependence of the reflectance depending on the angle of incidence of *p*−polarized light beam for wavelength you need (Figure 3);

2) to find the area of angles corresponding the area of minimum value of reflectance;

3) using the method of iterations by changing the pitch angle of the incident light of 1° to 0.04° to measure the angular spectral dependence of the reflectance depending on the determined in step 2 area of angles of incidence of *p*−polarized light beam for wavelength you need;

4) to determine the Brewster angle: it's the angle when the reflectance value is minimum;

5) using equation (1) to obtain the refractive index for this wavelength;

6) repeat steps 1 to 5 for another wavelengths;

7) approximate the refractive indices if necessary.

Determination of refractive index using the spectrum of reflection from one surface at low angle of incidence close to normal (Method 3.3).

The scheme for determination of the refractive index according to this method corresponds to the area 2 in Figure 3. According to Figure 3 at low angle of incidence close to normal (**up to 10°**) intensities of reflection of p- and s- polarized light become close.

In this case, the reflection coefficient of light from one surface can be represented as (2):

$$R = \frac{(n-1)^2 + \kappa^2}{(n+1)^2 + \kappa^2}$$

where k (λ) is the extinction coefficient.

According to the formula (3) in order to estimate the refractive index it is necessary to know not only the value of the reflection coefficient R but also the values of the extinction coefficient k. However, for single crystal $Gd_3Al_2Ga_3O_{12}$:Ce the values of the extinction coefficient k is negligibly small even in the absorption bands.

We can transform the formula (3) excluding the extinction coefficient k, and measure the reflection coefficient R at an angle of incidence close to the normal in the wavelength range of (200 – 720) nm with a step of 1 nm. This way we can calculate the refractive indices n and construct dispersion curves (Fig. 5) according to the foregoing formula:

$$n = \frac{1 + \sqrt{R}}{1 - \sqrt{R}}$$
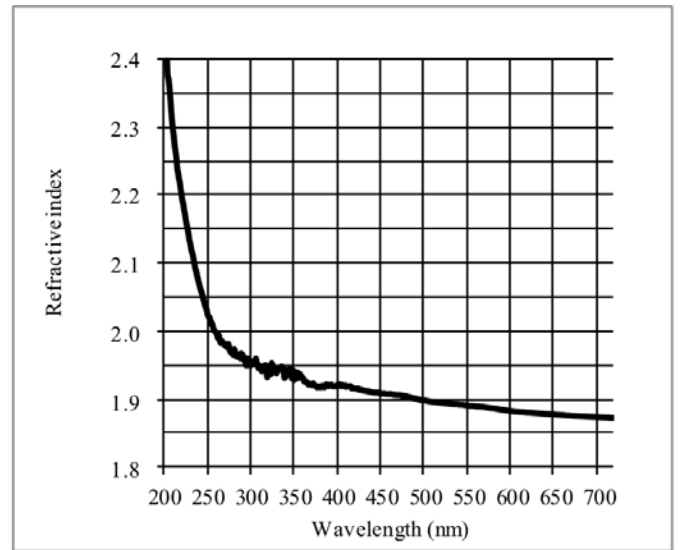
Figure 5. $Gd_3Al_2Ga_3O_{12}$:Ce refractive index dispersion obtained by reflection from one surface (4).

To avoid the reflection from the second face (the inner surface of the sample) it is better to use sample with a grinding finish surface on the opposite side or a sample with non-planar faces.

Values of n for GGAG obtained by these two methods are close. So both methods may be introduced in the practice of laboratories. Choice depends on the form of the sample.

To establish the confidence interval of this method we carried out metrological measurements on a reference sample of

fused quartz. We measured the reflection coefficients at the angle of light incidence close to normal, and then calculated the metrological characteristics of the method. For the reference sample, the accuracy was ± 0.4 %. This value falls in the confidence interval of the method.

Conclusion

1. A study of the use fo the Cary 5000 spectrophotometer with Universal Measurement Accessory was conducted to refractive indices of different type of materials, especially single crystal optical materials, by two spectrophotometric methods

    - Brewster's law method;

    - reflection from one surface at low angles of incidence close to normal.

2. Refractive indices obtained by the two methods were close enough. A laboratory equipped with the Cary 5000 and UMA may choose any method. The best choice depends on the form of the sample.

3. The accuracy of the spectrophotometry method is less than 0.4 %.

References

1. C.F. Bohren, D.R. Huffman Absorption and Scattering of Light by Small Particles. Wiley Professional Paperback Edition Published, **1998**, 545 p.

2. S.I. Borisenko "Refraction Index and methods for its experimental determination", Tomsk: Tomsk Polytechnic University, **2014**.

3. Kozlova N.S., Kozlova A.P., Goreeva Zh.A. "Spectrophotometric Methods and their Capabilities to Study Material Optical Parameters", Proceedings of the 2nd International Ural Conference on Measurements (UralCon) **2017**, p. 281-288

4. N.S. Kozlova, O.A. Busanov, E.V. Zabelina, A.P. Kozlova, V.M. Kasimova "Optical properties and refractive indices of $Gd_3Al_2Ga_3O_{12}$:Ce^{3+} crystals", Crystallography Reports, v. 61, No. 3, pp. 474-478, **2016**.

www.agilent.com/chem

Agilent

Trusted Answers

Optoelectronics

The field of optoelectronics concerns the intersection of optics and electronics. More specifically, optoelectronics often involves subsystems that convert light into electricity or electricity into light. Examples include photodiodes (photovoltaic cells or light emitting diodes, LEDs), imaging devices (cameras), and optical fiber communications. Optoelectronics commonly make use of UV, visible, or NIR wavelengths where attenuation losses can be most conveniently minimized. These inherent properties make UV-Vis-NIR spectrophotometers ideal for characterizing the basic materials used to make optoelectronics (e.g., the bandgap of diodes). The technique is also useful for the characterization of intermediary optical components (e.g., optical coatings, cube beam splitters, bi-refringent crystals) that are used to split, direct, or focus light at a specific wavelength or in select polarization states.

Agilent

Trusted Answers

A Faster, More Accurate Way of Characterizing Cube Beamsplitters

Using the Agilent Cary 7000 universal measurement spectrophotometer (UMS)
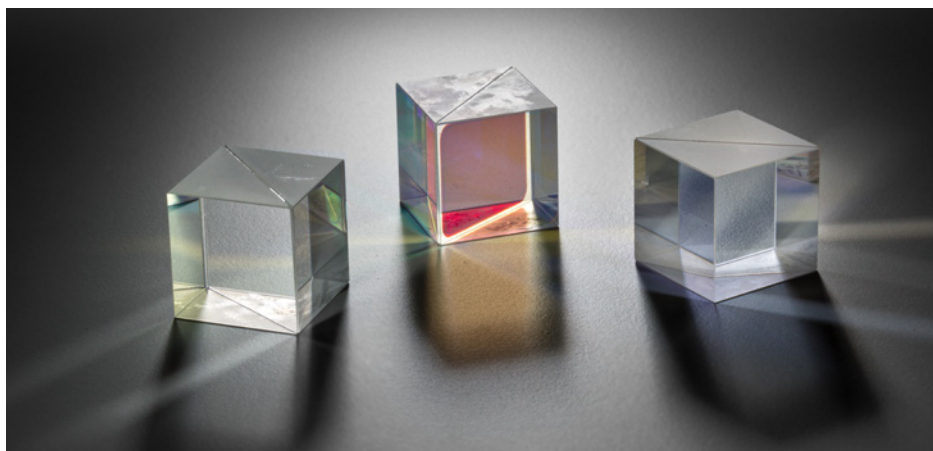
Authors

Travis Burt and Chris Colley
Agilent Technologies
Mulgrave, Victoria, Australia

Hakchu Lee
Agilent Technologies, Inc.
Santa Clara, California, USA

Abstract

Cube beamsplitters (CBS) are critical optical components that have a wide variety of uses in consumer products, high-tech micropositioning equipment, and fiber-optic-based telecommunication systems. This application note describes *in situ*, automated and unattended, transmission, reflection, and absorptance measurements of CBS using an Agilent Cary 7000 universal measurement spectrophotometer (UMS). Spectral information obtained is shown to provide useful insight for optical engineers at the design phase, and provide QA/QC departments better control metrics during final testing; all are obtained at highly productive rates amenable to routine volume analysis demands.

Introduction

Typically, not much larger than a die (0.5 to 1 in, 12.7 to 25.4 mm), the purpose of a CBS, as the name suggests, is to split a beam of light into two distinct paths — a reflected beam and a transmitted beam (Figure 1).
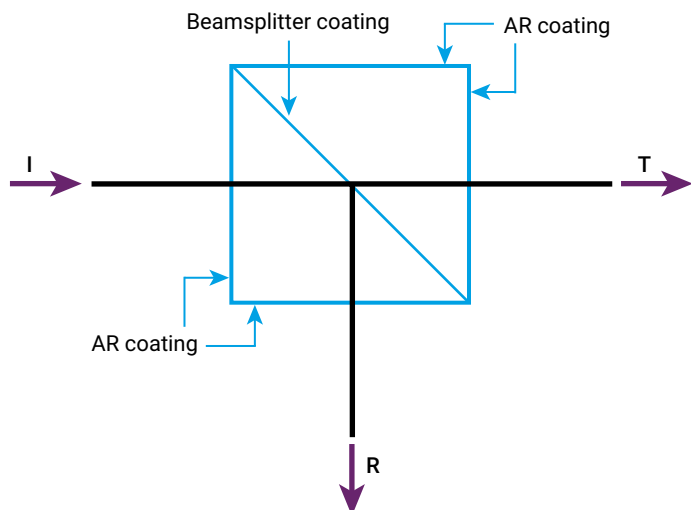

Figure 1. Plan view of a CBS showing reflection (R) and transmission (T) of the incident light (I).

The separated beam can be used to duplicate images, separate colors or polarization states, or in the case of laser applications, create compact interferometers for nano-positioning systems. In all cases, successful CBS design, implementation, and quality control rely on detailed spectral knowledge of both the transmitted and reflected beams. Dielectric (optical) coatings deposited on the central hypotenuse, and sometimes also the outside faces, determine the wavelength and polarization characteristics of the CBS. One of the measurement challenges is that the optical behavior of the internal multilayer coating is influenced by its immediate optomechanical environment, e.g., the refractive indices of the bonding agent used to combine the two halves. *In situ* measurement of the dielectric coating is imperative as an open-air characterization, performed before cementing the two prism halves together, renders different results to the completed cube assembly.

The Cary 7000 UMS permits spectral characterization of the transmitted and reflected beam on the same system without moving the sample, and hence the incident beam. The *in situ* measurement of transmission (T) and reflection (R) from identical locations on the sample permit accurate Absorptance (A = 1 − T − R) data to be calculated, providing greater insight into substrate and coating properties.

When analyzing total losses in spectra, researchers have previously reported artifacts which may cause doubt about the quality of the data. Sources of artifact have been reported[1] to include:

- The difference in angles of incidence (AOI) at which T and R are measured
- A slight thickness nonuniformity of the film
- Absorption in a thin film acting in combination with interference effects

In this application note, data collected using the Cary 7000 UMS are presented. Both T and R have been measured without moving the sample, thereby eliminating the source of AOI variations and coating thickness nonuniformities.

Beamsplitter types

Cube beamsplitters can be categorized broadly according to the optical requirements of their end use. A basic overview will be given here to highlight the optical performance drivers behind each type.

The wavelength range covered can be broadband, covering the entire visible spectrum for example, or narrow band, accommodating a specific laser line, such as from a 632.8 HeNe laser. The wavelength range is controlled by the beamsplitter coating but the substrate material must also transmit the required wavelength range. BK7 glass is a low-cost material useful for the visible spectrum but has strong attenuation in the UV and NIR wavelengths. Fused silica has a high cost but lower optical losses and broader wavelength range, making it the preferred choice for high-power laser applications.

The bonding method used to join the two halves can be an important consideration in their end use. Optical cement produces a highly stable (mechanical) CBS but this construction is more suited to lower optical power applications. Norland Optical Adhesive 61 (NOA 61) is an example of an optical cement. It is a clear, colorless, liquid photopolymer that cures when exposed to ultraviolet light. Higher-power laser applications, on the other hand, must avoid the use of cement and turn to optical contact methods or refractive index-matched oils instead. These have higher power thresholds but must be handled and used appropriately as they are less mechanically stable.

The polarization properties of a CBS are commonly used for laser-based interferometry devices. For example, the performance of interferometric nanopositioning systems is partially determined by the requirement for a CBS with a high T_p/T_s ratio and a correspondingly high R_s/R_p ratio. The CBS

measured in this application note is an example of such a polarizing beamsplitter and behaves as shown schematically in Figure 2.
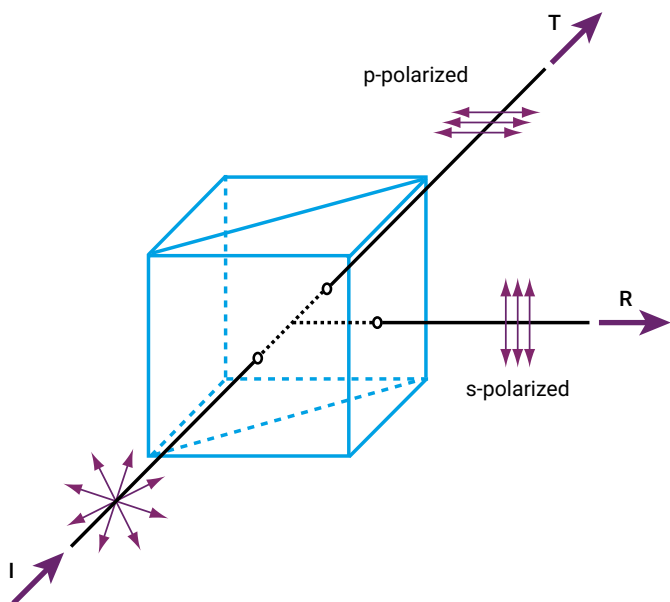

Figure 2. 3D schematic of the reflection and transmission of light incident on a polarizing CBS.

Experimental

Sample

The CBS was 25 mm cubed with a proprietary beamsplitter and antireflection coating made from titanium dioxide and silicon dioxide. The two prisms are bonded with optical adhesive.

Instrumentation

The data were collected using the Cary 7000 UMS, which is a highly automated variable-angle absolute specular reflectance and transmittance system. With the Cary 7000 UMS, operators have independent motorized control over the angle of incidence onto the sample and the position of the detector, which can be freely rotated in an arc around the sample. The independent control of sample rotation and detector position allow rapid, accurate, and unattended measurements of CBS.

Traditionally, reflectance and transmittance measurements have been performed using spectrophotometers fitted with different accessory attachments. In practice, this can lead to different areas of the sample being tested due to illumination beam patch size variations between measurement modes (accessories) and movement of the illumination beam over the sample.

If the deposition process produces a film with a nonuniform thickness, it is reasonable to expect that reflectance and transmittance measurements would be affected.

With the development of the Cary 7000 UMS, it is now possible to measure T and R at the same sample point without moving the sample, overcoming one source of artifacts on the results. In addition, the sample can automatically be rotated 180° to permit static T and R measurements in the forward or reverse direction. In either case, T and R are measured from the same point without moving the sample.

In this study, the Cary 7000 UMS was used to acquire transmittance data for s-polarized and p-polarized incident light at 0° AOI. Reflectance data were collected at 90° to the incoming beam and transmittance data at 0° (directly) as shown in Figure 3. The sample is mounted such that the center of the cube is at the focal point of the incident beam and on the axis of rotation of both the sample and detector. The cone angle of light incident on the sample was limited by 2° vertical and horizontal apertures.
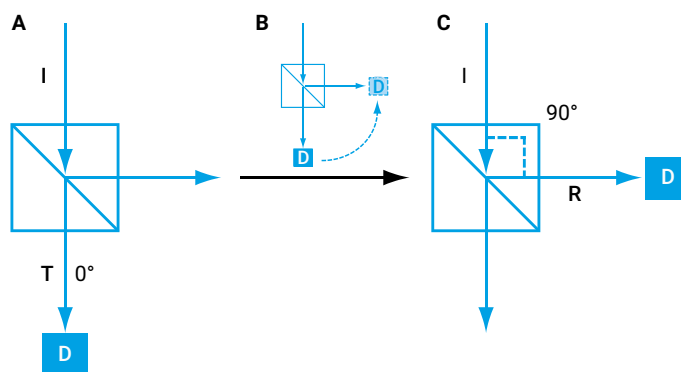
Figure 3. (A) CBS sample and detector (D) orientation for transmission measurement. (B) The detector is rotated around the sample in the plane of incidence so that for reflection measurements (C), the detector is at 90° to the incident beam and sample. **Note:** The sample does not move.

Spectra were measured over 500 to 720 nm with a data interval of 1 nm, a spectral bandwidth of 5 nm, and a 0.5-second spectral averaging time.

Results and discussion

The CBS is designed for use with a helium neon laser, which emits at 632.8 nm. At that wavelength the CBS would ideally transmit 100% p-polarized light and reflect 100% s-polarized light. In reality, the desired transmittance and reflectance of polarized light will not be perfect so it is important to be able to measure the true performance of the CBS.

Figure 4A shows s-polarization transmittance and reflectance spectra measured using the Cary 7000 UMS system. By zooming in on each of the spectra around 633 nm (see Figures 4B and 4C), the transmission and reflection values at 633 nm can be seen. The transmission of s-polarized light at 633 nm is 0.04% T, which is within the specification for the CBS of <0.2% T. The p-polarized spectra are shown in Figure 5. The transmission of p-polarized light at 633 nm is 98.19 %T, which is within the specification of >98% T.

B

633 nm, 98.19 %T

B

633 nm, 99.34 %R

A

T_P 0°

R_P 90°

A

R_S 90°

T_S 0°

C

633 nm, 0.11 %R

Figure 5. (A) Transmission and reflection spectra for p-polarized light measured on a CBS sample in an Agilent Cary 7000 UMS. (B) Transmission spectrum zoomed in around 633 nm. (C) Reflection spectrum zoomed in around 633 nm.
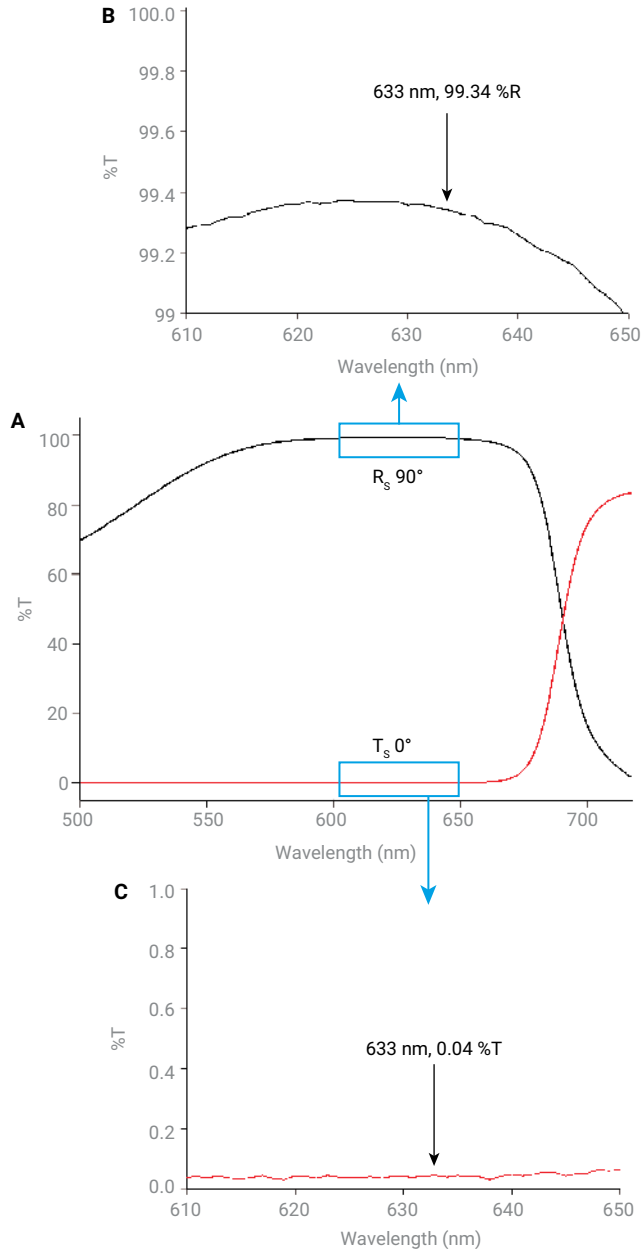

C

633 nm, 0.04 %T

Figure 4. (A) Transmission and reflection spectra for s-polarized light measured on a CBS sample in an Agilent Cary 7000 UMS. (B) Reflection spectrum zoomed in around 633 nm. (C) Transmission spectrum zoomed in around 633 nm.
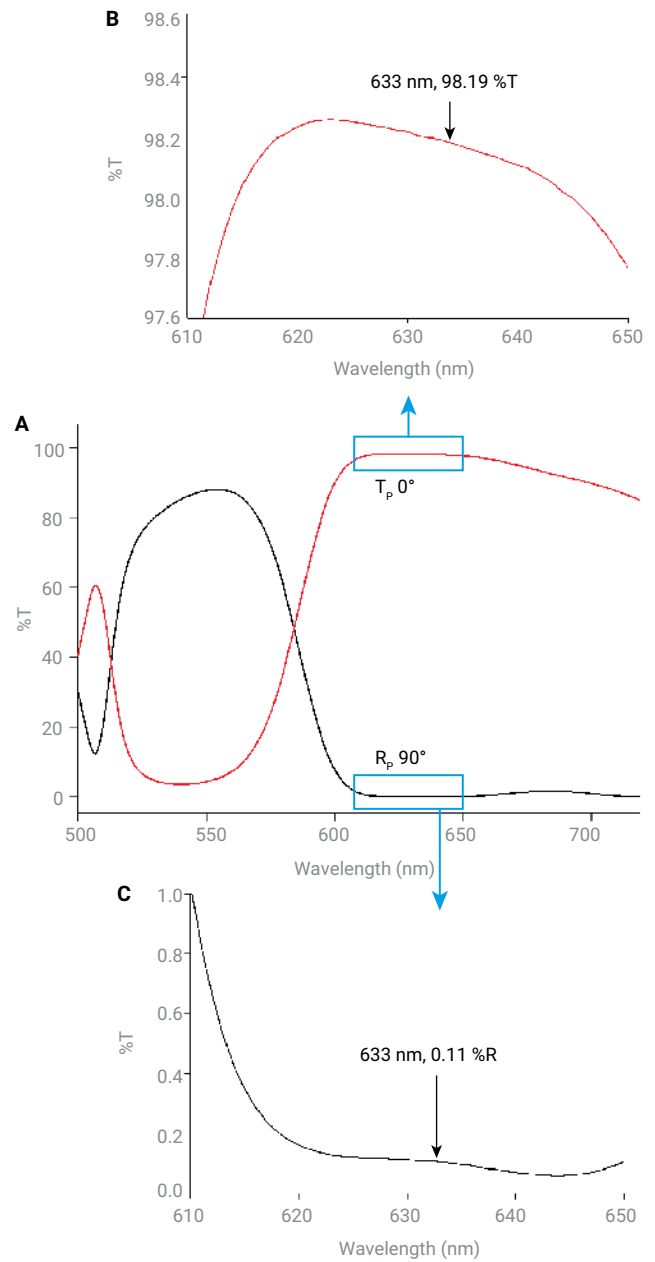
Since transmission and reflection have been measured without moving the sample, self-consistent spectral data have been collected, which are useful for determining total losses (e.g., retroreflection, internal absorption, or scattering). Absorptance (A) where A = 1 − T − R, for s- and p-polarized light are shown in Figure 6, which displays the spectral profile of light associated with these losses.
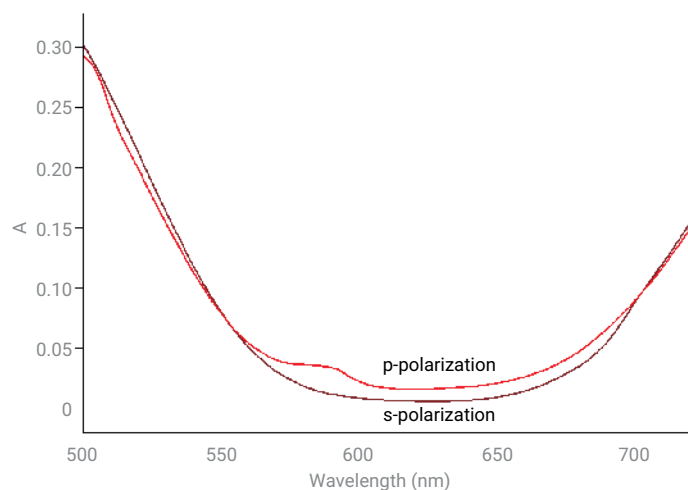
Figure 6. Absorptance spectra for s- and p-polarization

Conclusion

The Agilent Cary 7000 UMS has been shown to be a valuable tool for the characterization of cube beamsplitters. The system allows independent and automated control of the sample rotation and the detector position. The unique ability to measure T and R components without having to move the sample, keeping the incident light on the sample unchanged, has also provided detailed spectral information on the absorptance of the beamsplitter.

The Cary 7000 UMS is ideal for QA/QC environments because it offers convenience, ease-of-use, and completely unattended data collection.

Reference

1. Amotchkina, T. V. *et al.* Oscillations in Spectral Behavior of Total Losses (1 − R − T) in Thin Dielectric Films. *Optics Express* **2012**, *20(14)*, 16129−16144.

www.agilent.com/chem/cary7000ums

Agilent

Trusted Answers

Application Note

Glass, Ceramics and Optics

Agilent

Trusted Answers

Investigation of Dichroism by Spectrophotometric Methods

Authors

N.S. Kozlova, E.V. Zabelina,
I.S. Didenko, A.P. Kozlova,
Zh.A. Goreeva, T
NUST "MISiS", Russia

Introduction

Pleochroism (from ancient greek πλέον «more» + χρόμα «color») is an optical phenomenon when a transparent crystal will have different colors if it is viewed from different angles (1). Sometimes the color change is limited to shade changes such as from pale pink to dark pink (2).

Crystals are divided into optically isotropic (cubic crystal system), optically anisotropic uniaxial (hexagonal, trigonal, tetragonal crystal systems) and optically anisotropic biaxial (orthorhombic, monoclinic, triclinic crystal systems).

The greatest change is limited to three colors. It may be observed in biaxial crystals and is called trichroic. A two color change may be observed in uniaxial crystals and called dichroic. Pleochroic is often the term used to cover both (2).

Pleochroism is caused by optical anisotropy of the crystals (1-3). The absorption of light in the optically anisotropic crystals depends on the frequency of the light wave and its polarization (direction of the electric vector in it) (3, 4).

Generally, any ray of light in the optical anisotropic crystal is divided into two rays with perpendicular polarizations and different velocities (v_1, v_2) which are inversely proportional to the refractive indices (n_1, n_2) (4).

In uniaxial crystals there is a single direction governing the optical anisotropy whereas all directions perpendicular to it (or at a given angle to it) are optically equivalent. Thus, rotating the material around this axis does not change its optical behavior. This special direction is known as the optic axis of the material (5). This direction is parallel to the axis of symmetry of highest order: 6 for hexagonal, 3 for trigonal, 4 for tetragonal (6). Light whose polarization is perpendicular to the optic axis is governed by a refractive index n_o (for "ordinary"). Light whose polarization is in the direction of the optic axis sees an optical index n_e (for "extraordinary"). For any ray direction there is a linear polarization direction perpendicular to the optic axis, and this is called an ordinary ray. However, for ray directions not parallel to the optic axis, the polarization direction perpendicular to the ordinary ray's polarization will be partly in the direction of the optic axis, and this is called an extraordinary ray. The ordinary ray will always experience a refractive index of n_o, whereas the refractive index of the extraordinary ray will be in between n_o and n_e, depending on the ray direction as described by the index ellipsoid. (5)

So, if the light travels through the crystal along the optical axis there would be no change of color or shade with the rotation of the sample around the direction of light.

If light travels in the direction perpendicular to the optical axis then we may observe change of color or shade with the rotation of the sample around the direction of light – this is dichroism.

The main points of the dichroism are the following (2, 7, 8):

- dichroism may be observed only in uniaxial crystals

- colored uniaxial crystals may not be dichroic (or dichroism may be so small that it can't be observed by naked eyes but can be detected by highly precise optical instruments)

- colorless in visual wavelength range crystals may demonstrate dichroism in UV or IR wavelength ranges

Dichroism is an evidence of the anisotropy of the absorbing centers (7).

Dichroism can be observed in non-polarized light but in polarized light it may be more pronounced if the plane of polarization of incident light matches plane of polarization of light that propagates in the crystal—ordinary or extraordinary wave.

The difference in absorbance of ray lights may be minor, but it may be significant and should be considered both when reporting optical properties and when using the crystal. This is why any uniaxial crystal should the examined for dichroism.

Experimental

Equipment

To investigate dichroism we used an Agilent Cary 5000 UV-Vis-NIR spectrophotometer equipped with a Universal Measurement Accessary (UMA).

This system allows us to carry out experiments in wavelength ranges for

- non-polarized light - 190-2800 nm

- polarized light - 250-2500 nm.

To carry out experiments using polarized light, the system is equipped with an automatic polarizer controlled by the computer.

The accuracy of the Cary 5000 instrument is high enough to provide data on dichroism even in cases when dichroism is very small and the sample seems to be transparent and colorless when viewed with the naked eye.

Samples

Samples should have 2 plane-parallel polished surfaces parallel to the optic axis.

The best sample is the oriented sample—when you exactly know where crystallographic axes (axes related to the elements of symmetry) X and Y are located.

Method

Investigation of dichroism phenomenon consists of obtaining two spectra in the same region of the sample:

- in case of non-polarized light, the sample should be rotated in the sample holder by 90 degrees around the light ray;

- in case of polarized light, two spectra are measured with polarizer in the 0 degree and then the 90 degree position.

The Cary 5000 allows the measurement of transmission or absorption spectra. In addition, data obtained can be recalculated to any other demanded values.

Dichroism is characterized by the degree of dichroism (9, 10):

$$\Delta = \frac{D_1 - D_2}{D_1 + D_2} \qquad (1)$$

where D_1 is the optical density of the light transmitted through the sample in the sample position 1 ; D_2 - in the position 2.

or

$$\Delta = \frac{\mu_{max} - \mu_{min}}{\mu_{max} + \mu_{min}} \qquad (2)$$

where μ_{max} is the maximum spectral attenuation coefficient for the experimental wavelength and μ_{min} is the minimum spectral attenuation coefficient for that wavelength.

Spectral attenuation coefficient $\mu(\lambda)$ with consideration of multiple reflection is determined by calculations from measurements of spectral transmission $T(\lambda)$ using material refractive index n:

$$\mu(\lambda) = -\frac{1}{d} \lg \tau_i(\lambda), \qquad (3)$$

where d is the specimen thickness, cm; $\tau_i(\lambda)$ is the spectral coefficient of the internal transmission of the sample, arbitrary units.

Internal transmittance $\tau_i(\lambda)$:

$$\tau_i(\lambda) = \sqrt{\left[\frac{1}{T(\lambda)} \cdot \frac{8n^2(\lambda)}{(n(\lambda)-1)^4}\right]^2 + \left[\frac{n(\lambda)+1}{n(\lambda)-1}\right]^4} - \frac{1}{T(\lambda)} \cdot \frac{8n^2(\lambda)}{(n(\lambda)-1)^4}, \qquad (4)$$

where $T(\lambda)$ is the spectral transmission measured on the spectrophotometer; $n(\lambda)$ is the refractive index of the material.

Results

Oriented cubes of $CaMoO_4$ were measured with the Cary 5000 UMS instrument. The planes of the cubes were perpendicular to the optical axis (Z or axis of symmetry of 4th order) and the axis of 2nd order (X and Y). $CaMoO_4$ belongs to the tetragonal symmetry and is characterized by two refractive indices No and Ne.

The experiment was carried out along X, Y and Z axis.

Dichroism by naked eye

Dichroism in the samples of $CaMoO_4$ single crystals can be observed by naked eye, as shown in Figure 1.
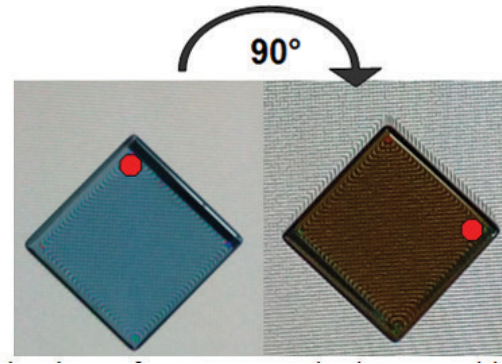
Figure 1. Image of a $CaMoO_4$ sample in two orientations; crystals x-axis parallel to optical axis (left) and (X + 90°) crystals x-axis perpendicular to the optical axis.

The cubic sample was rotated by 90 degrees relative to the axis of light passing along the direction perpendicular to the optical axis of the crystal. In one position the sample is blue, and in other is grey-orange.

The phenomenon is pronounced along axis of 2nd order (X, Y) and along axis of 4th order (Z) no change of color is observed.

Dichroism by spectrophotometer

We measured the optical transmission in the different positions of the sample in regard of incident light according to the scheme (Figure 2).

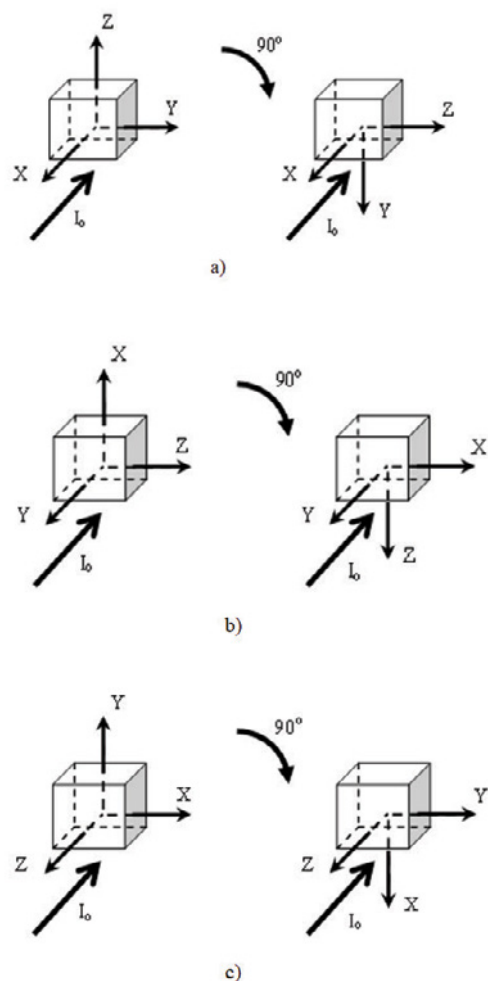**Figure. 2.** The measurement scheme of CaMoO$_4$ samples: a) measurements along the X-axis and (X + 90°); b) along the Y-axis and (Y + 90°); c) along the Z-axis and (Z + 90°); (X + 90°), (Y + 90°), (Y + 90°) - sample is rotated by 90° around the X, Y and Z axes respectively

According to the formula (3) we calculated the attenuation coefficients, according to formula (2) - the degree of dichroism, and plotted their spectral dependences (left-hand and right-hand scale in Figure 3 respectively):
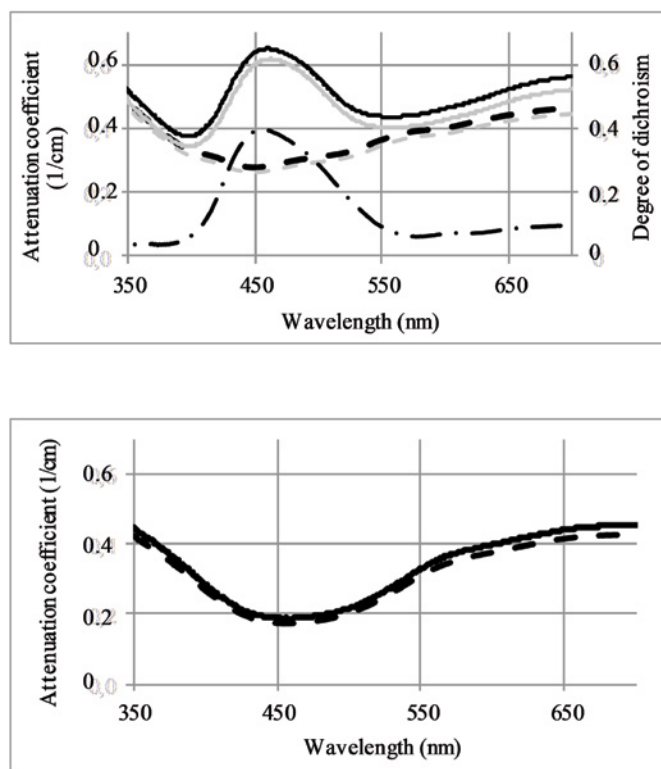

Figure 3. The spectral dependence of $\mu(\lambda)$ of CaMoO$_4$ single crystal and the degree of dichroism Δ:
Upper graph: Along X and Y axis, black and grey solid and dotes lines refer to left axis: black – crystallography X axis, grey – crystallography Y axis, solid line – initial position, dotes – sample was turned at 90° around the incident light ray; dash point curve refers to right axis;
Lower graph: Along the optical axis Z solid line – initial position, dotes – sample was turned at 90° around the incident light ray

If you compare the 2 solid or 2 dotted lines you will see that anisotropy of attenuation is insignificant: values in the X axis coincide values in Y (Figure 3, upper). But if you compare 2 black (measurements along X axis) or two grey lines (measurements along Y axis) you will see the difference between the attenuation in two positions - attenuation changes with the rotation by 90° around the incident light ray. This difference achieves its maximum 0.3 cm^{-1} at 450 nm (dot-dash curve, Figure 3, upper). This is dichroism on the spectral dependences.

Also with the rotation of the sample, the maximum of the attenuation bands shift and this result in the change of color.

Along Z-direction (parallel to the optical axis), there is no significant changes in the attenuation in two positions of the sample (Figure 3, lower).

This phenomenon also may occur in any other birefringent materials. For example, dichroism in trigonal crystals is reported by Kozlova N. S., Buzanov O. A., Zabelina E. V., Kozlova A. P., Bykova M. B. in "Point Defects and Dichroism in Langasite and Langatate Crystals" (Crystallography Reports. – 2016. - Vol. 61. - No. 2. - p. 275–284.)

Conclusions

The Cary 5000 UV-Vis-NIR spectrophotometer fitted with a Universal Measurement Accessory (UMA) provided the required measurement flexibility, and *S/P* polarization control determine the degree of dichroism of birefringent materials.

Measurements of %R and %T were made along crystal axes (X, Y, Z), with non-polarized light and polarized light (parallel to, and perpendicular to, the optical axis). Spectrophotometric measurements afforded by being able to automatically position the UMA detector at any point in a 340° arc around the sample.

Dichroism should be taken into account in the investigation, and interpretation, of the optical properties of birefringent materials. The Cary 5000 with UMA has proven to be a capable and convenient tool for such analysis.

References

1. Bloss, F. Donald, *An Introduction to the Methods of Optical Crystallography*, New York: Holt, Rinehart and Winston. pp. 147–149, **1961**

2. http://www.galleries.com/minerals/property/pleochro. htm. Accessed November 2018.

3. Sears F.W., Zemansky M.W., Young H.D., University Physics 6th ed, Pearson,

4. Sivukhin D. V. General course of physics. 3rd edition, stereotyped. M.: Fizmatlit, Moscow, 2002. Vol. IV. Optics. [in Russian] 792 p.

5. https://science-train.com/w/Birefringence/Explanation. html Accessed November 2018

6. http://reference.iucr.org/dictionary/Arithmetic_crystal_ class. Accessed November 2018.

7. Herbert Smith F.S., Revised by Phillips, G.F., *Gemstones,* London, Chapman & Hall, 1972.

8. Maier A. A., *Physical Chemistry of Solids: Crystal Optics* (Izd-vo MKhTI, Moscow, 1984) [in Russian], pp 84.N.

9. Kozlova, O. Buzanov, A. Kozlova, E. Zabelina, V. Shayapov, Nikita Siminel, Radiation-induced defects and dichroism in $La_3Ga_{5'5}Ta_{0'5}O_{14}$ crystals, *Radiation & Applications*, vol. 1, issue 3, pp. 171 – 176, **2016**

10. Tudor T., Manea V., Symmetry between partially polarized light and partial polarizers in the vectorial Pauli algebraic formalism, *J. Mod. Opt*., vol. 58, no 10, pp. 845-852, **2011**.
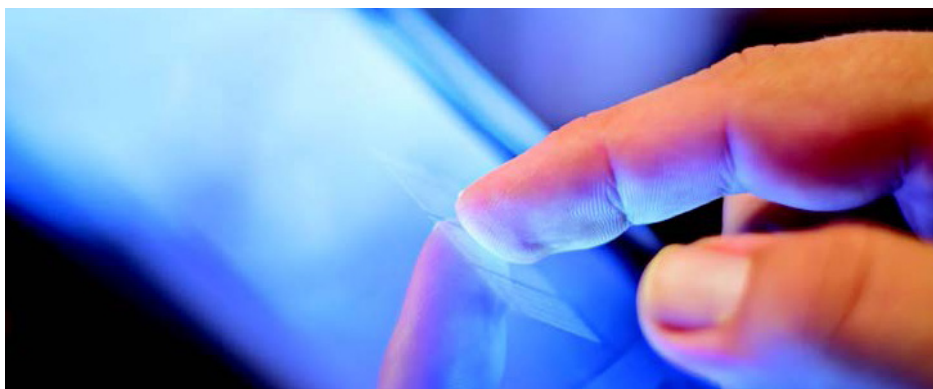
www.agilent.com/chem

Agilent

Trusted Answers

Agilent

Trusted Answers

Measuring the Performance of Compact Visual Displays

Angular reflectance measurements of optically active materials

Authors

Travis Burt, Huang ChuanXu*,
Andy Jiang*

Agilent Technologies
Mulgrave, Victoria, Australia

*Agilent Technologies
Shanghai, China

Introduction

The prevalence of visual displays in everyday use continues to grow as the size, weight and power consumption is reduced and device mobility is subsequently improved. Optical displays, based on light emitting diode (LED) and liquid crystal display (LCD) technology finds broad industrial and domestic use. Examples of devices include mobile telephones, portable computers ranging from hand-held personal digital assistants (PDAs) to laptop computers, portable digital music players, LED/LCD desktop computer monitors, and LED/LCD televisions. In an industry where thickness improvements are measured in tens of microns, LED/LCD packages are becoming thinner as the manufacturers of electronic devices strive for smaller package sizes.

Displays use backlighting to illuminate the full display area and liquid crystals to control the timing and color of the emissions presented to the viewer (Figure 1). The backlighting often takes the form of a solid light guide in the shape of a slab or wedge. The illumination source can be cold cathode fluorescent (CCFL) lighting, more commonly referred to as an LCD TV, or LED based backlighting often referred to as an LED TV. Due to the importance of backlighting on picture quality, the labels overlook the fact that both TV types employ the use of LCDs to control images presented to the viewer.

The solid light guides used in backlighting are often made of an optically transparent polymeric material which is mass produced by, for example, injection molding. The optical and electrical efficiency of solid light guides are enhanced by the use of reflectors. The reflector films are strategically positioned to more efficiently utilize light that would otherwise exit the back surface of the solid light guide or the illuminating source (Figure 1).

Backlight reflectors used in light guides need to have a high reflectivity for efficient transport of light. Reflection values of >98% are typical reflectance targets as multiple (tens of) reflections through the light guide would otherwise quickly extinguish available light if much more than 2% was lost at each reflection event.
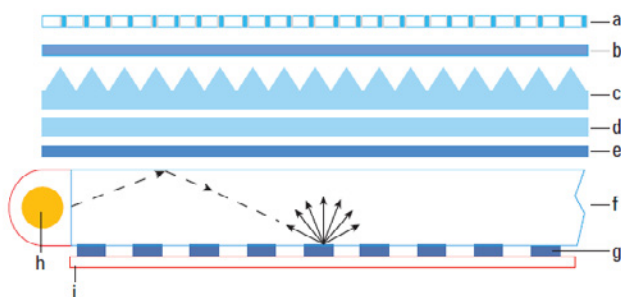
Multilayer optical coatings are used to generate the high reflectivities of the thin reflector films. The physical properties of the films, which are typically <100 µm thick, can be of a non-metallic multilayer polymeric material which can result in surfaces with optical activity. Optically active materials rotate the polarization state of light on a transmission or reflection event. More common are materials that are optically inactive where polarization interactions introduced by the sample only act to subdue a particular polarization component such as S, or P, not rotate it. While optical activity will typically have no direct consequence in end-use applications inside the display, accurate optical characterization (QA/QC) of the reflector prior to assembly requires careful consideration of these effects to ensure correct %R and %T values are recorded at the detector.

Experimental

Samples

The sample measured was approximately 50 x 50 mm (w x d) and approximately 100 µm thick (Figure 2). The reflective surface was protected by a semi-transparent clear film which could be easily peeled off before measurements were taken. The thickness of the sample and its flexibility was accommodated during mounting to ensure that a flat surface was presented to the incoming beam.

Figure 1. Cross section of products used in LCD construction:
a: LCD b-d: Varying film types to increase guide backlighting efficiency
e: Diffuser f: Light guide g: Dots for extracting light from the light guide
h: Fluorescent or LED light source i: Back reflector film (shown in red).
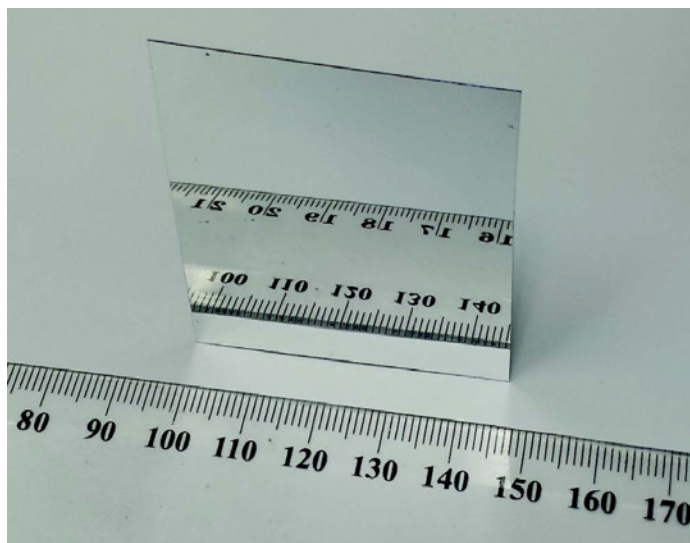

Figure 2. Reflector sample.

Optical activity of the sample was demonstrated before measurement in the Cary 7000 UMS by illuminating the sample with s-polarized visible white light at an angle, and viewing the specularly reflected beam from the sample by eye through a second polarizer. The Maximum intensity of the reflected beam was observed by rotating the viewing polarizer a few degrees from the S (0 deg) position.

The angular off-set between the incident s-polarized light and the visually detected light confirmed optical activity, or optical rotation of the light. This practical test confirmed that a depolarizer would be required to be inserted before the detector during the spectrophotometric measurements.

Instrumentation

– Agilent Cary 7000 Universal Measurement Spectrophotometer, p/n G6873AA

The Cary 7000 Universal Measurement Spectrophotometer (UMS) is a highly automated UV-Vis-NIR spectrophotometer system. The UMS performs variable angle transmission and absolute reflectance measurements. The linearly polarized beam that is incident on the sample can be used to measure transmission, and by rotating the detector assembly about an axis through the sample and perpendicular to the plane of incidence, in reflection, as indicated in Figure 3.
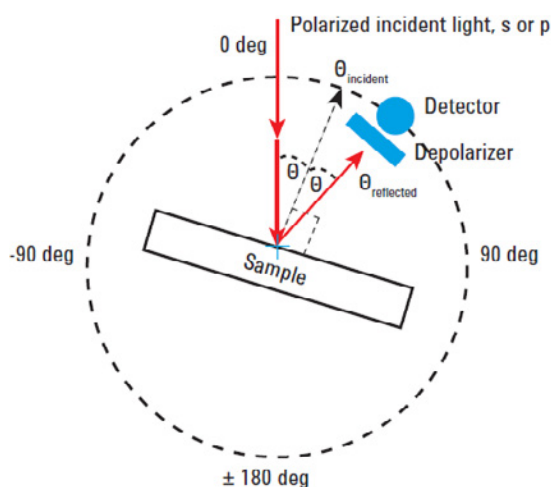

Figure 3. Schematic of the Cary 7000 UMS. Light incident onto the sample can be s, or p polarized. The detector module allows mounting of a depolarizer immediately before the detector. Absolute specular reflection of transmission can be measured.

A depolarizer was placed after the sample but before the detector to correct for the optical rotation imposed on the reflected light by the sample. The depolarizer before the detector and the polarizer before the sample were included in the single baseline measurement taken before each sample collection was made. The Cary 7000 UMS only requires a single baseline to be collected for all %R measurements at any angle for a given polarization. This unique feature dramatically improves the speed of analysis and sample throughput possible on this system.

Results and discussion

Reflectance data was collected at four angles of incidence (AOI); 70, 60, 45 and 30 deg over the spectral range 300–1200 nm (Figure 4). The sample demonstrated its design intent by displaying reflectance >98%R over the visible wavelength range (400–800 nm) (Figure 5).

The multi-angle measurements showed consistent performance over a broad angular range in the region of interest (400–800 nm) and angular dependence outside this range (>800 nm). High AOI >60 deg also showed some diminishing of the %R quality in the 600–700 nm and 800-900 nm region. The spectral dependence of the %R profile at these angles demonstrates that some color alterations are to be expected for high angles of incidence.

The importance of depolarizing the light after the sample, but just before the detector, is demonstrated in Figure 6. In this figure, absolute reflectance is measured with and without the use of a depolarizer. Without the use of the depolarizer the optical activity of the sample causes the %R values to artificially exceed 100%. This is compared directly to the result where a depolarizer is used which corrects for the optical rotation of the light and gives the correct values.

Figure 4. Reflection of backlight material at 70 (red), 60 (green), 45 (brown), 30 (black) degree s-polarized light.
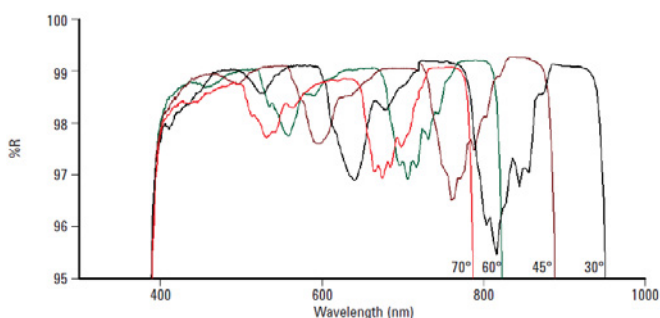
Figure 5. Magnified view of Figure 4 showing reflection of backlight material at 70 (red), 60 (green), 45 (brown), 30 (black) degree s-polarized light.
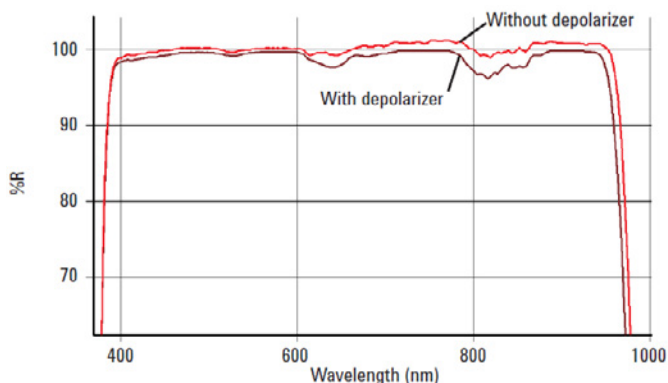
Figure 6. Demonstration of the importance of using a depolarizer after the sample but before the detector. Absolute reflection of backlight material at 30° s-polarized with a depolarizer before the detector (brown) and 30° s-polarized WITHOUT a depolarizer before the detector (red).

Conclusions

The Agilent Cary 7000 UMS was shown to be a valuable tool for measuring the optical properties of next generation materials used in optical displays. The optical rotation imposed by the specialized polymeric coating on the sample was accurately measured by using linearly polarized incident light and depolarizing the reflected light before it was detected and processed.
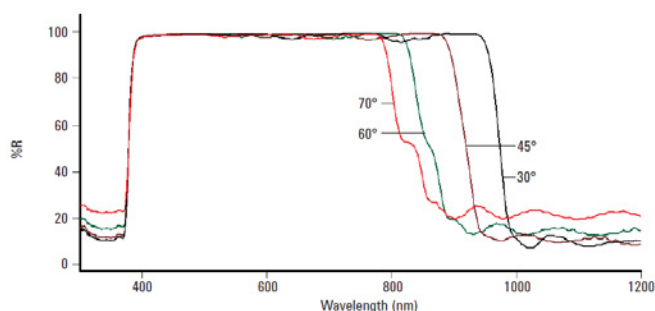
www.agilent.com/chem/cary7000ums

Agilent

Trusted Answers

Agilent

Trusted Answers

Quality Control of Beam Splitters and Quarter-Wave-Mirrors

Multi-angle UV-Vis-NIR measurements of multiple layer optical coatings
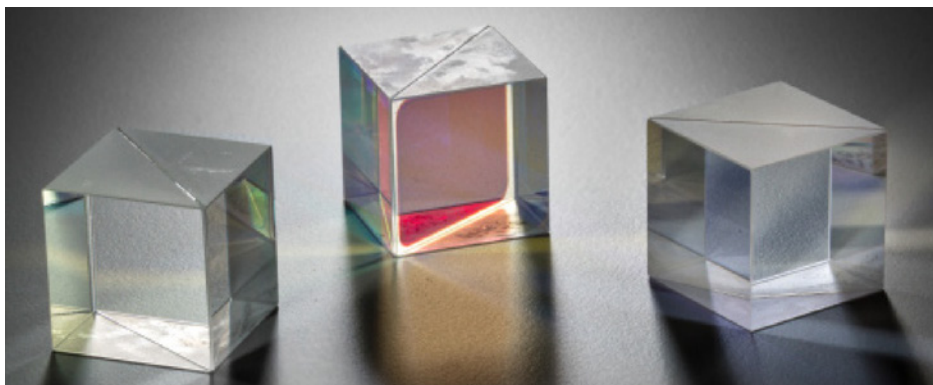
Author

David Death
Farinaz Haq
Agilent Technologies,
Australia

Introduction

Optical coatings and coating technologies have matured over many years in terms of the design, production and characterization processes. Today optical coatings are ubiquitous and can be found in applications from research and space optics to consumer items and industry. The variety of applications include eye wear, architectural and automotive glass, illumination and lighting systems, displays, optical filters, specialty mirrors, fiber optics and communications and medical optics. The performance of optical coatings depends on the specifications of the coating and substrate materials.

The design and manufacture of high quality multilayer optical coatings require accurate measurements of not only the final production component but also the optical constants of the materials in the thin film layers. These measurements enable the detailed design of sometimes very complex multilayer coatings. Measurements made at the end and during production can also be used to reverse engineer optical coatings to provide feedback on the design manufacturing

process (1). A primary aim of reverse engineering is to detect systematic and random errors in individual layer parameters. This helps to improve layer control and optimize the optical coating deposition.

Reliable reverse engineering of an optical coating depends critically on accurate measurements of reflection and transmission. Historically these measurements have been limited to normal incidence transmission (T) and/or near normal incidence reflection (R) data. As may be expected the ambiguity of multilayer reverse engineering grows as the number of coating layers increases. In general it is possible to minimize the ambiguity in reverse engineering by using more measured data. Both T and R measurements made at a range of angles of incidence (AOI) are valuable for the characterization of thin film materials and the reverse engineering of multilayer coatings. Most typical reverse engineering involves the detailed numerical analysis of normal or quasi-normal incidence T and R data related to the coating under study. While this approach is experimentally simple, it can lead to unreliable results due to the limited information available in near normal T and R data sets and the influence of measurement errors within those data sets (1). In particular, reflection data from broadband reflectors or transmission data from to broadband antireflection (AR) coatings can be considered as examples of such low-information data sets. Historically simple normal incidence T measurements have been available using a wide variety of spectrophotometers and near normal incidence R measurements similarly so by fitting an appropriate reflectance accessory.

This application note demonstrates a new form of multi-angle photometric spectroscopy using a unique automated double beam UV-VIS-NIR multi-angle spectrophotometer, the Cary 7000 Universal Measurement Spectrophotometer (UMS). Example measurements of multilayer coatings used to create a spectral beam splitter and two 43 layer quarter-wave stack mirrors on differing substrates are presented alongside the reverse engineering analysis enabled by the obtained multi-angle spectral photometric data set.

Experimental

Samples

Measurements of three different coatings are summarized from the work of Amotchkina et al. (2). The first coating, BS-AR-Suprasil, is a specialized beam splitter designed for an oblique AOI of 45°. The 52 layer reflector is deposited on a 1 mm thick Suprasil substrate. The front surface coating specification calls for a spectral transmission profile of greater than 98% T between 935 nm and 945 nm and greater than 98% R between 967nm and 971 nm. Additionally a 10-layer broadband AR coating is deposited on the rear

surface. Optical coatings typically consist of alternating layers of varying thickness of high and low refractive index materials. For this first sample the high index material used was Niobium Pentoxide (Nb_2O_5) and the low index material was Silica (SiO_2) and the coating was deposited using a Leybold Optics GmbH Helios magnetron-sputtering system.

Both the second and third samples are high reflectors constructed of 43 layer quarter-wave stacks with the design wavelength for the reflector at 800 nm. The coatings were deposited on two differing substrate types, 6.35 mm thick fused silica and 1.0 mm thick B260 glass. The sample names were HR800-FusedSilica and HR800-Glass. The high index material used in these coatings was Hafnia (HfO_2) and the low index material used was Silica (SiO_2). The coatings were deposited using e-beam evaporation in a Leybold Optics GmbH SYRUSPro 710 coating machine.

Instrumentation

The reflectance and transmittance of the completed coatings were obtained using the Cary 7000 UMS which is a highly automated variable-angle absolute specular reflectance and transmittance UV-Vis-NIR spectrophotometer. The Cary 7000 UMS provides users with automated independent motorized control over both the sample AOI and the angular positioning of the detector, see Figure 1. This independent control of both sample AOI and detector position allow for rapid, accurate and unattended measurements of optical multilayer coatings.

Reflectance and transmittance measurements have traditionally been performed using different spectrophotometer accessories. This leads to different areas of the sample being measured for reflectance and transmittance. Deposition processes, though well controlled, are not perfect and films are deposited of non-uniform thicknesses. As a result reflectance and transmittance measurements can vary across the surface as the coating thickness changes. With the development of the Cary 7000 UMS, it is now possible to measure R and T from the same point on the sample surface without moving the sample when changing from R to T measurement modes. Additionally the sample can be rotated 180° to permit static transmittance measurements to be performed in the forward or reverse direction. In a similar way the AOI in a reflectance measurement can be varied to either side of the sample normal and the detector can be moved to make R measurements at ±AOI. In either case both R and T can be measured from the same point without removing and replacing the sample in the spectrophotometer or changing to another accessory.
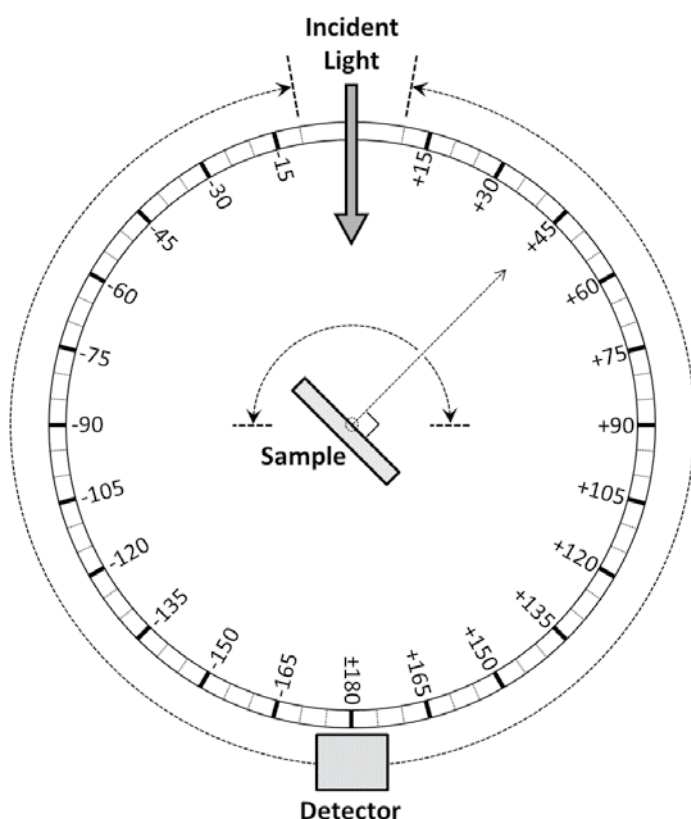
Figure 1. The AOI on the sample and the detector position can be set independently with 0.02° resolution. The AOI on the sample ranges from -85°~AOI~85°. The detector can be placed at angles ranging from -10° to 10°. As a result the Cary 7000 is able to determine R over the range 5°~|AOI|~85° and T over the range 0°~|AOI|~85°.

Results and discussion

Small variations in the layer thickness as each is deposited and variations in the optical characteristics of the materials used under differing coating conditions result in the overall performance of an optical coating not meeting the original design intent. The design and analysis of optical coatings are accomplished using sophisticated computer software packages which rely on the accurate knowledge of both the physical thickness of each layer and the optical constants of the materials used to build the coating. The three coatings described were designed using OptiLayer, a suite of software consisting of modules for the design of multilayer coatings, prediction of performance, characterization of optical materials and reverse engineering of coatings from measured transmittance and reflectance data.

Some modern coating machines have the facility to monitor the normal incidence transmission of the coating as it is deposited (*3-4*). These in-situ measurements made at

normal incidence are used as a basis for predicting the final design oblique incidence performance of the coating laid down. Detailed analysis of this in-situ data using OptiLayer typically shows rough agreement between positioning of the reflectance and transmittance bands with the initial design. However in-situ normal incidence measurements are no real substitute for actual oblique angle R and T measurements of the completed coating. In their article Amotchina et al. describe how measurements made using the Cary 7000 UMS allowed them to reverse engineer the deposited coating and hence fine tune the coating process using in-situ measurements to more closely match the original design intent of the coating.

In the example of the BSAR-Suprasil beam-splitter the primary uncertainties lie in the thicknesses of the individual layers as the optical properties of the Nb_2O_5 and SiO_2 are quite well understood. In this study, the Cary 7000 UMS was used to measure the sample after coating. The coating specification calls for the beam-splitter to be used at a 45° AOI. Using the Cary 7000 UMS it was possible to measure both R and T at a number of different AOI from the same patch on the surface of the sample. Increasing the number of measurements in the data set (more AOI) served to reduce the level of uncertainty in the results from reverse engineering the coating. Using this data and analysis it was then possible to correlate with in-situ measurements and construct an optimization strategy for the deposition. Finally measurements using the Cary 7000 UMS were used to validate the optimization.

Figure 2 compares the predicted and measured spectral transmittance of the optimized BSAR-Suprasil beam-splitter at an AOI of 45° Figure 2(a). The unpolarized transmittance measurements were made using the Cary 7000 UMS. The spectral agreement between the theoretical curve (Optilayer) and the measured data points is exceptionally good. Differences in peak heights are primarily due to the spectral bandwidth used to collect the measured data. Further measurements of the BSAR-Suprasil sample were also made at an AOI of 30° for both S and P incident polarization, this data is shown in Figure 2(b) along with the predicted spectral transmittance. Once again the agreement between measurement and theory is excellent. The close agreement between these measurements made at oblique AOI of 45° and 30° and the model predictions serves to validate the reverse engineering and model refinement used to optimize the coating deposition based on the in-situ normal incidence transmittance measurements.

The second and third samples measured were examples of multi-layer quarter wave stack mirrors designed to be oblique incidence high reflectors. Each mirror consisted of 43 quarter wave alternating layers of Hafnia (HfO_2 — high index material) and Silica (SiO_2 — low index material).

The difference between the samples being the type and thickness of the substrate used: HR800-FusedSilica — 6.35 mm thick fused silica; HR800-Glass — 1 mm thick B260 glass. In these coatings uncertainty in both the optical properties of the Hafnia and individual layer thickness need to be considered. Once again the mirror is designed for an oblique AOI of 45° with un-polarized incident light.
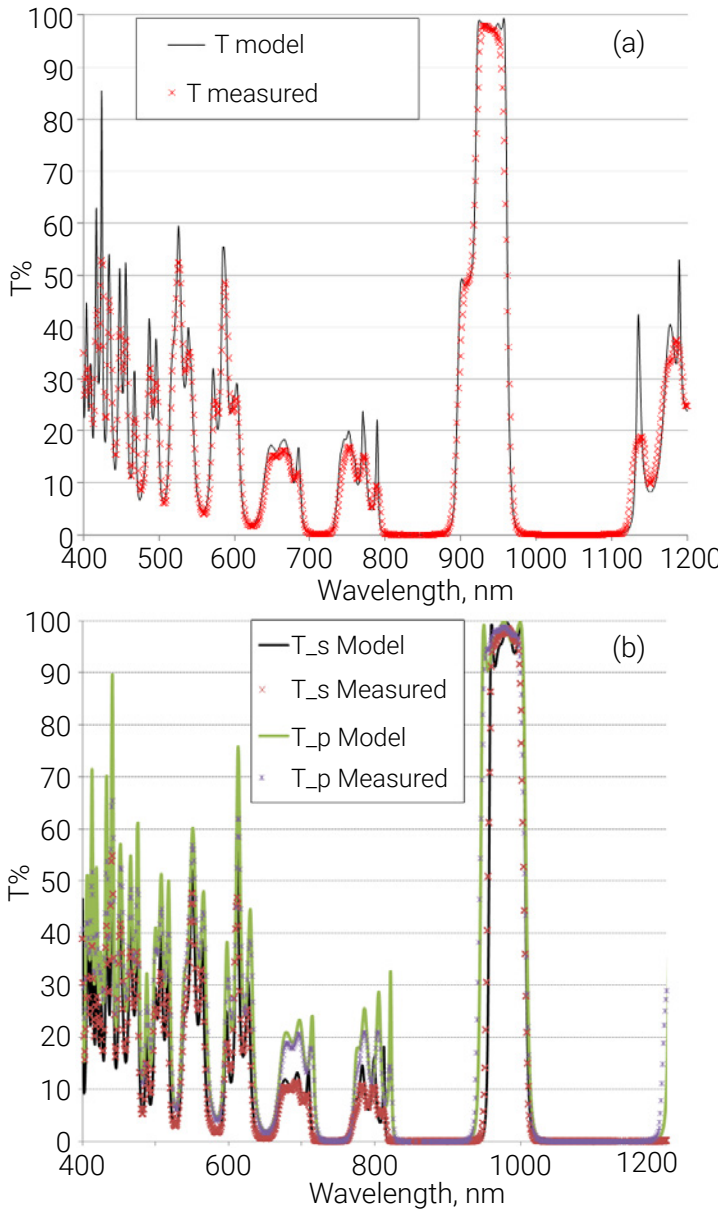

Figure 2. Comparison of oblique incidence experimental transmittance data for the sample BS-AR-Suprasil with model transmittance (a) non-polarized light at 45°, (b) s- and p-polarizations at 30°.
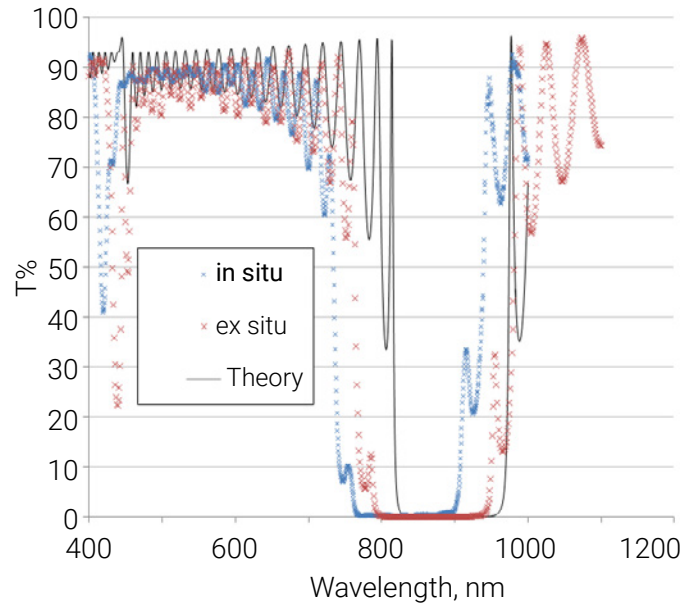

Figure 3. Comparison of in-situ normal incidence transmittance data, Cary 7000 UMS (ex-situ) measurements and theoretical transmittance for the HR800-Glass sample.

As with the first sample, measurements of these samples using the Cary 7000 UMS were used to characterize the final coating performance, optimize the coating strategy and validate the outcomes of the reverse engineering analysis. The strategy developed involved reverse engineering in-situ normal incidence measurements during the coating procedure to make adjustments on the fly. As an example of the influence of material and layer thickness variations, Figure 3 compares the desired design specification with the in-situ and final transmittance measurement using the Cary 7000 UMS of the un-optimized coating. As can be seen there is significant deviation between the three data sets. The primary difference is observed as a shift of the reflectance band toward shorter wavelength and differences in the width of the reflectance band.

The positioning of the reflectance band towards shorter wavelengths is understood in terms of an underestimation of the individual layer optical thicknesses as they are laid down. This may be associated with either an error in the physical thickness of the deposited layers and/or an uncertainty with respect to the optical properties of the layer materials (refractive index and absorption coefficient). Errors in the geometrical thickness of coating layers can arise from inaccurate calibration of the quartz crystal layer thickness monitors used to control the deposition. Errors in material properties on the other hand arise from incipient variation of the nominal refractive index with deposition temperature.
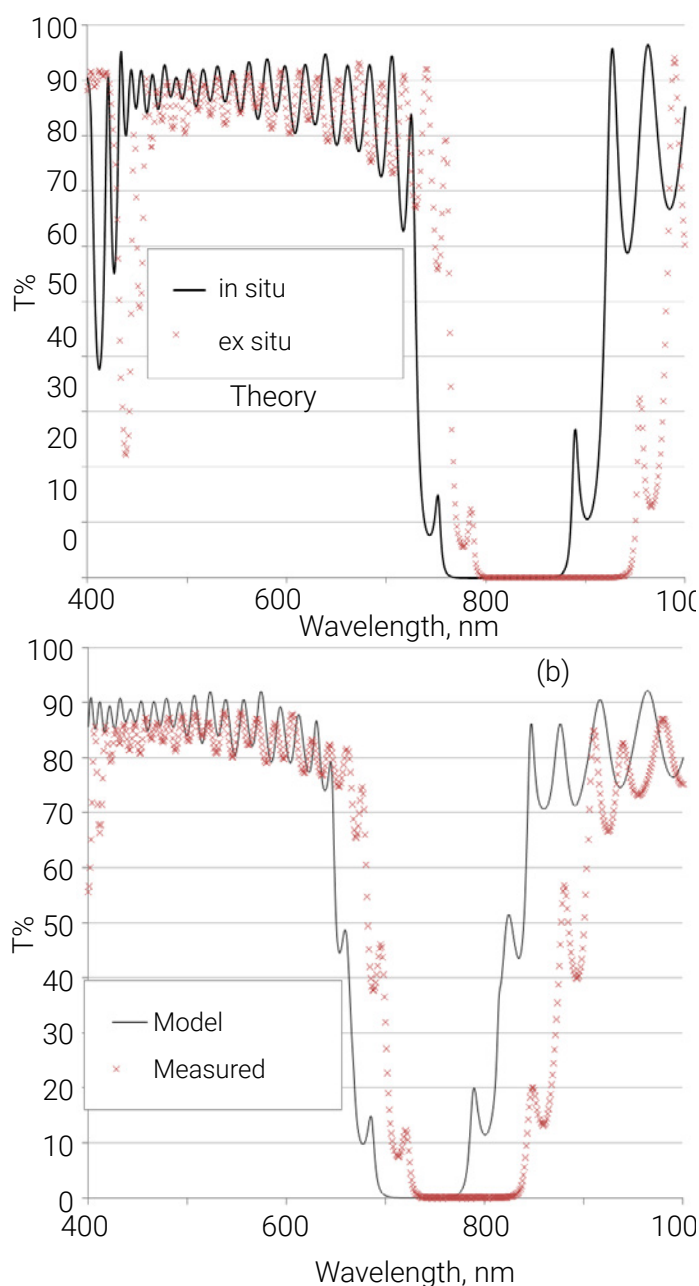
Figure 4. Comparison of normal (a) and AOI = 45° (b) experimental transmittance data related to HR800-FusedSilica sample with model transmittances calculated for intermediate design.

HfO_2 exhibits such a variation of refractive index as a function of deposition temperature and at the relatively low deposition temperature used here (120 °C) there is a degree of uncertainty in its value. Further, the width of the reflection band of a quarter wave mirror stack depends on the ratio of the high and low refractive indices used (5). On that basis the design specification should result in a width of 126 nm. The normal incidence in-situ measurements indicate a width of 133 nm and the Cary 7000 UMS measurements indicates a width approaching 143 nm. Considering that the uncertainties associated with the optical properties and porosity of the silica layers to be small it is apparent that the refractive index of the Hafnia layers is larger than the value assumed in the construction of the coating model. The apparently higher refractive index may be explained by the porous structure of the HfO_2 layers. Under vacuum the porous structure of the HfO_2 layers remains empty and the refractive index is correspondingly low. Exposing the coating to atmospheric air fills the pore structure with water vapor, thereby increasing the refractive index. This process is commonly known as a vacuum shift (6). These effects can be accounted for reasonably accurately by allowing for random errors in the layer thicknesses and random offsets in the refractive index of the HfO_2 layers (2).

Figure 4 shows the measured transmittance curves for normal and oblique incidence compared with the predicted design curve for the 800 nm high reflectance coating on the 6.35 mm fused silica substrate (HR800-FusedSilica). Once again a wavelength shift is observed, but this time it is toward longer wavelengths. The widths of the high reflectance regions are again also different. For this coating the physical layer thicknesses were found to be reasonably accurate. The shift in position of the reflectance band was in this case due to uncertainties in the refractive index values assumed for the HfO_2 layers. The HfO_2 layers are considered to be inhomogeneous due to inter-diffusion of the HfO_2 and SiO_2 coating materials (1). Random variations in the refractive index of the various HfO_2 layers were thus included in the model and the predicted transmittance recalculated for normal and oblique (45°) incidence and compared with measurements mad on the Cary 7000 UMS.

The final fitting of the normal incidence measurements by model data is shown in Figure 5(a). The model fit to the measurement is reasonable indicating that there is still room to improve the model. The model takes into account all the main features of the deposited coating however it may be further improved by allowing for variations in the degree of material inhomogeneity on a layer by layer basis and the definition of interlayers caused by diffusion of HfO_2 and SiO_2 materials. This level of sophistication cannot be based on the results of one set of transmittance or reflectance measurements at one particular angle of incidence. The Cary 7000 UMS is uniquely placed to provide both R and T data from a given sample at the multiple angles required to provide confidence in modelling these effects.

Figure 5(b) shows the comparison between the coating model and the measured transmittance at 45°. The results demonstrate good agreement between Cary 7000 UMS measurement and the predicted curve. Further the close agreement between measurement and model is confirmed in measurements at all angles made using the Cary 7000 UMS from AOI of 0° to 45° at 5° intervals.
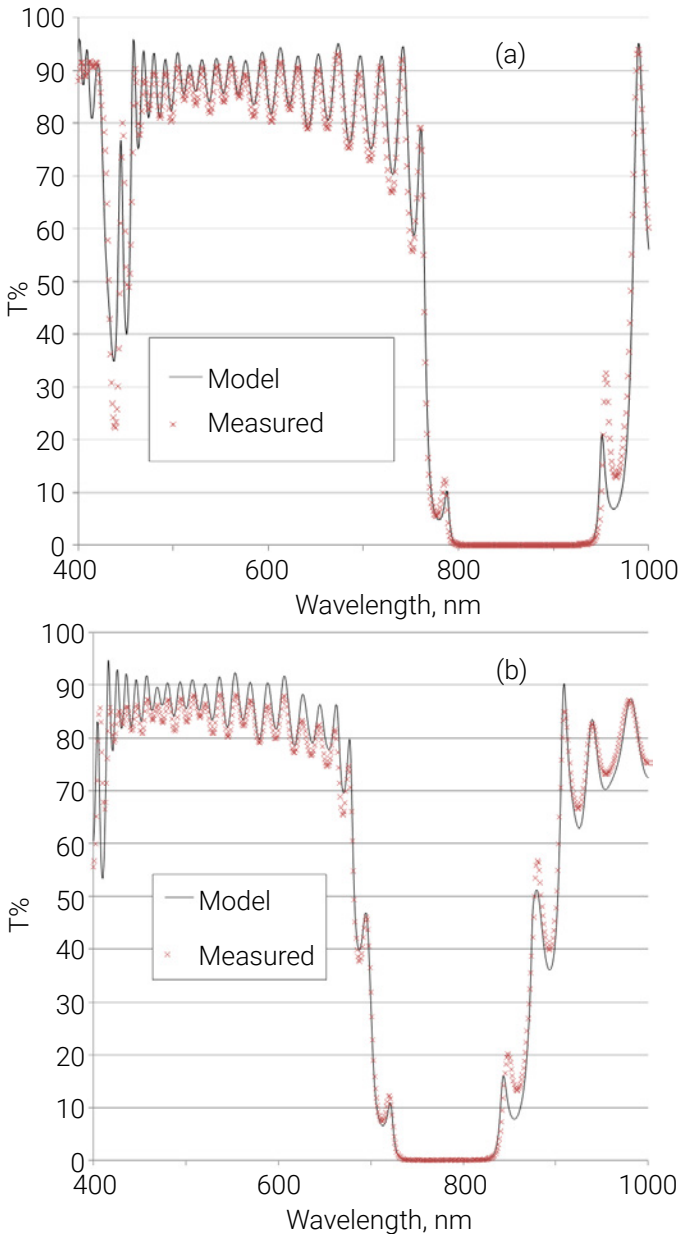
Figure 6 show the residual difference between the measured and calculated transmittance for both S and P polarization at 800 nm wavelength. As can be seen there is good agreement between the absolute transmittance measured by the Cary 7000 UMS and the value predicted by the model.
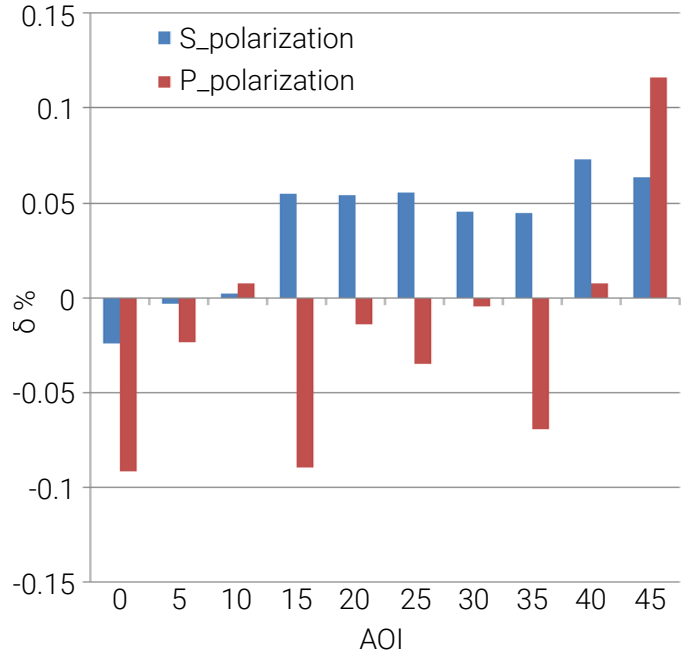

Figure 6. Residual differences between experimental and model transmission measurements data for the HR800-FusedSilica sample at the wavelength of 800 nm versus the AOI.

Conclusion

The Cary 7000 UMS has been shown to be a valuable tool for the measurement and characterization of complex multilayer optical coatings. The Cary 7000 UMS provides independent and automated control of sample rotation and detector position giving it the unique ability to measure both reflectance and transmittance at different angles without having to move the sample. The facility of an automated polarizer gives the added benefit of being able to address both S and P polarization measurements, all done with the light incident on exactly the same place on the surface of the sample. The Cary 7000 UMS is an ideal candidate for QA/QC in optical coating environments because of its convenience, ease-of-use and ability to operate and produce accurate data completely unattended.

Figure 5. Final fitting of normal (a) and oblique incidence AOI = 45° (b) experimental Transmittance data related to HR800-FusedSilica sample by model transmittances.

Amotchkina et al. demonstrate the value that accurate measurements of optical coatings made at a multiplicity of angles has for the accurate characterization, control and optimization of complex optical coatings. Such measurements enable and validate the adoption of intricate optimization strategies in coating deposition, particularly for coatings designed for application at oblique incidence. Such strategies often involve in-situ measurements made at normal incidence only followed by reverse engineering of the coating from a limited dataset. The Cary 7000 UMS enables optimization and validation through the provision of accurate measurement across a range of angles.

References

1. A.V. Tikhonravov, T.V. Amotchkina, M.K. Trubetskov, R.J. Francis, V. Janicki, J. Sancho-Parramon, H. Zorc and V. Pervak, "Optical characterisation and reverse engineering based on multiangle spectroscopy," *Appl. Opt.* 51(2), 245-254 (**2012**).

2. T.V. Amotchkina, M.K. Trubetskov, A.V. Tikhonravov, S. Schlichting, H. Ehlers, D. Ristau, D. Death, R.J. Francis, and V. Pervak, "Quality control of oblique incidence optical coatings based on normal incidence measurement data," *Optics Express*, 21,18, 21508–21522 (**2013**).

3. D. Ristau, H. Ehlers, S. Schlichting, and M. Lappschies, "State of the art in deterministic production of optical thin films," Proc. SPIE 7101, 71010C, 71010C-14 (**2008**).

4. H.E. Ehlers, S.S. Schlichting, C.S. Schmitz and D.R. Ristau, "Adaptive manufacturing of high-precision optics based on virtual deposition and hybrid process control techniques," Chin. Opt, Lett., 8, 62–66 (**2010**).

5. S.A. Furman and A.V. Tikhonravov, "Basics of Optics of Multilayer Systems, Editions Frontieres, (**1992**).

6. O. Stenzel, S. Wilbrandt, S. Yulin, N. Kaiser, M. Held, A. Tunnermann, J. Biskupek, and U. Kaiser, "Plasma ion assisted deposition of hafnium dioxide using argon and xenon as process gases," *Opt. Mater. Express*, 1(2), 278–292 (**2011**).

Agilent

Trusted Answers

Semiconductor

Semiconducting materials control the flow of electricity in analog or digital circuits. The electrical conductivity of a semiconductor, which lies between an efficient conductor (metal) and strong insulator (glass), changes predictably under light and temperature exposure. Semiconductor materials are often made from silicon (integrated circuits, photovoltaics), silicon carbide (power devices), or gallium arsenide (high-frequency transistors). These materials facilitate the performance of digital tasks at a micro scale in microelectronics and integrated circuits (transistors) or light conversion tasks at the macro scale of LED and photovoltaics. Analysts use molecular spectroscopic techniques to calculate the bandgap of doped semiconductors and quantify operating efficiencies under light exposure, typically after purpose-designed optical coatings have been applied to the semiconductor. Also, the spectral transmission and reflection of semiconductor wafers of varying sizes, from 1 to 8 inch (2.54 to 20.32 cm) diameters, can be measured using the spatial mapping features of a UV-Vis-NIR spectrophotometer fitted with a solids autosampler.

Agilent

Trusted Answers

Coated Wafer Mapping Using UV-Vis Spectral Reflection and Transmission Measurements

Using an Agilent Cary 7000 Universal Measurement Spectrophotometer (UMS) with Solids Autosampler

Author

Travis Burt

Farinaz Haq

Agilent Technologies, Inc.

Introduction

Spectral reflection (R) and transmission (T) are the fundamental measurements for characterizing the optical properties of materials and optical coatings. Mutli-angle Photometric Spectroscopy (MPS) measures the reflectance and/or transmittance of a sample across a range of angles (Θi) from near normal to oblique angles of incidence (AOI). The development in the field of MPS by Agilent Technologies, the Cary 7000 Universal Measurement Spectrophotometer (UMS), combines both reflection and transmission measurements from the same point on a sample's surface, without moving the sample between measurements. Alleviating the need for multiple accessories and accessory changeover or reconfiguration ensures unprecedented data quality and prevents sample non-uniformity effects or spectral inconsistencies that occur when multiple analysis techniques are used to perform a single measurement.

In this paper we describe a new autosampler capability for the Agilent Cary 7000 UMS with rotational (Φ) and radial (z) sample positioning control. The Agilent Solids Autosampler allows for the automated and unattended mapping of single large diameter samples (up to 8 in diameter). Examples are provided which demonstrate spatial spectroscopic information obtained on a zinc tin oxide (ZTO) layer deposited onto a 4 in diameter sapphire substrate to a resolution of 2 mm x 2 mm square. The method allows the band gap energy to be mapped across the diameter of the substrate.

Experimental

Instrumentation

- Agilent Cary 7000 Universal Measurement Spectrophotometer

- Agilent Solids Autosampler

The Cary 7000 UMS is a versatile new system designed for MPS applications over the UV-Vis-NIR wavelength range 250–2500 nm. MPS measures the absolute reflectance and/or transmittance of a sample across a range of angles from near normal to oblique incidence (*1*). The Cary 7000 UMS combines both reflection and transmission measurements from the same patch of a sample's surface in a single automated platform for angles of incidence in the range $5° \leq |\Theta_i| \leq 85°$. The Cary 7000 UMS also provides diffuse reflectance measurements of non-specular surfaces and diffuse transmittance measurements of translucent materials. The addition of an automated polarizer further enables accurate measurement at S, P or user specified polarization angles.

The accessory component of the Cary 7000 UMS, the Cary UMA (Universal Measurement Accessory), is available as an upgrade option for existing Cary 4000/5000/6000i UV-Vis-NIR spectrophotometer users.

The Solids Autosampler is an independently controlled sample holder designed specifically for the Cary UMA. It can be mounted inside the Cary UMA measurement chamber as shown in Figure 1a. In addition to the AOI control (Θ_i) provided by the UMS, the Solids Autosampler provides two additional degrees of freedom; radial (z) and rotational direction (Φ) about the incident beams axis (I_o). A variety of sample holders allow mounting of multiple individual samples (up to 32 x 1 in diameter) or single large diameter samples (8 in diameter). Figure 1b shows the 8 in diameter sample holder. The autosampler was operated in spatial mapping mode for the large sample characterization study of ZTO. In the mapping mode spectra can be collected at user defined points within the sample holder.

Figure 1a. Plan view of the Cary 7000 UMS measurement chamber with the Solids Autosampler installed.

Figure 1b. Image of the 8 in diameter sample holder.

Mapping analysis

The optical or electronic band gap properties of semiconductors are core to their effectiveness in end-use devices such as sensors (e.g. detectors) or emitters (e.g., LED's). The band gap energy of a semiconductor can be determined from diffuse reflection spectra when the material is in a powdered form[2] or from transmission spectra where an epitaxial semiconductor layer has been deposited on a transparent substrate.

In this experiment, the band gap energy was mapped across the diameter of a wafer coated with a ternary metal oxide by acquiring transmission spectra using a Cary 7000 UMS with Solids Autosampler. Transmission spectral were collected from 700 nm (1.7 eV) to 200 nm (7.8 eV) with a 4 nm spectral band witdth and 0.1 s signal averaging time. UV-Vis spectral data was acquired at 5 mm intervals from the bottom of the wafer (-40 mm) to the top (45 mm) as indicated in Figure 2b.

Samples

The sample was comprised of a graded zinc tin oxide (ZTO) layer deposited onto a 100 mm (4 in) diameter sapphire substrate thickness was 600 µm, Figure 2a. Zinc and tin metal targets were sputtered in an oxygen ambient atmosphere from opposite ends of the wafer simultaneously by high power impulse magnetron sputtering (HiPIMS) and direct current magnetron sputtering (DCMS) respectively producing a coating of approx 14 nm (140 Å). The epitaxial layer formed a graded ZTO layer stretching from almost pure tin at the bottom of the wafer to almost pure zinc the top as indicated in Figure 2b.

ZnO has a large direct band gap of ~ 3.4 eV at room temperature where tin has an optical band gap of 3.6 eV as SnO_2 (3). The optical band gap of the amorphous phase of ZTO has been reported as low as ~ 2.8 eV (4), which is of interest as it may be a suitable replacement for the widely used but relatively expensive indium tin oxide (ITO) in a range of applications including organic photovoltaics and flexible displays.

Figure 2a. 100 mm (4 in) diameter sapphire substrate coated with Zn/Sn.
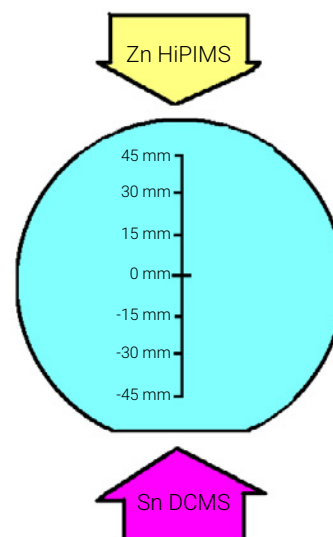

Figure 2b. Schematic of deposition direction and coordinate system with respect to wafer orientation. Tin (Sn) was deposited by DCMS and zinc (Zn) by HiPIMS. Spectral measurements were made at 5 mm intervals from -40 mm to 45 mm.

Results and discussion

Transmission spectra

Transmission spectra were collected at 18 evenly spaced (~5 mm) intervals through the diameter of the wafer from bottom to top position. The absorption edge of the transmission spectra (Figure 3a) can be seen to shift to lower frequencies at the top of the wafer where the Zn concentration is highest. Band gap was determined by extrapolating a linear fit through the absorption edge to zero absorption in a plot of (Absorption)2 vs eV. The intercept in eV at zero Abs was taken as the band gap energy. Figure 3b shows band gap energies determined through the diameter of the wafer. This profile can help to extract smaller samples from the wafer with very specific, targeted, band gap energies without the need to have precise control of the coating conditions.
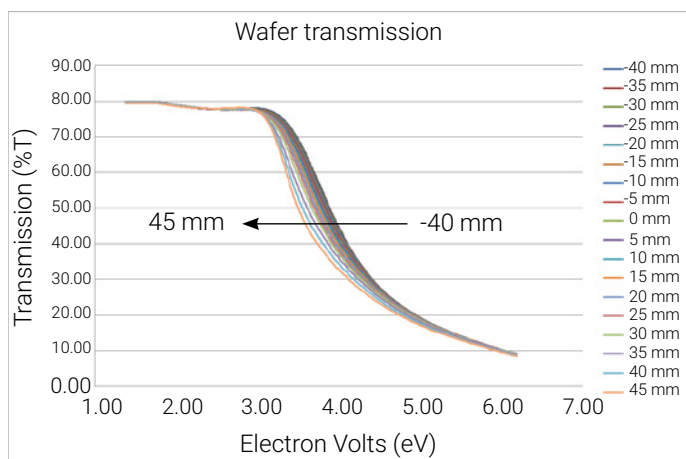
Wafer transmission

Figure 3a. Transmission spectra through wafer at 11 positions through its diameter, at 5 mm increments.
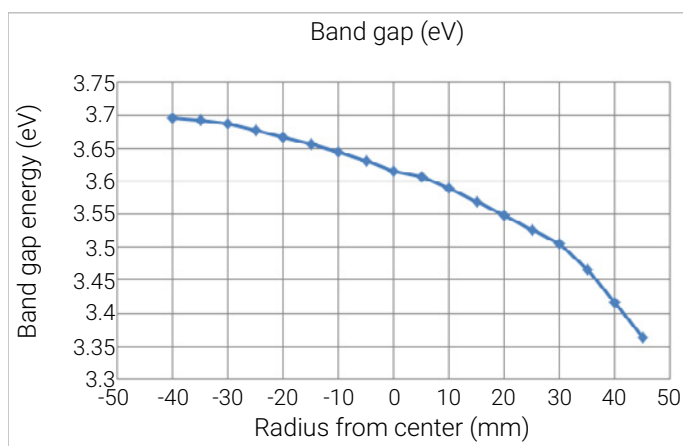
Band gap (eV)

Figure 3b. Band gap was determined from the intercept of the extrapolation of absorption edge, (Absorption)2 vs Energy (eV), to zero absorption.

Conclusion

The Agilent Cary 7000 UMS with Solids Autosampler has been used successfully for the large sample characterization of thin-film substrates. The autosampler was operated in spatial mapping mode for study of ZTO. The band gap energy of the ZTO substrate was mapped across the diameter of the wafer through the acquisition of transmission spectra. The data showed some variation; for example lower frequencies were observed at the top of the wafer where, as a result of the deposition process, the Zn concentration was highest.

As suitable replacements for relatively expensive substrates such as indium tin oxide (ITO) are being sought, materials with similar optical band gap energies can be characterized using this method.

It is expected that the Cary 7000 UMS and Solids Autosampler will prove to be a valuable tool for the characterization of optical materials, coatings and components in a wide range of industrial and laboratory applications.

Acknowledgements

References

1. Death, D.L.; Francis, R.J.; Bricker, C.; Burt, T.; Colley, C. *The UMA: A new tool for Multi-angle Photometric Spectroscopy.* Optical Interference Coatings (OIC) OSA Topical Meeting, Canada. 2013.

2. Uchida, S.; Yamamoto, Y.; Fujishiro, Y.; Watanabe, A., Ito, O.; and Sato, T. Intercalation of titanium oxide in layered $H_2Ti_4O_9$ and $H_4Nb_6O_{17}$ and photocatalytic water cleavage with $H_2Ti_4O_9/(TiO_2, Pt)$ and $H_4Nb_6O_{17}/(TiO_2, Pt)$ nanocomposites *J. Chem. Soc.***1997**, Farady Trans., 93, 17, 3229.

3. Batzill, M.; Diebold, U. Review: The surface and materials science of tin oxide *Progress in Surface Science.* **2005** 79, 47–154.

4. Madambi, K.; Jayaraj; Kachirayil J.; Saji; Nomura, K.; Kamiya, T.; Hosono, H. Optical and electrical properties of amorphous zinc tin oxide thin films examined for thin film transistor application. *J. Vac. Sci. Technol.* **2008**, B 26, 495.
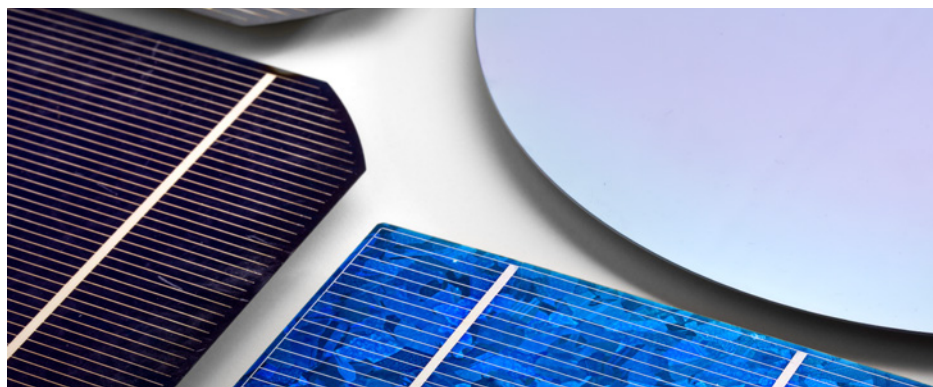
www.agilent.com/chem

Agilent

Trusted Answers

Agilent

Trusted Answers

Investigating the Angular Dependence of Absolute Specular Reflection

Using the Agilent Cary 7000 universal measurement spectrophotometer (UMS)

Authors

Travis Burt and Chris Colley
Agilent Technologies, Inc.
Mulgrave, Victoria
Australia

Introduction

When characterizing an optical sample it is common to measure reflection or transmission properties at a single angle of incidence (AOI). However, for a more complete characterization of the sample, it is desirable to measure reflection and/or transmission at multiple AOI's as this can provide a much deeper insight into the sample's optical properties.

This application note illustrates how the Agilent Cary 7000 universal measurement spectrophotometer (UMS) can provide rapid and automated absolute specular reflection measurements at multiple AOIs. The value of using three-dimensional (3D) plots and two-dimensional (2D) contour plots to visualize the data is also demonstrated.

Experimental

Sample

The sample was a large silicon wafer measuring 200 mm in diameter and 0.80 mm in thickness. A proprietary optical coating had been applied to the front surface after polishing. A summary of the sample and collect conditions is given in Table 1.

Instrumentation

The data were collected using the Cary 7000 UMS, which is a highly automated variable-angle absolute specular reflectance and transmittance system. With the Cary 7000 UMS, operators have independent motorized control over the angle of incidence onto the sample and the position of the detector, which can be freely rotated in an arc around the sample. The independent control of sample rotation and detector position allows rapid, accurate, and unattended measurements.

Traditionally, reflectance and transmittance measurements have been performed using spectrophotometers fitted with different accessory attachments. In practice, this can lead to different areas of the sample being tested due to illumination beam geometry variations between measurement modes (accessories) and movement of the illumination beam over the sample.
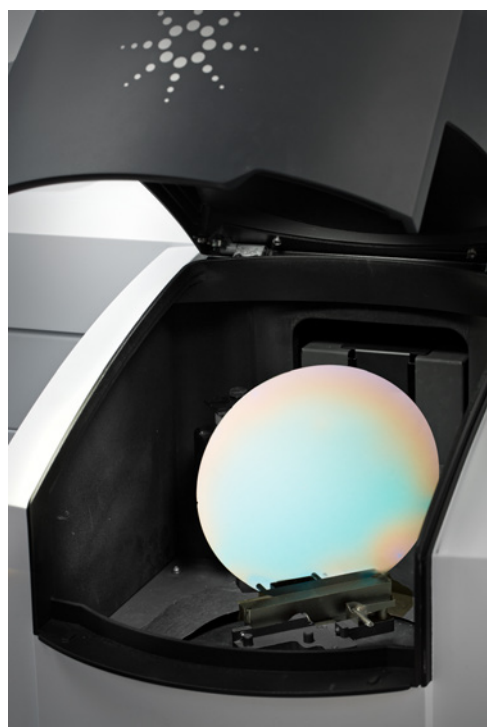

Figure 1. Agilent Cary 7000 UMS with a 200 mm diameter silicon wafer sample mounted in the measurement chamber.

If the deposition process produces a film with a nonuniform thickness, it is reasonable to expect that reflectance and transmittance measurements would be affected.

With the development of the Agilent Cary 7000 UMS, it is now possible to measure T and R at the same sample point, without moving the sample, thus overcoming one source of artifacts on the results.

Measurements

Specular reflection measurements were made with AOIs from 6° to 86° in 1° increments. The polarization of the light incident on the sample was controlled with an automated rotatable wire grid polarizer. Reflection with both s- and p-polarization was measured.

The collect conditions were set up using the Cary WinUV software method editor. Only two baselines are required at the start of the full data collection sequence, one for s- and one for p-polarization. These baselines were used for all angles, and the software applied the appropriate baseline to the individual collected spectra. In contrast, other systems require a unique baseline for each polarization at each angle, which dramatically increases the total time of collect. Once the two baselines had been collected, the system was left unattended to collect the entire data set.

As has already been noted, the silicon wafer was particularly large at 200 mm diameter. The Cary 7000 UMS is designed to accommodate samples as large as 275 mm in diameter enabling very high grazing angles of incidence to be measured. With the largest possible samples, angles close to 90° can be measured without the incident light "falling off" the sample.

Table 1. Agilent Cary 7000 UMS collect conditions.

Parameter	Value
AOI	6° to 86° in 1.0° intervals
Wavelength Range	2,500 to 250 nm
Data Interval	UV-Vis 1.0 nm, NIR 4.0 nm
Spectral Bandwidth	UV-Vis 4.0 nm, NIR 4.0 nm
Signal Averaging Time	0.26 sec
Polarization	s and p
Incident Beam Aperture	3° × 3° (vertical × horizontal)

Results and discussion

Specular reflectance

Figure 2 shows the absolute specular reflection spectra with angles of incidence ranging from 6° to 86° in 1° increments for s-polarized light. A similar plot was generated for p-polarized light as well (not shown in this document).

Analyzing such a large number of spectra can be a significant challenge. Figures 3 and 4 show 2D contour plots and 3D plots generated using Scilab software[1], respectively, for the same data set. It can be seen that the reflective properties, in terms of the positions of minima and the associated %R values, are highly dependent on AOI.
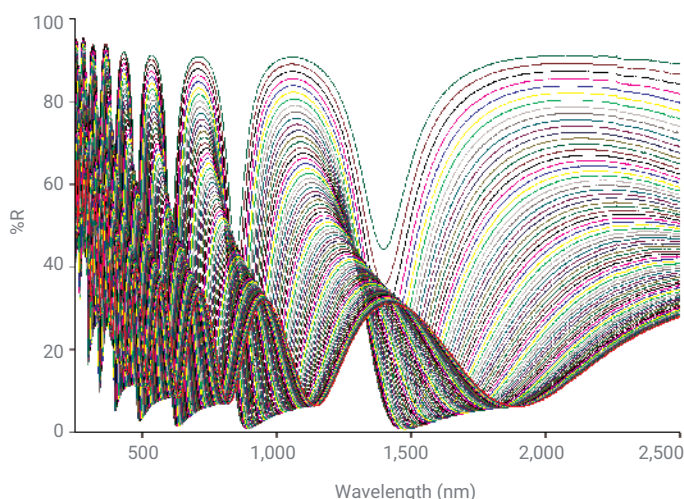

Figure 2. Absolute specular reflectance of s-polarized light from the silicon wafer from 6° AOI to 86° AOI at 1° intervals.

For example, in the infrared region, at near normal AOI, there is a broad minimum centered at approximately 1,900 nm. At much higher angles of incidence, at approximately 70°, the minimum is centered at approximately 1,400 nm. In addition, the minimum is narrower and reaches a %R value that is much closer to zero.

Depending on the intended end use of reflective coatings and the associated performance requirements in terms of AOI, spectral region, and %R, these types of observations can be fed back into coating design. Measuring the coating at one AOI only, as is common, gives no indication of this strong angular dependence.
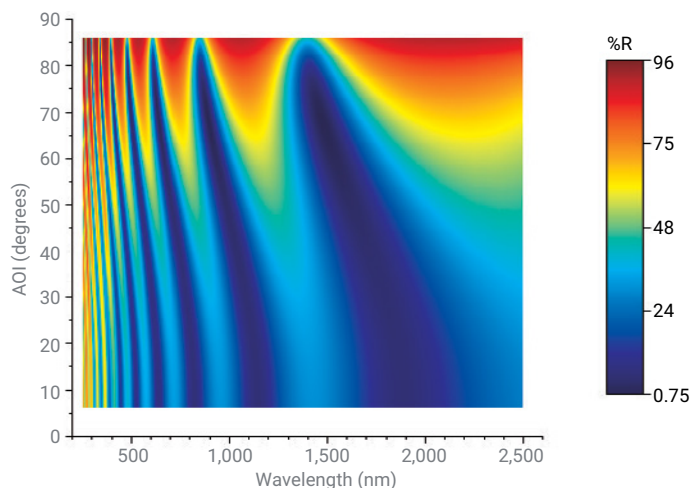

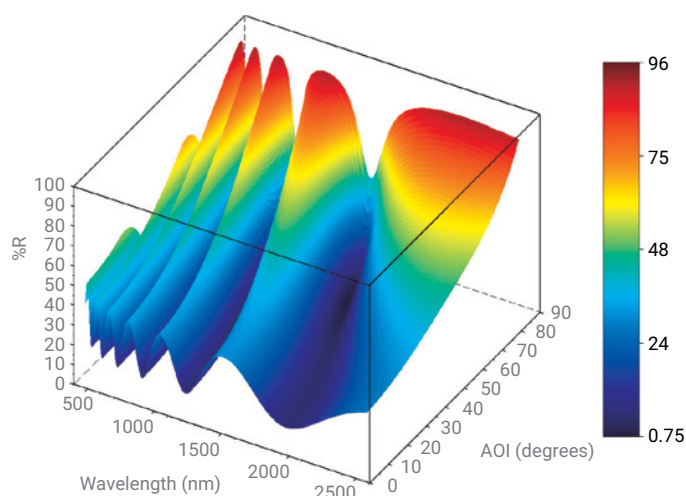**Figure 3.** 2D contour plot of the same data displayed in Figure 2.

Figure 4. 3D plot of the same data displayed in Figure 2.

Conclusion

It has been demonstrated that the Agilent Cary 7000 UMS can be used to automatically collect high quality spectra for a large, coated sample at a wide range of AOIs, in both s- and p-polarization. The measurement is made under complete software control and, once the sample is mounted, data collection is entirely unattended. The complete characterization of this sample over a wide wavelength range, AOI and polarization allowed greater insight into the angular dependence of the optical coating.

Furthermore, using 3D and 2D contour plots to visualize the large data sets provides a more thorough understanding of the properties of an optical coating. This valuable information can be used to aid coating design and optimization.

References

1. Scilab is free open source software available at
   https://www.scilab.org

www.agilent.com/chem/cary7000ums

Agilent
Trusted Answers

Application Note

Materials

Agilent

Trusted Answers

Measuring the Optical Properties of Photovoltaic Cells

Using the Agilent Cary 5000 UV-Vis-NIR spectrophotometer and the External DRA-2500

Authors

Dr. Andrew R. Hind and
Dr. Marcus Schulz
Agilent Technologies, Inc.

Introduction

The term "photovoltaic" stems from the Greek word for light (photo) and the physicist Volta[1] (the inventor of the electric battery). It is applied to the direct conversion of sunlight into energy by means of solar cells. The conversion process is based on the photoelectric effect (discovered by Bequerel[2] in 1839), which involves the release of positive and negative charge carriers in a solid when light strikes its surface.

Solar cells are composed of various semiconducting materials, with the majority (>95%) of solar cells manufactured made primarily of silicon. To produce a solar cell, the semiconductor is "doped". Doping involves the intentional introduction of other elements, with the aim of obtaining a surplus of either positive (p) or negative (n) charge carriers within the semiconductor material. When two differently contaminated semiconductor layers are combined, a so-called "p-n" junction results at the boundary of the layers. This junction results in an electric field, which leads to the separation of the charge carriers that are released by light. By using metal contacts, an electric charge can be drawn and, if the outer circuit is closed, direct current flows. Silicon solar cells are generally 10 × 10 cm in size, with a transparent anti-reflection (AR) coating used to protect the cell and decrease reflective losses on the cell surface. Figure 1 shows a schematic diagram of a typical photovoltaic cell.
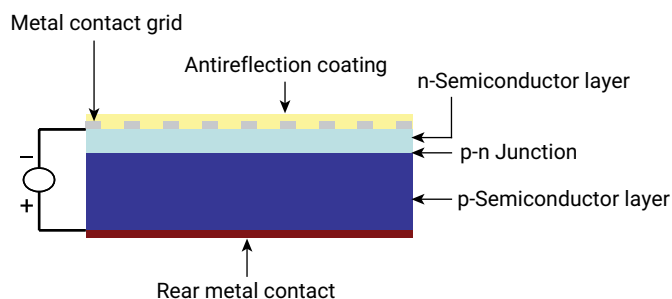
Figure 1. Schematic diagram of a typical solar cell.

In any photovoltaic cell, the current intensity obtained increases with higher light flux. And, while many factors can affect the efficiency of a particular cell, reflectance of light at the surface of the cell is a parameter of obvious importance. To perform these types of reflectance measurements, a high-performance UV-Vis-NIR spectrophotometer equipped with integrating sphere is required. An integrating sphere is designed to collect reflected radiation (diffuse or total) from a solid surface (such as a photovoltaic cell). Using the appropriate sampling geometry, integrating spheres can also be used for the measurement of the diffuse transmission properties of solar cells.

This application note demonstrates how the reflectance properties of a solar cell and its precursors can be measured at various stages of the manufacturing process using an Agilent Cary 5000 UV-Vis-NIR spectrophotometer equipped with an External Diffuse Reflectance Accessory 2500 and Small Spot Kit attachment.

Experimental

Instrumentation[3]

– Agilent Cary 5000 UV-Vis-NIR spectrophotometer

– Agilent External DRA-2500

– Small Spot Kit attachment

Conditions

The External DRA-2500 was installed into the spectrophotometer and aligned.[4] UV-Vis-NIR spectra were, in general, acquired in the region of 250 to 2,500 nm using appropriate baseline correction (Zero/baseline correction). Indicative instrumental parameters were as follows: 2 nm SBW, 0.1 s SAT, 1 nm data interval (UV-Vis) and Energy 3, 0.2 s SAT, 3 nm data interval (NIR); double-beam mode using full slit height. The reflectance spectra were collected using a Cary 5000 UV-Vis-NIR spectrophotometer equipped with an External DRA-2500 and a Small Spot Kit when small beam images were required.

Results and discussion

Figure 2 shows diffuse reflectance spectra of the finished solar cell and its precursors. Obvious spectral differences are evident between the uncoated, textured wafer (TS3), the AR-coated wafer (TS2), and the "finished" wafer (TS4) with metal contact grid (see Figure 3). The spectra were acquired at two different locations on each sample to test for surface homogeneity.
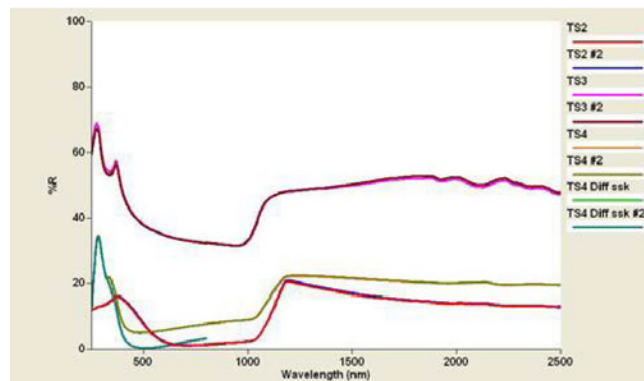

Figure 2. UV-Vis-NIR diffuse reflectance spectra of solar cells.
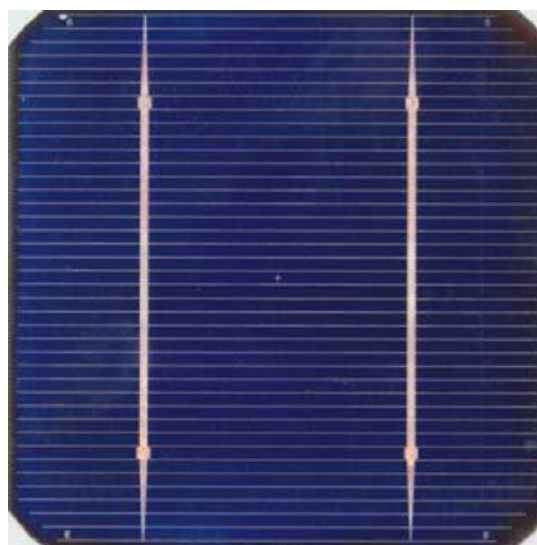
Figure 3. A finished solar cell with metal contact grid and anti-reflection coating.

Furthermore, additional differences are evident between the average reflectance spectrum of the finished cell (TS4, where the area sampled includes both cell surface and metal contact grid), and the spectrum of the cell surface only (TS4 Diff ssk, without reflectance contribution from the reflective metal contacts). This highlights the advantage of being able to reduce beam size to the point where it is small

enough (~1 mm diameter) to allow the collection of spectra from an area between the metal contacts of the grid itself. Not surprisingly, the results confirmed the relatively high reflectivity of the metal grid compared to the active surface of the cell itself.

Conclusion

Both the reflectance and transmission properties of solar cells are readily measured using UV-Vis-NIR spectrophotometry. Using a high-performance spectrophotometer (such as the Agilent Cary 5000 UV-Vis-NIR spectrophotometer) equipped with an integrating sphere permits the fast acquisition of high quality spectra (high resolution, low noise). For the measurement of small areas of solar cells, some type of focusing optics are required to reduce the size of the beam image focused on the sample surface. The External DRA-2500 with Small Spot Kit attachment available from Agilent allows such measurements to be made.

References

1. Allssandro Volta (1745–1827)

2. Alexandre-Edmond Bequerel (1820–1891)

3. Part numbers:

Product	Part Number
Agilent Cary 5000 UV-Vis-NIR spectrophotometer	G9825AA
External DRA-2500	G9832A
Small Spot Kit	G9850A#006

4. Cary WinUV Software, online help, Version 3.0.

www.agilent.com/chem/cary5000

Agilent

Trusted Answers

Glass

The visual transparency and structural rigidity properties of glass have been appreciated for thousands of years. In the early 20th century, the development of cheaper, float glass production processes transformed glass into an everyday material for buildings and automobiles. More recently, the ultraviolet and infrared properties of glass used in construction are being investigated. New materials could help to better regulate ambient temperatures and reduce the amount of energy needed to heat or cool a building. Reflectance, transmittance, and absorption of glass products can be measured using a UV-Vis-NIR spectrophotometer over the critical solar wavelengths from 250 to 2500 nm. Quick and simple spectrophotometric measurements can be made using standard sample holders, diffuse reflectance accessories, or multi-angle specular reflectance/transmission accessories.
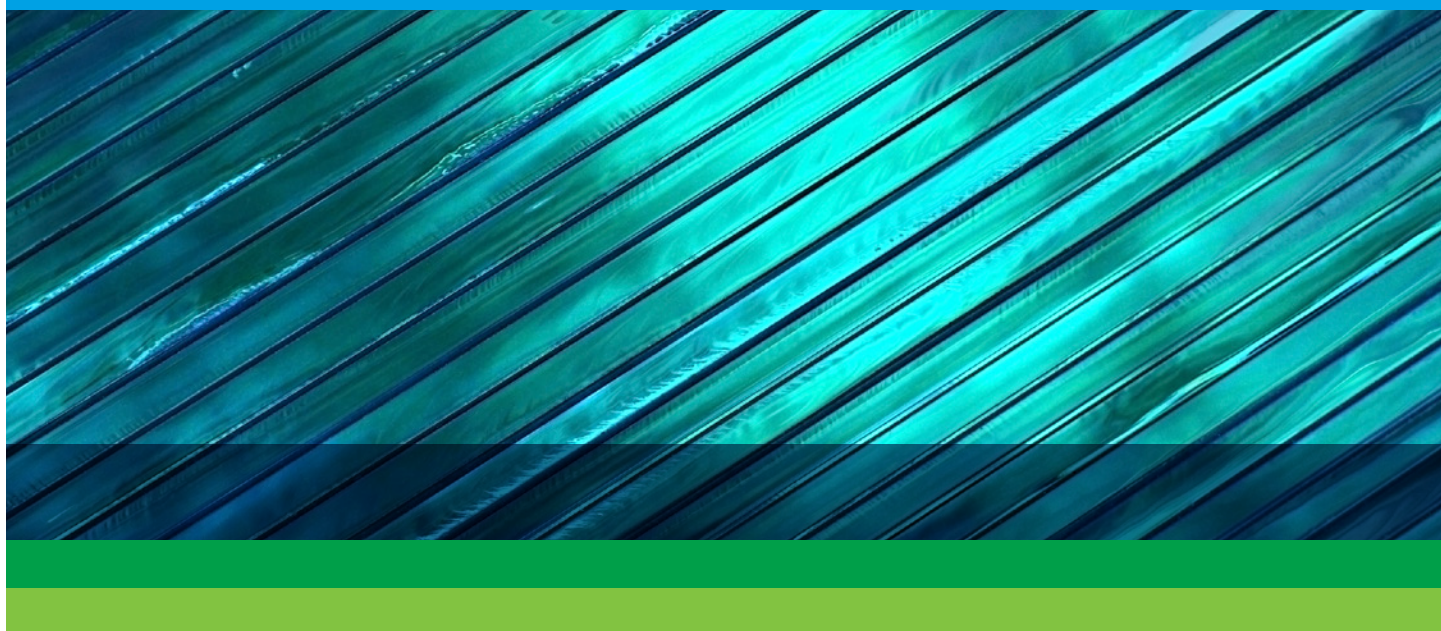
Agilent

Trusted Answers

Automated, Unattended, Multi-Angle Transmission and Absolute Reflection Measurements

Using the Agilent Cary 7000 universal measurement spectrophotometer (UMS)

Authors

Travis Burt and Chris Colley
Agilent Technologies, Inc.
Mulgrave, Victoria
Australia

Introduction

Glass and glass-based products have been in use for thousands of years, providing form and function to people all around the world. The last century witnessed a significant acceleration in both the production and variety of uses of glass products, predominantly due to the advent of automobiles, skyscrapers, domestic housing, and consumer packaging. This increase in demand has been met by the development and refinement of high-volume commercial float glass production starting in the 1950s.

More recent development in composite products and specialty coating technology has allowed glass products to be tailored to very specific functional needs, environmental conditions, and lighting demands. In addition, developers and users today are equally focused on the energy efficiency of the product and the fit-for-purpose general requirements to block UV radiation, transmit visible light, repel thermal radiation (heat) in summer, and retain heat in winter.

Nationally and internationally recognized standards have been developed to ensure that measurement and classification of glass products is performed in a controlled and comparable manner. The use of three such standards will be used in this application note using an Agilent Cary 7000 universal measurement spectrophotometer (UMS):

 – **ISO 9050 (2003)**: Glass in building — Determination of light transmittance, solar direct transmittance, total solar energy transmittance, ultraviolet transmittance, and related glazing factors

 – **EN 410**: Glass in building — Determination of luminous and solar characteristics of glazing

 – **ISO 13837 (2008)**: Road vehicles — Safety glazing materials — Method for the determination of solar transmittance

Experimental

Samples

A variety of automotive and architectural glazing products were measured and characterized using a Cary 7000 UMS. The Cary 7000 UMS is a powerful and versatile spectral characterization tool that provides multi-angle transmission and absolute reflection measurements in a motorized, fully automated package.

The Cary 7000 UMS performs transmission and absolute reflection measurements from the same point on the sample — without having to move the sample between measurements. The *in situ* measurement of %T and %R from identical locations on the sample permits highly accurate absorptance (A = 1 − T − R) data to be calculated providing far greater insights into substrate (internal transmission) and coating properties. This capability ensures the highest quality R and T data for QA/QC operation as well as providing a better understanding for the research and development of glazing and coated glazing products.

In addition to the versatile T, R, A collections, dedicated calculations can be executed for the major international and regional glazing standards. In this application example, a complete set of transmission and reflection data was collected using standard glazing methods supplied with the Cary WinUV version 6 software. Calculations were performed using the in-built glass calculation and reporting tool. Examples of the test report, spectral data, and parameters calculated are shown in the following section.

Instrumentation

Agilent Cary 7000 Universal Measurement Spectrophotometer (part number G6873AA)

The Cary 7000 UMS is a highly automated UV-Vis-NIR spectrophotometer system. The Cary 7000 UMS performs variable angle transmission and absolute reflectance measurements. The linearly polarized beam that is incident on the sample can be used to measure in transmission, and by rotating the detector assembly about an axis through the sample and perpendicular to the plane of incidence, in reflection.

Results and discussion

Each of the standards have their specific reporting parameters, which were automatically calculated and displayed in the Cary WinUV software report. Furthermore, each set of data was collected automatically and unattended, highlighting the true productivity benefit provided by the Cary 7000 UMS. After the initial configuration and baseline collection, each collection was set and executed in <3 minutes. Testing requiring reflection and transmission measurement on the same sample required no further user interaction as the collection was run for any user-specified angle of incidence or reflection. As shown in Figures 1 to 3, the high quality data lead to accurate characterization of these types of samples.

EN 410

EN 410 calculations:
Color Rendering, Light Reflectance, Light Transmittance,
Total Solar Energy Transmittance (Solar Factor) and Shading
Coefficients, UV Transmittance

A

Scan Analysis Report

Report Time :	Mon 03 Jun 02:39:24 PM 2013
Method	
Batch:	C:\Documents\glass sample.BSW
Software version:	6.0.0.1547
Operator:	

Sample Name: Sample S +-60 +-180

Test Report	Determination of Luminous and Solar Characteristics of Glazing
EN410 Glass in Building	5_2 and 5_5

Light Transmittance of Glazing	
780 nm - 380 nm	0.6767
UV Transmittance of Glazing	
380 nm -300 nm	0.5110

This report was generated from data
supplied to EN410 Light and UV
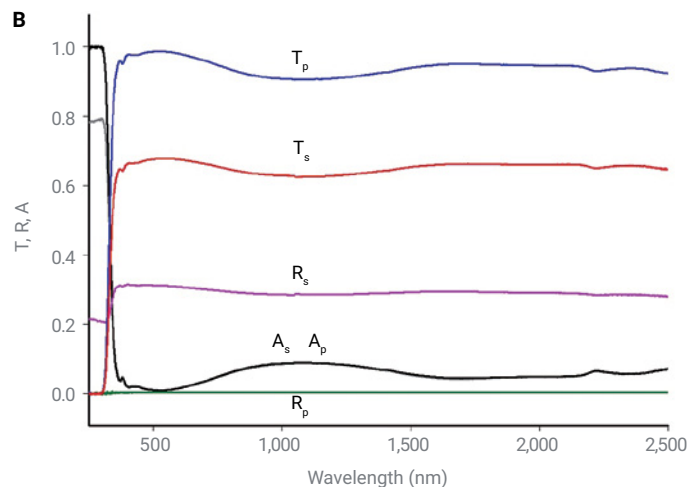Transmittance 5_2 and 5_5_Agilent.xlsx.

B

Figure 1. (A) Example of a EN 410 test report generated for an architectural glass sample. (B) Transmission, reflection, and the associated absorptance spectra (A = 1 − T − R) for an architectural glass sample (2 mm thick). Both s- and p-polarized spectral data were collected at 60° angle of incidence.

ISO 9050

ISO 9050 calculations:
CIE Damage Factor, Light Reflectance, Light Transmittance,
Skin Damage Factor, Total Solar Energy Transmittance
(Solar Factor), UV Transmittance

A

Scan Analysis Report

Report Time :	Mon 03 Jun 02:47:38 PM 2013
Method	
Batch:	C:\Documents\glass sample.BSW
Software version:	6.0.0.1547
Operator:	

Sample Name: Sample S +-7 +-14

Test Report	Determination of Luminous and Solar Characteristics of Glazing
ISO9050 Glass in Building	3_5

Solar direct Transmittance	0.823
Solar Direct Reflectance	0.074
Direct Solar Absorptance	0.109
Secondary Heat Transfer factor of glazing towards inside*, Single Glazing	0.028
Secondary Heat Transfer factor of glazing towards outside*, Single Glazing	0.081
Total Solar Energy of Transmittance (Solar Factor)	0.851

This report was generated from data supplied
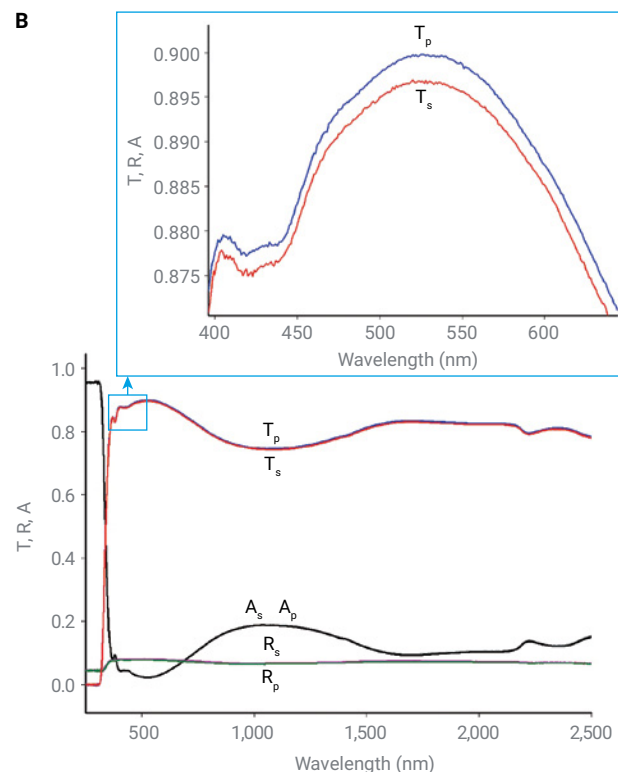to ISO9050 Solar Energy Transmittance
3_5_Agilent.xlsx.

B

Figure 2. (A) Example of an ISO 9050 test report generated for an architectural glass sample. (B)Transmission, reflection, and the associated absorptance spectra (A = 1 − T − R) for an architectural glass sample (2 mm thick). Both s- and p-polarized spectral data were collected at 7° angle of incidence. Inset: A closer look at the T_p and T_s spectra in Figure 2B reveals an expected separation of approximately 0.003 between s- and p-polarized spectra.

ISO 13837

ISO 13837 calculations:
Solar UV Transmittance $T_{UV}(400)$, Solar Direct Transmittance $T_{DS}(1.5)$, Solar UV Transmittance $T_{UV}(380)$, Solar Direct Transmittance $T_{DS}(1.0)$

Scan Analysis Report

Report Time :   Mon 03 Jun 03:13:02 PM 2013
Method
Batch: C:\Documents\glass sample.BSW
Software version: 6.0.0.1547
Operator:

Sample Name: Sample S +-45 +-180

Test Report   Road Vehicles Safety Glazing Materials

Solar UV Transmittance TUV(400)   61.78
Solar Direct Transmittance TDS(1.5) 72.50
Solar UV Transmittance TUV(380)   51.69
Solar Direct Transmittance TDS(1.0) 71.47

This report was generated from data supplied
to ISO13837_Agilent.xlsx.

Figure 3. Example of an ISO 13837 test report generated for an automotive glass sample.

Conclusions

The Agilent Cary 7000 UMS, standard software methods, and reporting tools were used to calculate the optical properties of three different glass products used in automotive and building products. The optical properties were reported according to the regional and international glass standards, ISO 9050, ISO 13837, and EN 410. The Cary 7000 UMS is a powerful, productive, and ideal turn-key solution for routine QA/QC testing and research and development of glass and glazing products.

www.agilent.com/chem/cary7000ums

Agilent
Trusted Answers

Catalysis

Catalysts are compounds that increase the rate of chemical reactions. They occur naturally in living systems (e.g., enzymes). Synthesized catalysts have a range of uses such as boosting food production, driving yields of fine or bulk chemicals, or improving energy-producing reactions. Catalysts in powder form comprise either coarse sand grain-sized particles or nanoparticles. Light that is diffusely reflected from the surface of the particles can be measured by UV-Vis-NIR. The data provides insights into the molecular and electronic structure of the catalyst, as well as its effectiveness. In cases where temperature or atmospheric gasses play a significant role in catalysis, efficacy control over these variables also becomes essential. Cary UV-Vis-NIR accessories that facilitate studies of catalysis reactions include diffuse reflectance accessories (DRAs) and the Praying Mantis accessory with a high-temperature reaction chamber.

Agilent

Trusted Answers
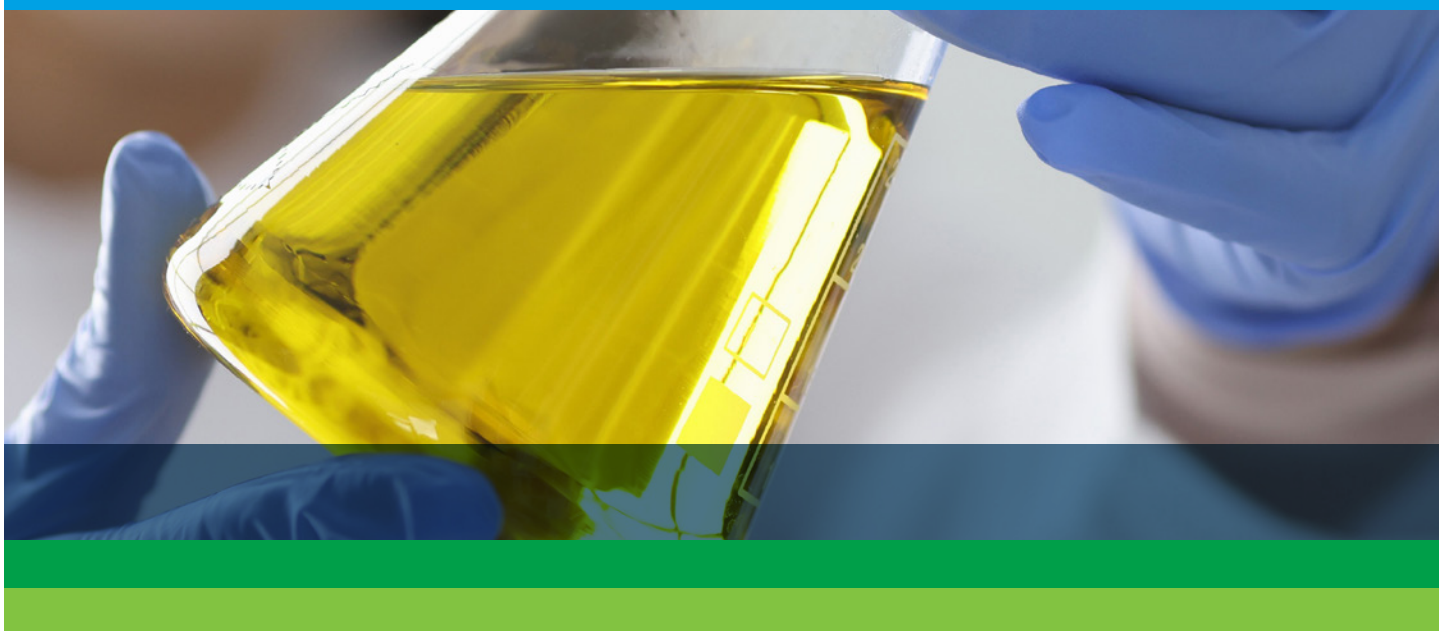
Measurement of Diffuse Reflection from Catalyst Powders

Using the Praying Mantis accessory and Agilent Cary 5000 UV-Vis-NIR spectrophotometer

Authors

Eric Marceau
UPMC — Laboratoire de
Réactivité de Surface
(UMR 7197 CNRS)
Paris, France

Caroline Perier
Agilent Technologies
Les Ulis, France

Travis Burt
Agilent Technologies
Melbourne, Australia

Introduction

Aluminum oxide (Al_2O_3), commonly known as alumina, is a widespread naturally occurring compound that has a broad range of industrial applications. Besides its use as a pigment or abrasive, alumina also plays a vital role as a catalyst support for desulfurization or hydrogenation reactions. In the latter case, the active phase on the catalyst often consists of nickel metal nanoparticles. The interactions initially established between nickel (II) salt and the alumina surface during the first steps of the Ni/Al_2O_3 catalyst preparation ultimately determine the active phase dispersion and the activity of the catalyst. It is thus of prime importance to follow the evolution of nickel speciation upon thermal treatments to improve the catalyst preparation.

The Agilent Cary 5000 UV-Vis-NIR spectrophotometer coupled with a Praying Mantis diffuse reflectance accessory is suited for gaining greater understanding of the chemical transformations taking place over wide temperature ranges. UV-Vis-NIR spectroscopy allows investigating electronic absorption spectra of transition metal ions. The spectra are interpreted by the number and position of absorption bands, which provides the electronic configuration of the element as well as the nature and symmetry of its chemical environment. Moreover, the near-infrared part of the spectrum provides information on the narrow IR overtone and combination bands originating from the metal ligands or from the support, which may effectively complement mid-range IR spectra.

The flexibility of the Praying Mantis sampling accessory allows reflection studies on solid samples within an environmental cell where temperature and gas atmosphere can be controlled. In this study, samples were measured using a small volume powder cup of the reaction chamber set inside the Praying Mantis. The Praying Mantis accessory gives results that are qualitatively very similar to an alternative diffuse reflectance accessory — an integrating sphere — but with the advantage of the measurement geometry being downward-looking, permitting the samples to be mounted horizontally, and with an ability to measure very small samples (approximately 0.1 cm^3) without loss of performance.

Further to its flexibility, the Cary UV-Vis-NIR system delivers a very high level of data for small power volumes. The Praying Mantis DRA uses mirrors rather than a sphere, which has a reflective coating. This gives better optical control over illumination and detection conditions, creating a highly efficient system over a defined range of reflection angles. This type of measurement is always made as a "percent of reference reflectance", making it qualitative in nature; the result is dependent on the reference material used. But, similar results can be obtained from the two approaches.

A primary advantage of Cary UV-Vis-NIR spectrophotometers is their ability to work with very small signals and very low light levels (very high absorbance or very low transmittance/reflectance). High-precision readings can be obtained even where the sample has low reflectance or when measurements are made under extreme sampling conditions, such as with the reaction chamber.

Experimental

Instrumentation

All readings were made using a standard Cary 5000 UV-Vis-NIR spectrophotometer (Figure 1) with a Praying Mantis accessory (Figure 2) fitted with a high-temperature reaction chamber, which had been mounted and aligned for use with the standard powder cell holders. The windows of the reaction chamber were SiO_2. The reference spectrum was collected on PTFE under ambient conditions (20 °C), and air flow was used for sample measurements.

Figure 1. Agilent Cary 5000 spectrophotometer.

Figure 2. Praying Mantis accessory with alignment tools and powder cell sample cups.

Reaction chamber

The reaction chamber (Figure 3) enables a reaction gas to be introduced and reacted with the sample so that the reactions can be studied *in vivo*, reaction rates determined, and intermediate and reaction products identified. The reaction chamber is enclosed with a dome with three windows — two for the spectrometer radiation to enter and exit the chamber and the third for viewing, illuminating, or irradiating the sample. This enables the use of the reaction chambers for photochemical studies. The standard material provided with all three windows is UV quartz.
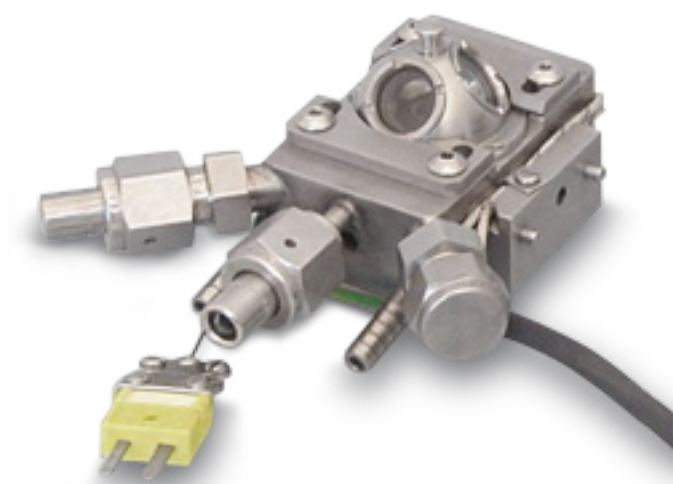

Figure 3. Reaction chamber.

Results and discussion

Spectral results are presented in Kubelka-Munk (F(R)) units versus wavelength in nanometers. F(R) are a mathematical transformation of the %R to aid in the correlation between reflectance and concentration.

Ni^{2+} ions in an octahedral geometry exhibit three absorption bands, two in the visible region (around 400 and 600 nm) and a broader one in the NIR region (around 1,200 nm). Shifts of the 390 nm band with temperature up to 110 °C evidence the changes around nickel ions upon transformation of hydrated nickel nitrate to nickel hydroxynitrate, while NiO forms above 230 °C.

Spectra in the NIR range both highlight development of hydroxynitrates between room temperature and 110 °C, (shift of the 1,153 nm band to 1,240 nm), but also dehydration of the nickel salt and support (loss of the -OH overtone band at 1,450 nm). Two more bands by adsorbed water and alumina hydroxyl groups are found at 1,950 and 2,300 nm.

The dehydration process is clearly seen through the decrease of the initially intense band at 1,950 nm, with some hydroxyl groups remaining on the alumina surface after thermal treatment at 250 °C.
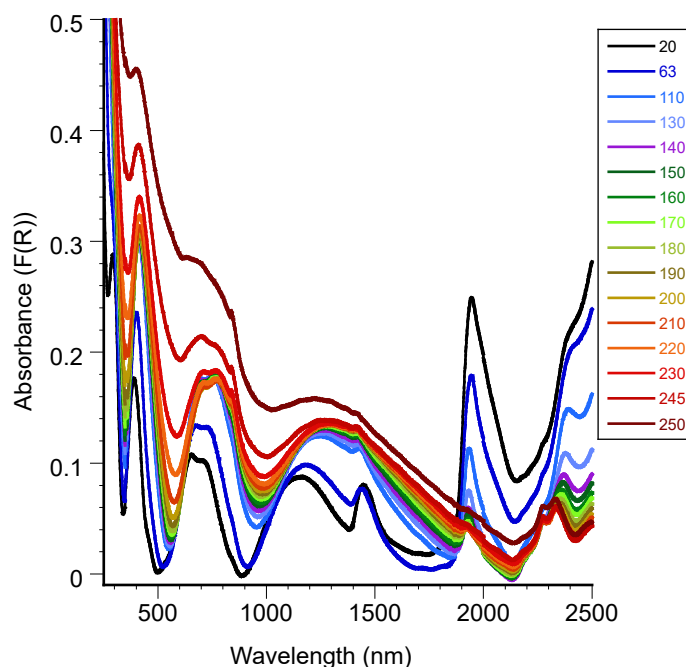

Figure 4. Praying Mantis in an Agilent Cary 5000 UV-Vis-NIR (overlaid scans). Thermal transformations of $Ni[H_2O]_6(NO_3)_2/Al_2O_3$ from 20 °C up to 250 °C.
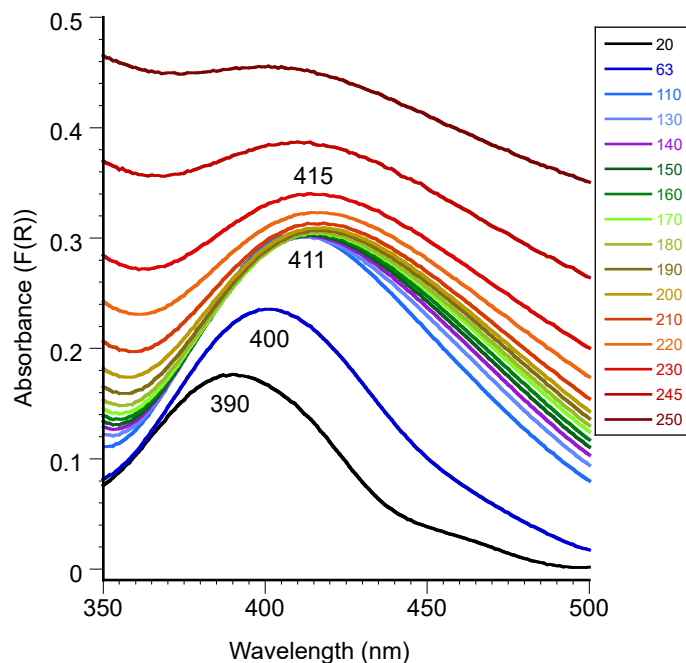
Figure 5. UV-Vis range.
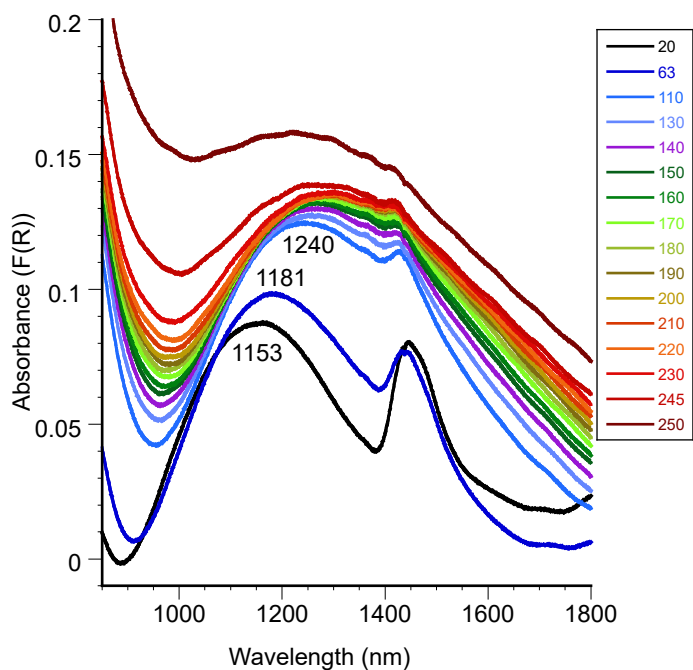
Figure 6. NIR range.
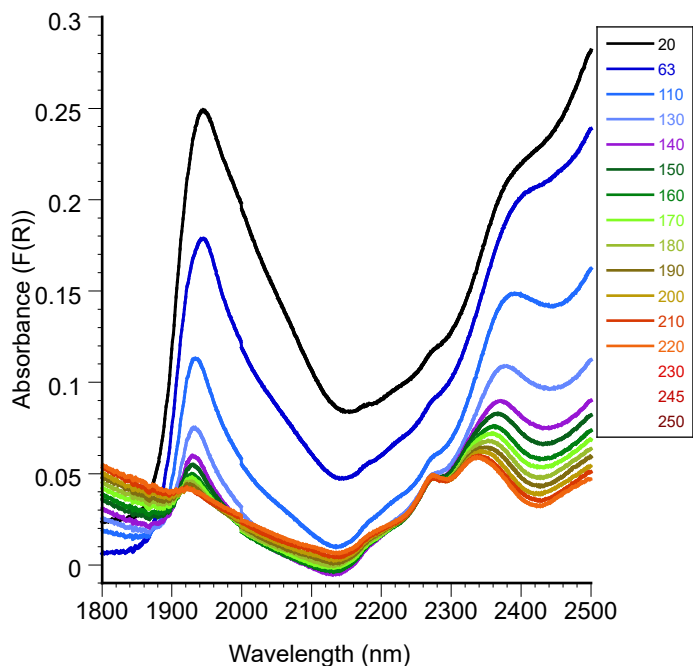
Figure 7. NIR range up to 1,800 nm.

Conclusion

The results demonstrate the use of the Agilent Cary 5000 UV-Vis-NIR system in the analysis of a small volume of catalyst powder samples over temperatures from 20 to 250 °C. The combination of the wide dynamic range of the Cary 5000 and excellent signal-to-noise ratio evidenced the transformation of nickel salt and dehydration of the supported system using a high-temperature reaction chamber in combination with the Praying Mantis accessory. This makes diffuse reflectance a valuable tool for studying powders involved in heterogeneous catalysis or reactions at the gas-solid interface.

www.agilent.com/chem/cary5000

Agilent

Trusted Answers

Personal Protective Equipment (PPE)

Personal protective equipment is mainly associated with workplace safety and includes items such as safety helmets, gloves, eye, hearing, or respiratory protection, high-visibility clothing, safety footwear, and harnesses. Spectrophotometry is especially useful for the assessment of PPE designed to protect against strong light sources (natural or manufactured) and electromagnetic radiation in both workplace and domestic settings. Applications of domestic protective materials include clothing, sunscreen, and sunglasses while industrial PPE includes laser goggles, welding masks, and viewports. Manufacturers and distributors of PPE must often comply with regulatory standards and/or QA requirements, so need to use reliable and accurate molecular analysis methods.

Application Note

Materials

Agilent

Trusted Answers

The Measurement of High Optical Densities in the Near-Infrared

Authors

Andrew R Hind Ph.D.
Agilent Technologies, Inc. UK

Jan Wuelfken Ph.D.
Agilent Technologies, Inc
Germany

Abstract

The optical densities of various materials used in the manufacture of laser safety eyewear have been determined in the NIR. The lens materials were measured over wavelength ranges corresponding to the laser wavelengths for which the eyewear was designed (InGaAs, 980 nm and Nd:YAG, 1064 nm). Prior to measurement, a variety of filters of known optical density were used to validate the photometric performance of the spectrophotometer. Using the addition of filters technique, photometric range, accuracy and linearity were demonstrated up to 8 Absorbance units at 1200 nm in the near-infrared.

Introduction

The measurement of high optical density (or absorbance) in the NIR is of significant importance to scientists and engineers in applications ranging from the rapidly expanding area of biophotonics to the manufacture of designer sunglasses. Other areas where measurement of high optical density is important include the design, production and validation of bandpass, blocking and cut-off filters, quantitative analysis of strongly absorbing liquid media (such as potassium permangenate [1]) and the measurement of turbid biological samples (such as those containing cytochrome P450[2]). Central to the ability to make these high optical density measurements are the photometric accuracy, linearity and dynamic range of the spectrophotometer in question.

Photometric linearity determines how accurately a spectrophotometer measures absorbance with increasing optical density or concentration. If an instrument has poor linearity, calibration curves (for instance) may deviate from linearity at high absorbance levels, reducing the photometric range of the instrument and accuracy of high optical density measurements. Together with linearity, photometric accuracy defines the ability of a spectrophotometer to accurately measure a given optical density or absorbance.

Photometric accuracy and linearity are obviously vital wherever accurate and precise measurements are required. Of similar importance is the range over which the spectrophotometer response remains linear. This is known as the linear dynamic range and is traditionally defined as the range over which absorbance and concentration remain directly proportional to each other[3]. A wide linear dynamic range permits the measurement of a wide range of sample concentrations (optical densities) and can significantly reduce sample analysis and preparation (dilution) times. In this instance, optical densities of materials used in the manufacture of laser safety eyewear have been determined in the NIR. Prior to sample measurement, filters of known optical density were used to confirm the photometric performance of the spectrophotometer. Using this addition of filters technique, photometric range, accuracy and linearity were demonstrated up to 8 Absorbance units at 1200 nm in the near-infrared. Having demonstrated photometric accuracy, linearity and range, the lens materials in question were then measured at the appropriate wavelengths in the nearinfrared.

Theory

The 'addition of filters' technique provides a straightforward and inexpensive means of determining the photometric linearity and range of a spectrophotometer without the need for expensive, calibrated standards. This method, applied to the visible portion of the electromagnetic spectrum, has been described elsewhere[4]. In this case, the same principle has been applied in the NIR to confirm photometric performance prior to sample analysis.

Rear beam attenuation was used when appropriate. Rear beam attenuation (RBA) is useful when the apparatus (or sample) in the sample beam attenuates the light beam considerably. In such situations, attenuation of the rear beam considerably increases the dynamic range of the instrument, as the detector does not 'see' two dramatically different signals (or light intensities). Typical situations where RBA may be of use include measuring the transmittance of dense optical filters, compensating for sample holders/accessories that restrict the light beam, or (in general) measuring samples with high absorbance. RBA may be achieved using mesh filters of the type described below, or by using the fully automated Cary Rear Beam Attenuator[5].

Materials and method

(For part numbers, please see Reference 6)

Equipment
- Agilent Cary 6000i UV-Vis-NIR Spectrophotomter
- Lockdown Solid Sample Holder and Lockdown Cuvette Holder
- Mesh filter kit for attenuating reference beam

Protocol
Using the Lockdown Solid Sample Holder and Cuvette Holder, a Lockdown plate was prepared with optical rails and sample slide in the sample beam and cuvette base in the reference beam. The optical rails and sample slide were used to mount filters and samples, whilst the cuvette base was used to provide a platform for rear beam attenuation (RBA). This was achieved using V-holder and mesh filters (mesh filter kit for attenuating reference beam[6]). RBA of ~3.5 A was used for all filter and sample measurements. Measurements were made using independent UV-Vis and NIR control (fixed spectral bandwidth in the UV-Vis; variable spectral bandwidth in the NIR). Indicative parameters were as follows (longer signal averaging times were used in some instances):

- UV-Vis: 5 nm SBW, 1 nm data interval, 0.1 s signal averaging time
- NIR: 3 nm data interval, 0.3 s signal averaging time, Energy 3.00

All measurements were made in 'double beam' mode using a full slit height. Baseline correction (Zero/Baseline correction) was used in all cases.

Filters having nominal absorbance values ranging from 1 to 3 over the desired wavelength range were used for the addition of filter experiments (all filters were manufactured by Schott; www.schott.com). Particular care was taken with respect to filter positioning and movement between measurements.

In the case of the two-filter addition, the first filter was measured, followed by the two together and then the second (by careful removal of the first).[4] A similar approach was used for the three-filter addition.

Results and discussion

The The results of the addition of filters measurements can be seen in Figure 1. For the two- filter addition, the actual and predicted measurements show excellent correlation across the entire NIR wavelength range measured, up to an absorbance maximum of 7.19 Abs at 1248 nm. In the case of the three-filter addition, where an additional absorbance of ~1 Abs is measured, good correlation between actual and predicted is again observed up to a maximum of 8.10 Abs at 1208 nm.
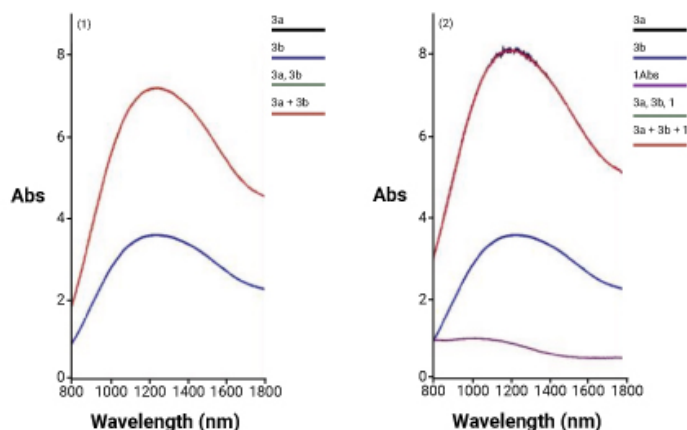

Figure 1. Addition of filters: (1) addition of two filters for an absorbance maximum of 7.19 (1248 nm) and (2) addition of three filters for an absorbance maximum of 8.10 (1208 nm). In each case, the red trace is the result of the mathematical addition of the individual filter spectra, and is overlaid on the spectrum of the combined filter measurement.

The noise evident in the combined three-filter measurement is indicative of the very low light throughput around the absorbance maximum. However, the profile of the measured spectrum is essentially identical to that of the mathematical addition of the three separate filters. The noise is distributed symmetrically about the expected profile, and could be minimized using a longer signal averaging (acquisition) time.

Whilst not exhaustive, the addition of filter experiments described confirm the ability of the spectrophotometer to make photometrically accurate and precise absorbance measurements at optical densities up to 8 Abs. High optical density samples were subsequently analyzed using parameters similar to those used for the filter measurements. The results can be seen in Figures 2 and 3.

The spectra obtained show excellent signal-to-noise across the wavelength and absorbance ranges investigated. Furthermore, they clearly demonstrate the ability of the spectrophotometer to make accurate high optical density measurements.
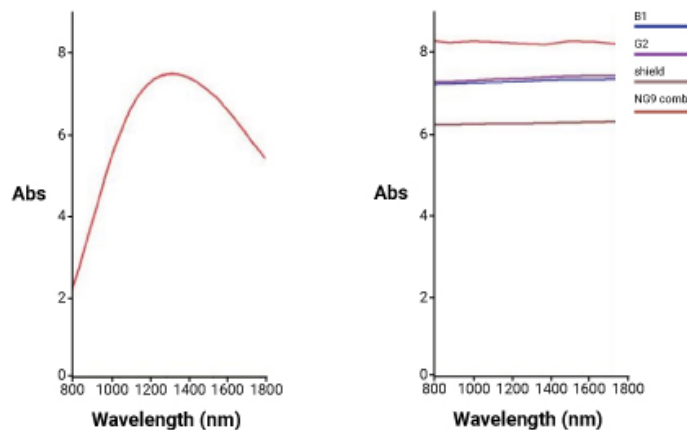

Figure 2. Sample scans of (left) high optical density lens material (absorbance maximum of 7.45 at 1230 nm, and (right) two plastic and two glass lens materials for use at 1064 nm (Nd:YAG).
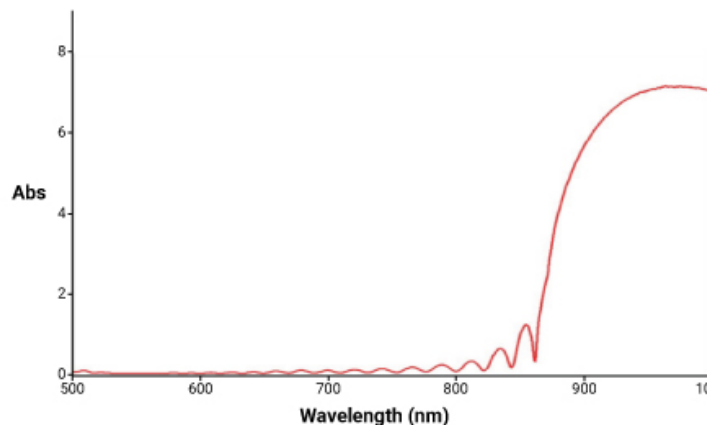

Figure 3. Visible-NIR spectrum of blocking filter for use over the 900 –1100 nm wavelength range (e.g. InGaAs lasers at 980 nm). Maximum absorbance of 7.16 Abs observed at 964 nm.

Conclusion

The addition of filters technique has been successfully used to demonstrate the photometric range, accuracy and linearity of the Cary 6000i UVVis-NIR spectrophotometer. Using the same instrument, spectra of a number of samples having absorbance maxima ranging from 7 to 8 were readily acquired.

Acknowledgements

References

1. The Linear Dynamic Range of the New Generation Cary 4000, 5000 and 6000i spectrophotometers. Data Sheet **2011**, www.agilent.com.

2. Josephy, D and Logan, D., A whole cell assay for spectroscopic measurement of recombinant cytochrome P450 expression in bacteria. **2011**, UV-VisNIR At Work No.87, www.agilent.com.

3. Hind, A.R., *To improvements in spectrophotometry*, American Laboratory, 34(24) **2002** 32

4. Photometric Linearity Range of the New Generation Cary 4000/5000/6000i spectrophotometers. **2011**, Data Sheet, www.agilent.com

5. Cary Rear Beam Attenuator accessory; part number 00 100441 00

6. Part numbers:

Product	Part Number
Agilent Cary 6000i UV-Vis-NIR Spectrophotometer*	00 100794 00
Mesh filter kit for attenuating reference beam	99 100477 00
Cary Win UV Analysis Pack Software	85 101950 00

* includes Lockdown Solid Sample Holder and Cuvette Holder as standard

www.agilent.com/chem/cary6000i

Agilent

Trusted Answers

Instrument Overview

Cary 4000 UV-Vis Spectrophotometer (175–900 nm)

The Cary 4000 sets the standard for photometric noise, range, and linearity, providing excellent resolution across the UV-Vis spectrum. The Cary 4000 is ideal for challenging research applications in materials science and is the industry-leading solution for all biological research.

Cary 5000 UV-Vis-NIR Spectrophotometer (175–3300 nm)

The Cary 5000 combines PbSmart detector technology with the optimized optical design and performance of all Cary instruments. It requires only one detector—the PbSmart—to extend that performance from the UV-Vis into the NIR.

Cary 6000i UV-Vis-NIR Spectrophotometer (175–1800 nm)

The Cary 6000i uses a high-performance InGaAs detector that is optimized for the shortwave NIR, delivering superior resolution in the 1200–1800 nm region. No instrument can match the NIR performance of the Cary 6000i.

Cary 7000 Universal Measurement Spectrophotometer (175–3300 nm)

Measure virtually any sample; measure absolute reflectance and transmission at any angle; and measure them all unattended. The Agilent Cary 7000 Universal Measurement Spectrophotometer (UMS) will satisfy all your solid sampling needs. Collect hundreds of UV-Vis-NIR spectra overnight, or characterize optical components or thin films in minutes to hours rather than hours to days. Delivering a turnkey solution for research, development, and QA/QC in optics, thin films/coatings, solar, and glass, the Cary 7000 UMS will advance your materials analysis. Design experiments never before possible, expand your research, and save time and money with the ground-breaking Cary 7000 UMS.

Common Applications

Cary 4000/5000/6000i

Materials Testing and Research	Chemicals and Petrochemicals	Energy and Fuels	Food and Agriculture	Biotech and Pharmaceuticals
− Thin film thickness analysis and anti-reflection coating analysis − Analysis of novel nanocomposite materials − Color measurements and color matching − Optical density measurements, e.g., optical filters and safety eyewear	− Spectro-electrochemical measurements, for, e.g., reduction of CO_2 − Measuring suspensions and highly scattering samples − Analysis of heavy metals in water − Quantitative analysis of strongly absorbing liquid media or suspensions	− Analysis of the functionality of photoresists − Measurement of oil yield in oil shale samples − Analysis of the reflectance properties of solar cells − Study of paints and the effect of pigments in the automotive industry	− Assessment of crop conditions, such as chlorophyll, water, and dry matter content − Quantitative analysis of additives − QC applications	− Measurement of turbid biological samples − Characterization of intracellular biochemical pathways − Analysis of potential sun-blocking agents for sun cream and cosmetics

Cary 7000 Universal Measurement Spectrophotometer

Optics, Thin Films, and Coatings	Solar	Glass	Academic and Industrial Research
− QA/QC coating quality − Film thickness control − Bulk optic performance and characterization − Coating uniformity − Color/visual appearance − Coatings and materials used in fashion eyewear (sunglasses) and safety eyewear (laser/welding goggles)	− QA/QC and development of parabolic trough and Fresnel reflectors − Photovoltaics – optimizing raw material and module efficiency at various stages of construction − Coated silicon homogeneity − Performance longevity and lowering PM costs under environmental exposure − Optical constant confirmation; purity and surface finish	− QA/QC optical performance testing − Conformance to regulatory standards (e.g., EN 410, ISO 9050, EN 13837) − Coated/composite properties (construction quality) − Optical robustness/longevity under environmental testing (e.g., temperature, light exposure, aging, physical abuse) − Confirmation of final design intent	− Optical constant measurements (refractive index, n, and k) − Film thickness modeling/measurement − Nanocomposite bandgap measurements − Characterizing fundamental scattering from Bragg grating surface plasmon polaritons − Diffuse scattering

Learn more:
www.agilent.com/chem/uv-vis

Buy online:
www.agilent.com/chem/store

Get answers to your technical questions and access resources in the Agilent Community:
community.agilent.com

U.S. and Canada
1-800-227-9770
agilent_inquiries@agilent.com

Europe
info_agilent@agilent.com

Asia Pacific
inquiry_lsca@agilent.com

Agilent
Trusted Answers